

EVALUATION AND DEVELOPMENT OF A STRUCTURALLY
ENHANCED PVC WATER PIPE

by

AMEYA BRAHMANAND PARADKAR

Presented to the Faculty of the Graduate School of
The University of Texas at Arlington in Partial Fulfillment
of the Requirements
for the Degree of

DOCTOR OF PHILOSOPHY

THE UNIVERSITY OF TEXAS AT ARLINGTON

August 2016

Copyright © by Ameya Brahmanand Paradkar 2016

All Rights Reserved



Acknowledgements

I would like to acknowledge the chair of my committee, Dr. Mohammad Najafi, P.E., F. ASCE, and Director of Center for Underground Infrastructure Research and Education (CUIRE) and Professor at the University of Texas at Arlington. Dr. Najafi has always been a teacher, a great motivator and was always supportive throughout all phases of my research. It would have been impossible for me to complete my research without his guidance, expertise and knowledge. His insight has significantly assisted me in choosing my career path, presently and in the future.

I would like to thank my dissertation committee members, Dr. Chien-Pai Han, Dr. Shih-Ho Chao and Dr. Mostafa Ghandehari for their suggestions on improving my dissertation and for taking the time out from their extremely busy schedules for my dissertation.

This dissertation research was funded by the Water Research Foundation (WRF), Denver, CO and American Water (AW), Voorhees, NJ. I would like to express my sincere appreciation to Jonathan Cuppett from WRF, David Hughes, Chandan Venkatesh and Robert Goeltz from AW and Agnes HJ Lee from Pyungwha Pipe Industry Inc. (PPI), South Korea. I could not have accomplished this work without their input, support, and direction. I would like to acknowledge Microbac Laboratories for performing some of the tests included here. This dissertation research would not have been possible without the funding received from Water Research Foundation and without the efforts of American Water. These organizations and their principles should be commended for their contributions and leadership to this research.

I would like to thank my colleagues at CUIRE who helped me throughout my research, and mention Amir Tabesh, Saeed Janbaz, Niloofar Rezaei, Marjan Shahrokh Esfahani and Taha Ashoori.

I would like to thank all my relatives and friends who have always encouraged me to work hard and fulfill my dreams. Lastly but most importantly, I would like to express my gratitude to my parents Mrs. Vijaya Paradkar and Mr. Brahmanand Paradkar, my wife Manasi and my brother Aniket, Mandar and my wife's parents for their love, support and unwavering trust in me and my abilities.

July 28, 2016

Abstract

EVALUATION AND DEVELOPMENT OF A STRUCTURALLY ENHANCED PVC WATER PIPE

Ameya Brahmanand Paradkar, PhD

The University of Texas at Arlington, 2016

Supervising Professor: Mohammad Najafi

Many U.S. utilities rely upon iron pipe to deliver water through their distribution network. It has only been in the past 50 years that other products have penetrated into the water utilities' pipeline. The industry has turned to various cementitious and plastic materials largely to overcome aggressive soil and water that can be corrosive to metallic pipes. This dissertation will discuss a new pipe material called iPVC pipe manufactured by Pyungwha Pipe Industry Inc. (PPI), South Korea. The iPVC pipe was evaluated by a series of selective testing on the pipe, including impact, stiffness, tensile, short-term hydrostatic burst pressure, fatigue and bedding tests as well as a pilot installation and operation of the pipe as part of an active system. The testing described here was funded by American Water (AW), a water utility company based in Voorhees, NJ through a grant from Water Research Foundation (WRF), Denver, CO.

The iPVC pipe parameters such as modulus of elasticity, pipe stiffness, design fatigue life, tensile strength, short-term burst pressure, impact strength, hoop stress and deflections of iPVC pipe are computed based on the tests performed. The iPVC pipe properties exceeds the American Water Works Association (AWWA) minimum standards requirements. The results of this dissertation show that iPVC exceeds the American Water Works Association (AWWA) minimum standards requirements for PVC C900 for

hydrostatic short-term burst pressure, impact strength, pipe stiffness, and tensile strength. The average hydrostatic short-term burst pressure recorded was 1,042 psi (40% higher than AWWA standards requirements), average impact strength recorded was 1,200 foot-pounds at 73 °F (12 times higher) and 1,080 foot-pounds at 32 °F (10 times higher), average pipe stiffness recorded was 479 psi (32% higher) and average tensile strength recorded was 7,930 psi (13% higher).

The fatigue design life for 8 in. DR 18 iPVC pipe is 125 years considering only the surge pressure experienced by the pipe. A finite element analyses is performed to evaluate the deflection of iPVC pipe under earth load and earth plus live (truck) load simulations. The pipe deflection values obtained during bedding test as well as theoretical calculations are compared with finite element analyses. The maximum deflection experienced by the iPVC pipe is less than the AWWA maximum allowable deflection of 5% for 8 in. DR 18 PVC pipe.

Table of Contents

Acknowledgements	iii
Abstract	v
Table of Contents	vii
List of Illustrations	xiv
List of Tables	xxi
Chapter 1 INTRODUCTION AND BACKGROUND	1
1.1 History of Pipelines	1
1.2 Classification of Pipes	2
1.3 Types of Pipe Materials	4
1.3.1 Metallic Pipes	5
1.3.1.1 Cast Iron Pipe (CIP).....	5
1.3.1.2 Ductile Iron Pipe (DIP).....	5
1.3.1.3 Steel Pipe (SP)	5
1.3.2 Concrete Pipes	6
1.3.2.1 Prestressed Concrete Cylinder Pipe (PCCP)	6
1.3.2.2 Reinforced Concrete Pipe (RCP)	6
1.3.2.3 Bar-wrapped Steel-cylinder Concrete Pipe (BWP).....	6
1.3.2.4 Asbestos Cement Pipe (AC).....	6
1.3.3 Plastic Pipes	7
1.3.3.1 Polyvinyl Chloride Pipe (PVC)	7
1.3.3.2 Polyethylene Pipe (PE).....	7
1.3.3.3 Glass Reinforced Polyester Pipe (GRP).....	7
1.4 Introduction to Polyvinyl Chloride (PVC).....	8
1.4.1 Development of PVC	8

1.4.2	Manufacturing of PVC Resins.....	11
1.4.3	Types of PVC Pipe as per Manufacturing Process	12
1.4.3.1	PVC-U Pipe	13
1.4.3.2	PVC-O Pipe	13
1.4.3.3	PVC-M Pipe	14
1.4.4	Types of Joints for PVC Pipe.....	14
1.4.4.1	Gasketed Joint.....	14
1.4.4.2	Heat Fused Joint.....	15
1.4.5	Current Standards for PVC Pipes.....	15
1.4.6	Characteristics of PVC Pipes.....	16
1.4.6.1	Lightweight.....	16
1.4.6.2	Strength and Flexibility	17
1.4.6.3	Resistance to Corrosion	17
1.4.6.4	Resistance to Chemical.....	17
1.4.6.5	Joint Tightness.....	18
1.4.6.6	Flame-retardant and Insulation Properties	18
1.4.6.7	Simplicity in Manufacturing Processes	18
1.4.6.8	Prevention from Oxidation	19
1.4.7	Limitations of PVC Pipes	19
1.4.7.1	Photo-oxidative and Thermo-oxidative Degradation	19
1.4.7.2	Hydrocarbon Compounds and their Effects on the PVC Pipe	20
1.4.7.3	PVC Pipe Cracks	20
1.4.7.4	Joint Failures in PVC Pipes	21
1.4.7.5	Effects of PVC Resin on Environment.....	23

1.4.7.6	PVC Pipe Failure Case Studies.....	23
1.4.8	Installation Requirements for PVC Pipe	24
1.4.9	Introduction to iPVC Pipe.....	26
1.5	Introduction to iPVC Pipe Project.....	26
1.6	Research Needs	27
1.7	Research Objectives	27
1.8	Research Methodology	27
1.9	Expected Outcome.....	29
1.10	Dissertation Organization.....	30
1.11	Chapter Summary.....	30
Chapter 2 Literature Review		31
2.1	Introduction	31
2.2	Hydrostatic Short-term Burst Pressure Test.....	31
2.3	Impact Test	37
2.4	Stiffness Test	40
2.5	Tensile Test.....	44
2.6	Fatigue Test	46
2.7	Bedding Test.....	51
2.8	Previous Tests on iPVC Pipe.....	65
2.9	Chapter Summary.....	69
Chapter 3 Testing Methodology		70
3.1	Introduction	70
3.2	Hydrostatic Short-term Burst Pressure Test (Adapted from WRF Report No. 4650, 2016).....	71
3.2.1	Purpose.....	71

3.2.2	Procedure	71
3.2.3	Expected Outcome	71
3.2.4	Benefit to the Industry	72
3.3	Impact Test (Adapted from WRF Report No. 4650, 2016)	72
3.3.1	Purpose.....	72
3.3.2	Procedure	72
3.3.3	Expected Outcome	73
3.3.4	Benefit to the Industry	73
3.4	Stiffness Test (Adapted from WRF Report No. 4650, 2016)	73
3.4.1	Purpose.....	73
3.4.2	Procedure	73
3.4.3	Expected Outcome	74
3.4.4	Benefit to the Industry	75
3.5	Tensile Test (Adapted from WRF Report No. 4650, 2016).....	75
3.5.1	Purpose.....	75
3.5.2	Procedure	75
3.5.3	Expected Outcome	76
3.5.4	Benefit to the Industry	77
3.6	Fatigue Test (Adapted from WRF Report No. 4650, 2016)	77
3.6.1	Purpose.....	77
3.6.2	Procedure	77
3.6.3	Expected Outcome	79
3.6.4	Benefit to the Industry	79
3.7	Bedding Test (Adapted from WRF Report No. 4650, 2016)	79
3.7.1	Purpose.....	79

3.7.2	Procedure	80
3.7.3	Test Pit.....	80
3.7.4	Test Pipe.....	81
3.7.5	Instrumentation	82
3.7.5.1	Earth Pressure Cells.....	82
3.7.5.2	Displacement Sensors.....	83
3.7.5.3	Strain Gauges.....	84
3.7.5.4	Data Loggers	85
3.7.5.5	Installation of the Sensors	87
3.7.5.6	Nomenclature	89
3.7.5.7	Data Collection and Monitoring	91
3.7.5.8	Sign Conventions.....	92
3.7.6	Pipe Installation	92
3.7.7	Live Load Simulation	93
3.8	Pipe Modeling using Finite Element.....	94
3.9	Chapter Summary.....	95
	Chapter 4 Research Results.....	96
4.1	Hydrostatic Short-term Burst Pressure Test.....	96
4.2	Impact Test	98
4.3	Stiffness Test	101
4.4	Tensile Test.....	104
4.5	Fatigue Test	109
4.6	Bedding Test.....	111
4.6.1	Effect of Only Earth Load on iPVC Pipe	112
4.6.2	Effect of Earth plus Truck Load on iPVC pipe	117

4.7	Field Installation of iPVC Pipe.....	123
4.8	Chapter Summary.....	124
	Chapter 5 Discussion of Results.....	125
5.1	Introduction	125
5.2	Hydrostatic Short-term Burst Pressure Test.....	125
5.3	Stiffness Test	129
5.4	Fatigue Test	132
5.5	Bedding Test.....	136
	5.5.1 Deflection of iPVC Pipe due to Earth Load.....	136
	5.5.2 Deflection of iPVC Pipe due to Earth plus Truck Load.....	139
5.6	Pipe-Soil Interaction with Finite Element analyses	140
	5.6.1 Introduction	140
	5.6.2 Assumptions and Parameters for FEM Model.....	140
	5.6.3 FEM Analysis in PLAXIS 2D.....	141
	5.6.4 FEM Analysis in ABAQUS 6.14-3.....	146
5.7	Contribution to the Body of Knowledge.....	157
	5.7.1 Overall Approach to Evaluate a New Pipe	157
	5.7.2 Uniqueness of Fatigue and Bedding Test	157
	5.7.3 Comparison of Evaluation of New Pipe with Other Pipe Materials....	158
	5.7.4 Marketing of iPVC Pipe in U.S.....	160
5.8	Chapter Summary.....	161
	Chapter 6 Conclusions and Recommendations for Future Research	162
6.1	Conclusions.....	162
6.2	Recommendations for Future Research	165
	Appendix A Abbreviations	167

Appendix B Bedding Test Instrumentation.....	171
Appendix C Strain Gauge Readings	177
References.....	180
Biographical Information	192

List of Illustrations

Figure 1-1 Comparison of Typical Soil Loads on Rigid and Flexible Pipe (Adapted from: Watkins and Anderson, 2000).....	3
Figure 1-2 Arching over the Flexible Pipe (Adapted from: Watkins and Anderson, 2000).....	3
Figure 1-3 Types of Pipe Based on Material (Adapted from: Al-Barqawi and Zayed, 2006).....	4
Figure 1-4 PVC Resin Consumption in 2007 in U.S. and Canada (Source: American Chemistry Council, 2008).....	8
Figure 1-5 (a) Vinyl Chloride Molecule and (b) Molecular Chain in PVC (Rahman, 2004)	9
Figure 1-6 PVC Pipe and Fittings Worldwide Consumption (Uni-Bell, 2012)	10
Figure 1-7 Process Flow Diagram for PVC Resin Manufacturing (Chan et al., 2007)	11
Figure 1-8 Heat Fused Joint Operation for PVC Pipe (Underground Solutions, 2016).....	15
Figure 1-9 Process of Contamination in PVC Pipe (Ong et al., 2008)	20
Figure 1-10 Crack in PVC Pipe (Burn et al., 2005)	21
Figure 1-11 Failure Steps Leading to a Blown Section (Adapted from: Burn et al., 2005).....	21
Figure 1-12 (a) New Rieber Type Gasket, and (b) Older Type of Gasket (Balkaya et al., 2013)	22

Figure 1-13 Failure of PVC Pipe due to Improper Bedding Conditions (Lackey, 2010)	24
Figure 1-14 Terms used in Pipe Installation (Uni-Bell, 2013)	25
Figure 1-15 PVC and iPVC pipe Structure under SEM (Source: AW and PPI, 2015).....	26
Figure 1-16 Project Methodology Overview (Source: Adapted from WRF Report No. 4650, 2016)	29
Figure 2-1 Cross-section of RTP (Adapted from: Bai and Bai, 2014).....	32
Figure 2-2 Equations for Predicting Burst Pressure (Law and Bowie, 2007)	34
Figure 2-3 Burst Pressure Results and Predictions in MPa (Law and Bowie, 2007)	35
Figure 2-4 Test Specimens after Burst Test (Netto et al. 2005)	36
Figure 2-5 Small Scale Impact Test Setup (Gabet et al. 2011)	38
Figure 2-6 Full Scale Impact Test Setup (Gabet et al. 2011)	39
Figure 2-7 Parallel Plate Load Test	41
Figure 2-8 Parallel Plate Test for 18 in. PVC Pipe (Sargand et al., 1998)	42
Figure 2-9 Parallel Plate Test for 18 in. HDPE Pipe (Sargand et al., 1998)	42

Figure 2-10 Stress Relaxation of PVC Pipe (Sargand et al., 1998)	43
Figure 2-11 Stress Relaxation of HDPE Pipe (Sargand et al., 1998)	44
Figure 2-12 Moser's S-N Plot (Jeffrey et al., 2004)	49
Figure 2-13 Illustration of Stress Terms (Jeffrey et al., 2004)	50
Figure 2-14 Schematic Diagram of Buried Pipe (Alam and Allouche 2010).....	51
Figure 2-15 Earth Pressure Diagrams for: a) Spangler's Analysis, b) Simplified Analysis by JSWA and c) Proposed Analysis for High Fills (Kawabata et al., 2006)	54
Figure 2-16 Typical Section of Renewal and Bypass Mains in Edmonton, Canada (Zhan and Rajani, 1997)	58
Figure 2-17 (a) Peaking Load due to Lateral Forces of Embedment and (b) Deflection due to Backfill Cover (Najafi et al. 2013).....	63
Figure 2-18 Bulldog™ Restrained Joint Pipe Components (Najafi et al. 2011-b).....	64
Figure 2-19 9 in. OD DR 18 iPVC pipe Thickness (Source: AW and PPI, 2015).....	66
Figure 2-20 PVC and iPVC pipe Impact Test Results (Source: AW and PPI, 2015).....	67

Figure 2-21 iPVC pipe Pressurized with Freezing Water (Source: AW and PPI, 2015).....	68
Figure 2-22 Crawl Test (Source: AW and PPI, 2015).....	68
Figure 2-23 Bucket Test (Source: AW and PPI, 2015).....	69
Figure 3-1 Specimen Dimensions (ASTM D638-14, 2010)	76
Figure 3-2 CUIRE Fatigue Test Schematic Diagram (Divyashree et al. 2015).....	78
Figure 3-3 CUIRE Fatigue Test Experiment Setup.....	79
Figure 3-4 Bedding Test Location.....	80
Figure 3-5 Trench 1 and Trench 2 Pit.....	80
Figure 3-6 Cross Section of Bedding Test 2 Setup	81
Figure 3-7 Earth Pressure Cells used in Test.....	83
Figure 3-8 Displacement Sensors Attached to iPVC pipe for Round 2 Test	83
Figure 3-9 Strain Gauge attached to iPVC pipe	85
Figure 3-10 Geokon™ 8002-16 (LC-2 x 16) Data Logger used in Test 2 (Geokon 2016)	86
Figure 3-11 (a) P3 Data Logger for Test 1, (b) System 7000 Data Logger for Test 2.....	86
Figure 3-12 (a) Schematic diagram showing location of instruments, (b) Actual photographs for displacement sensors and strain gauge location	88
Figure 3-13 Sectional View of a Typical Pipe	89
Figure 3-14 Nomenclature Used for Sensors in Bedding Test 2	90
Figure 3-15 iPVC Pipe Installation	93

Figure 3-16 Boundary Conditions	94
Figure 4-1 iPVC pipe Failure in Short-term Burst Pressure Test: (a) Brittle Failure and (b) Ductile Failure (Source: WRF Report No. 4650, 2016).....	97
Figure 4-2 Graphical Illustration of Hydrostatic Burst Test Results (WRF Report No. 4650, 2016)	98
Figure 4-3 (a) Falling Weight TUP A and (b) Impact Test Results at Microbac.....	99
Figure 4-4 Deflection of Pipe during Stiffness Test (Source: WRF Report No. 4650, 2016).....	102
Figure 4-5 Load vs. Deflection in Stiffness Test (Source: Microbac).....	104
Figure 4-6 Type I Tensile Test (Mid-wall) in Action at Microbac.....	105
Figure 4-7 Tensile Strength of Type I iPVC pipe Specimen (Source: WRF Report No. 4650, 2016).....	106
Figure 4-8 Modulus of Elasticity of Type I iPVC pipe Specimen (Source: WRF Report No. 4650, 2016).....	106
Figure 4-9 Tensile Test Type III (Full-wall) Testing at CUIRE	107
Figure 4-10 Tensile Strength of Type III iPVC pipe Specimen	108
Figure 4-11 Modulus of Elasticity of Type III iPVC pipe Specimen	109
Figure 4-12 Change of Pipe Circumference Measurement Locations on iPVC pipe	110
Figure 4-13 Change in Circumference at Various Stages	111
Figure 4-14 Deflection at Joint of Pipe.....	113
Figure 4-15 Deflection at End of Pipe	114
Figure 4-16 Strain Measurements at Joint of Pipe	115
Figure 4-17 Strain Measurements at End of Pipe.....	115

Figure 4-18 Earth Pressures for Bedding Test 2	117
Figure 4-19 20-Ton Truck used to Create Live Load Simulation	118
Figure 4-20 Deflection at Joint of Pipe due to Earth plus Truck Load	119
Figure 4-21 Deflection at End of Pipe due to Earth plus Truck Load	120
Figure 4-22 Strain Measurements at Joint of Pipe due to Earth plus Truck Load	121
Figure 4-23 Strain Measurements at End of Pipe due to Earth plus Truck Load	121
Figure 4-24 Earth Pressures for Bedding Test 2 due to Earth plus Truck Load.....	122
Figure 4-25 Tapping of iPVC pipe (Source: AW).....	123
Figure 4-26 iPVC pipe Pilot Installation by MOAW at Meramec River Bottom Road, St Louis County, MO. (Source: AW).....	124
Figure 5-1 Hoop Stress due to Internal Pressure (Uni-Bell, 2012)	126
Figure 5-2 Hydrostatic Life of PVC Operation at STR (Uni-Bell, 2012)	128
Figure 5-3 Graphical presentation of PS for iPVC pipe	131
Figure 5-4 Graphical Illustration of SF for iPVC pipe.....	131
Figure 5-5 Graphical Illustration of Flexural Modulus (E) for iPVC pipe	132
Figure 5-6 Hydrostatic Design Basis Values Corresponding to LTHS Values (ASTM D2837-13e1, 2013).....	134
Figure 5-7 Standard Prism Load Soil Pressure (Source: JM Eagle, 2016)	137
Figure 5-8 Bureau of Reclamation Values of E' (for Initial Flexible Pipe Deflection) (Howard, 1977)	138

Figure 5-9 Transmitted Live Loads to Pipe (Source: JM Eagle, 2016)	139
Figure 5-10 Screenshot of Soil Properties used for FEM analysis	141
Figure 5-11 Screenshot of iPVC pipe Properties used for FEM Analysis.....	142
Figure 5-12 Distribution of Mesh for Soil Box in Initial Phase using Plaxis 2D.....	143
Figure 5-13 Initial Phase before FEM Analysis.....	144
Figure 5-14 Vertical Displacement due to Earth Load	144
Figure 5-15 Vertical Displacement due to Earth plus Truck Load	145
Figure 5-16 Horizontal Displacement due to Earth Load.....	145
Figure 5-17 Horizontal Displacement due to Earth plus Truck Load	146
Figure 5-18 Geometry of Pipe-Soil Model in ABAQUS.....	147
Figure 5-19 Contact Surface between Soil and Pipe.....	148
Figure 5-20 Meshing of Model in ABAQUS	148
Figure 5-21 Vertical Deflection Contours (a) Front View (b) 3D View	149
Figure 5-22 Vertical Deflection Contours - Front View	151
Figure 5-23 Vertical Deflection Contours - 3D View	151
Figure 5-24 Arrows showing the Direction of Resultant Deflection in Pipe	152
Figure 5-25 Deflection Values for Earth Load Application	155
Figure 5-26 Deflection Values for Earth plus Truck Load Application	155

List of Tables

Table 1-1 Rigid and Flexible Pipe Classification (Najafi, 2010).....	4
Table 1-2 Milestones of PVC Pipe in North America (Uni-Bell, 2015)	10
Table 2-1 Measured Burst Pressure of RTP Samples (Bai and Bai, 2014)	33
Table 2-2 Burst Pressure Results for Small-scale Steel Specimens (Adapted from: Netto et al. 2005).....	36
Table 2-3 Pipe Stiffness of Parallel Plate Test at Two Different Loading Rates (Adapted from: Sargand et al., 1998).....	43
Table 2-4 Pipe Stiffness Results of Stress Relaxation Tests (Adapted from: Sargand et al., 1998).....	44
Table 2-5 Elastic Parameters for PVC Pipe (Adapted from: Neelam and Kalaga, 2002)	46
Table 2-6 iPVC pipe Test Results by PPI (Source: AW and PPI, 2015).....	66
Table 3-1 Details of Sensors used for Bedding Test 2	91
Table 4-1 Short-term Burst Pressure Test Results from Microbac and CUIRE.....	97
Table 4-2 Impact Test Results at 73 °F at Microbac for Partial Number of Test Samples	99
Table 4-3 Impact Test Results at 32 °F at Microbac for Partial Number of Test Samples	100
Table 4-4 Impact Retest Results at 32 °F at Microbac for Partial Number of Test Samples	100

Table 4-5 Partial Stiffness Test Results for iPVC pipe at Microbac.....	103
Table 4-6 Type I Mid-wall Pipe Sample Tensile Test Results at Microbac.....	105
Table 4-7 Type III Full-wall Pipe Sample Tensile Test Results at Microbac and CUIRE	108
Table 4-8 Pipe Deflection at Joint and End of Pipe due to Earth Load	112
Table 4-9 Earth Pressures at Joint and End of Pipe.....	116
Table 4-10 Pipe Deflection at Joint and End of Pipe due to Earth plus Truck Load.....	118
Table 4-11 Earth Pressure at Joint and End of Pipe due to Earth plus Truck Load.....	122
Table 5-1 Hoop Stress for iPVC pipe.....	126
Table 5-2 STR Rating for iPVC pipe	128
Table 5-3 Stiffness Factor for selected iPVC pipe Samples	129
Table 5-4 Corrected PS, SF and E for iPVC pipe.....	130
Table 5-5 Soil Properties for FEM Analysis (Source: Sharma, 2013).....	141
Table 5-6 Summary of Vertical and Horizontal Deflections for Earth Load only.....	150
Table 5-7 Summary of Vertical and Horizontal Deflections for Earth plus Truck Loads.....	153
Table 5-8 Deflection Values obtained from FEM Analysis.....	154
Table 5-9 Comparison of DI, PVC, HDPE and iPVC pipe (Source: DIPRA, Uni-Bell, Plastics Pipe Institute)	159
Table C-1 Strain in iPVC pipe at joint and end of pipe	178
Table C-2 Strain in iPVC pipe at joint and end of pipe due to earth plus truck load.....	179

Chapter 1

INTRODUCTION AND BACKGROUND

1.1 History of Pipelines

Use of pipelines began thousands of years ago in countries such as Persia, China, Crete, Greece, etc. The people of Mesopotamia started using aqueducts around 2000 B.C. to transport drinking water from rivers through desert to housing communities. People of Egypt started using canals to divert the Nile River to irrigate farming fields and communities in 3000 B.C. To reduce evaporation from the aqueducts, communities then started using clay pipes (Antaki, 2003). In 400 B.C., bamboo wrapped with waxed clothes was used by the Chinese to supply natural gas to Beijing for lighting purposes (Venkatesh, 2012).

In the United States (U.S.), settlers first invented log pipes and later adapted wooden pipes connected by steel hoops soon after migrating from Europe (Najafi, 2010). The technology of pipelines saw a vast improvement with the introduction of cast iron pipes in the 1800s. Before that, most small diameter pipes were made of wood. Cast iron was first manufactured in the early 1800's in New Jersey and gradually replaced the wooden pipes of the 1800s (CISPI, 2006). These cast iron pipes were cast vertically in pits and later replaced by centrifugally spun cast iron in the 1920s. In 1922, cement mortar lining of pipes took place. Ductile iron pipe was first manufactured and used in 1948 and the polyethylene encasement was first developed and used in 1951. Steel pipe has been in use since the 19th century and concrete cylinder pipe since the 1940s for water distribution. Bar-wrapped pipe was developed in 1942 with large-scale production starting in 1950 (Walski, 2006). Asbestos cement was introduced in the late 1920s and was heavily used around the world — especially in the mid-1900s (Wang et. al, 2011).

Modern piping materials such as polyvinyl chloride (PVC), high density polyethylene pipe (HDPE) and medium density polyethylene pipe (MDPE), glass-

reinforced polyester pipe (GRP) and polymer concrete pipe (PCP) have been in use in North America for the last 40 years (Najafi and Gokhale, 2005).

1.2 Classification of Pipes

Pipes are classified based on the following criteria (Mays, 2000):

- a. Nature of applications: gas, water, sewer, oil.
- b. Environment or topographical applications: offshore, inland, in-plant, mountain pipelines.
- c. Type of burial or support: underground, aboveground, elevated and underwater.
- d. Material: cast iron, ductile iron, PVC, HDPE, concrete pipe, etc.

Based on the mode of withstanding loads, pipes are classified into two major categories, rigid and flexible. Rigid pipes are resistant to longitudinal and circumferential (ring) bending and they do not deform under the applied loads. Rigid pipe is designed to withstand external dead and live loads and internal pressure loads without deformation and with minimum support of the side soil column (Sharma, 2013).

Flexible pipes are deformable pipes capable of deforming without causing any damage to the pipe. Flexible pipes are designed with an allowance to deform within a specified limit depending upon the pipe material and type of coatings and linings on the pipe (Najafi, 2010). Flexible pipes derive their soil load carrying capacity from their flexibility. The pipe tends to deflect under soil load thereby developing passive soil support at the sides of the pipe. During the same time, the ring deflection relieves the pipe of the major portion of the vertical soil load which is picked up by the surrounding soil in an arching action over the pipe. The reduction in load imposed on a pipe because of its flexibility is referred to as arching. The pipe and the soil work as a system in resisting the vertical load in a buried flexible pipe. The pipe-soil system eventually reaches a point of equilibrium where the soil above the pipe forms an arch and further deflection of the pipe stops (Moser

and Folkman, 2008). Figure 1-1 compares the typical soil loads on a rigid and flexible pipe and shows how the deflection of flexible pipe is just enough to equalize the horizontal and vertical forces. Figure 1-2 illustrates the formation of an arch over the flexible pipe. Table 1-1 classifies pipe materials as either rigid or flexible.

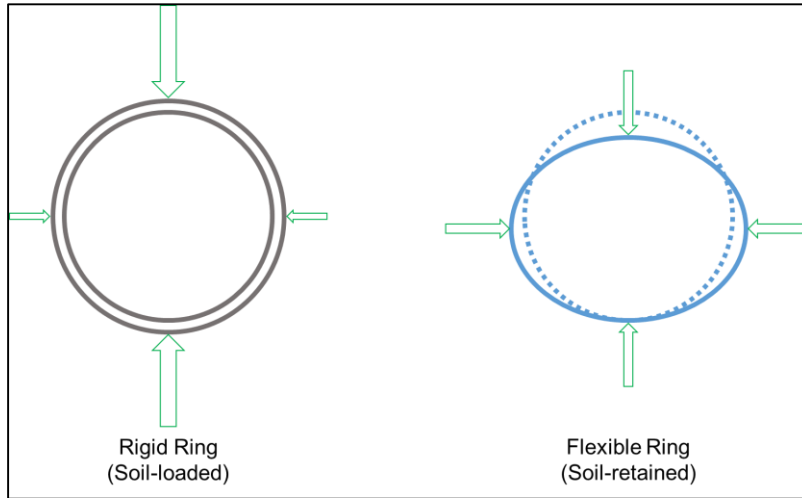


Figure 1-1 Comparison of Typical Soil Loads on Rigid and Flexible Pipe
(Adapted from: Watkins and Anderson, 2000)

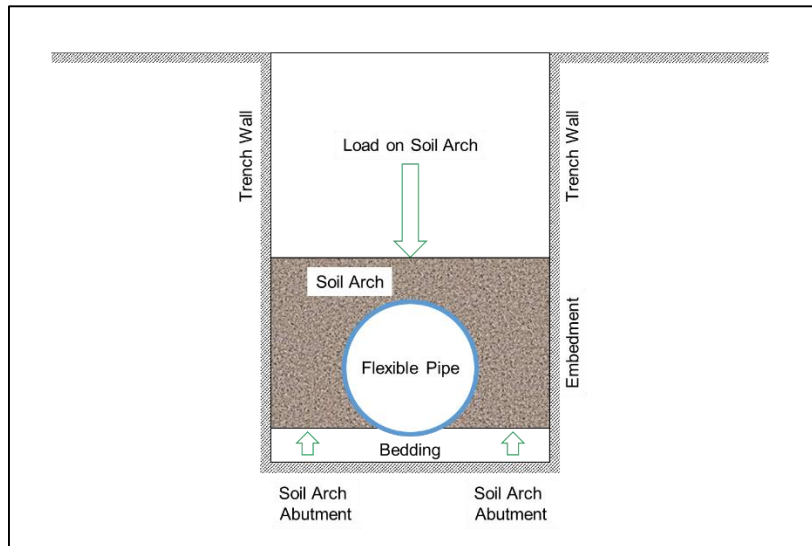


Figure 1-2 Arching over the Flexible Pipe
(Adapted from: Watkins and Anderson, 2000)

Table 1-1 Rigid and Flexible Pipe Classification (Najafi, 2010)

Rigid Pipes	Flexible Pipes
Cast Iron Pipe (CIP)	Steel Pipe (SP)
Vitrified Clay Pipe (VCP)	Ductile Iron Pipe (DIP)
Prestressed Concrete Cylinder Pipe (PCCP)	Polyvinyl Chloride Pipe (PVC)
Reinforced Concrete Pipe (RCP)	Polyethylene Pipe (PE)
Bar-wrapped Steel-cylinder Concrete Pipe (BWP)	Glass Reinforced Polyester Pipe (GRP)
Asbestos-Cement Pipe (AC)	-
Polymer Concrete Pipe (PCP)	-

1.3 Types of Pipe Materials

Based on the material used in manufacturing, pipes are classified into three types: metallic pipes, concrete pipes and plastic pipes. Figure 1-3 presents the different types of pipes available on the market.

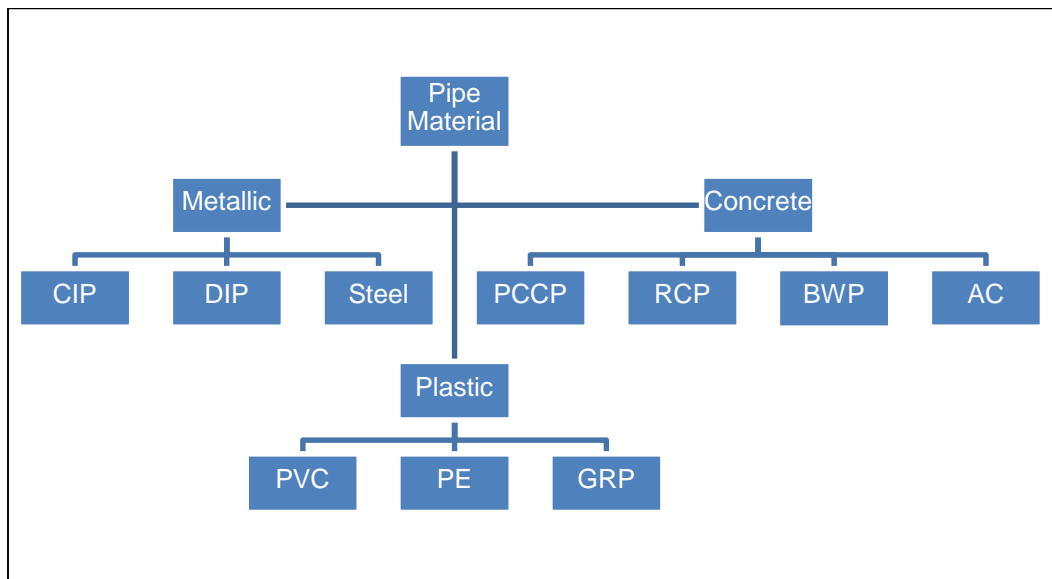


Figure 1-3 Types of Pipe Based on Material
(Adapted from: Al-Barqawi and Zayed, 2006)

1.3.1 *Metallic Pipes*

1.3.1.1 Cast Iron Pipe (CIP)

Since the 1800's, cast iron pipe (CIP) has been widely used in North America. About 50% of the total length of installed water mains is cast iron pipe (Makar et al., 2001). Cast iron is also referred as gray cast iron and is a strong but brittle material (Najafi and Gokhale, 2005). Pit cast gray iron and centrifugal cast gray iron are two types of cast iron pipe.

1.3.1.2 Ductile Iron Pipe (DIP)

The graphite composition in the CIP was changed from flake form to spherical form by adding inoculants such as magnesium to the molten iron to have an improved pipe material. This procedure led to the development of ductile iron pipe (DIP) which has an improved strength, impact resistance and some other properties compared to CIP (Najafi and Gokhale, 2005).

1.3.1.3 Steel Pipe (SP)

Steel pipes are manufactured in different ways to give them their respective characteristics. Steel pipes can be manufactured using seamless welds, butt-welds or spiral welds. Seamless pipe is formed when a molten steel rod is combined with a clamp. Butt welded steel pipe is formed when hot steel is rolled into a hollow cylinder-like shape giving the pipe a joint. Finally, a spiral welded steel pipe is formed when strips of steel metal are twisted and welded where the edges join each other. Steel pipes are known for their strength and ability to transport water at high pressures.

Carbon steel pipes are most commonly used in industry today. The carbon steel material's drawback is the ability to corrode easily via ferrous oxide formation on the inside of the walls, which can sometimes slow down the water flow (Parisher and Rhea, 2012).

1.3.2 Concrete Pipes

1.3.2.1 Prestressed Concrete Cylinder Pipe (PCCP)

Prestressed concrete cylinder pipes (PCCP) has a cement mortar inside a steel cylinder mold. After the concrete hardens, the cylinder is again wrapped with a hot-rolled steel bar and then wrapped with a dense mortar layer of cement. The engineers noticed premature failures on pipes made of this material in the 1990's. Lined cylinder pipe and embedded cylinder pipe are the two types of PCCP (Najafi and Gokhale, 2005).

1.3.2.2 Reinforced Concrete Pipe (RCP)

Reinforced concrete pipes (RCP) are reinforced with welded wire fabric, hot-rolled rod made of Grade 40 steel or cold-drawn steel wire made from hot-rolled rods. RCP is used for pressure applications up to 55 psi (Najafi and Gokhale, 2005).

1.3.2.3 Bar-wrapped Steel-cylinder Concrete Pipe (BWP)

Bar-wrapped steel-cylinder concrete pipes (BWP) were known as pre-tensioned concrete cylinder pipes before 1995. BWP are currently used in high pressure water and sewer applications. BWP are manufactured by first forming a steel cylinder and lining it with cement mortar. The cement mortar is steam cured and a steel bar is wrapped around it (Arnaout, 2000).

Cement mortar coating allows for an alkaline environment which prohibits corrosion in the bar-wrapped pipe. However, this mortar is prone to damage due to improper handling, aggressive environments, etc., which can then lead to corrosion and eventually lead to leakage/failure. It is typically used for pressures of 300 psi or less. It is produced in diameters of 10-72 in. (Pure Technologies, 2016).

1.3.2.4 Asbestos Cement Pipe (AC)

Asbestos cement (AC) was introduced in North America in the late 1920s and was used to carry water from the 1940s to 1970s. It was manufactured by mixing slurry of

Portland cement (80-85%) with a mixture of chrysotile asbestos fibers (15-20%). The pipes experienced degradation over time leading to chemically corrupted water. The AC pipes would lose free lime due to acidic pH which led to their eventual softening and a significant decrease in mechanical strength (Wang et. al, 2011). Due to the harmful effects of asbestos fibers to the human health, its use was discontinued in the early 1980s in North America (Najafi, 2010). However, utilities in U.S. have a small percentage of AC pipe in their distribution network which are still in service.

1.3.3 *Plastic Pipes*

1.3.3.1 Polyvinyl Chloride Pipe (PVC)

PVC material was an accidental discovery in the 19th century made by German scientists when vinyl chloride was being observed and it resulted in the creation of an off-white accumulation of solid material when it got exposed to the sunlight. The technology was brought to U.S. in mid-1950s and by 2000 the use of PVC resin had reached 5 billion pounds (Najafi and Gokhale, 2005).

1.3.3.2 Polyethylene Pipe (PE)

Polyethylene was discovered in 1933 and its use in pipe applications started in 1950. A variety of materials which are low, medium, high or linear low density abbreviated as LDPE, MDPE, HDPE and LLDPE are used for PE pipes. PE pipes has been an alternative choice for tuberculation and corrosion issues of traditional iron, steel and concrete pipes (Storm and Rasmussen, 2011).

1.3.3.3 Glass Reinforced Polyester Pipe (GRP)

The manufacturing for this pipe in the U.S. started in the 1950s and is commonly known as fiberglass pipe. The fiberglass composites are made from glass fiber reinforcements, thermosetting resins and other additives such as fillers, catalysts, hardeners, accelerators, and so on. Epoxy, polyester and vinyl ester are the types of resins

used for its manufacturing. The use of GRP in large diameter water applications is growing rapidly in North America (Najafi and Gokhale, 2005).

1.4 Introduction to Polyvinyl Chloride (PVC)

Polyvinyl chloride (also called vinyl or simply PVC) is a versatile thermoplastic material. PVC resin is currently used in the production of hundreds of day-to-day products that consumers use. PVC resin is also used in many other products in construction, electronics, healthcare, and other applications. The low cost and desirable physical and mechanical properties are some of the reasons for its widespread use. Figure 1-4 explains the consumption of PVC resin in U.S. and Canada in 2007 (American Chemistry Council, 2008).

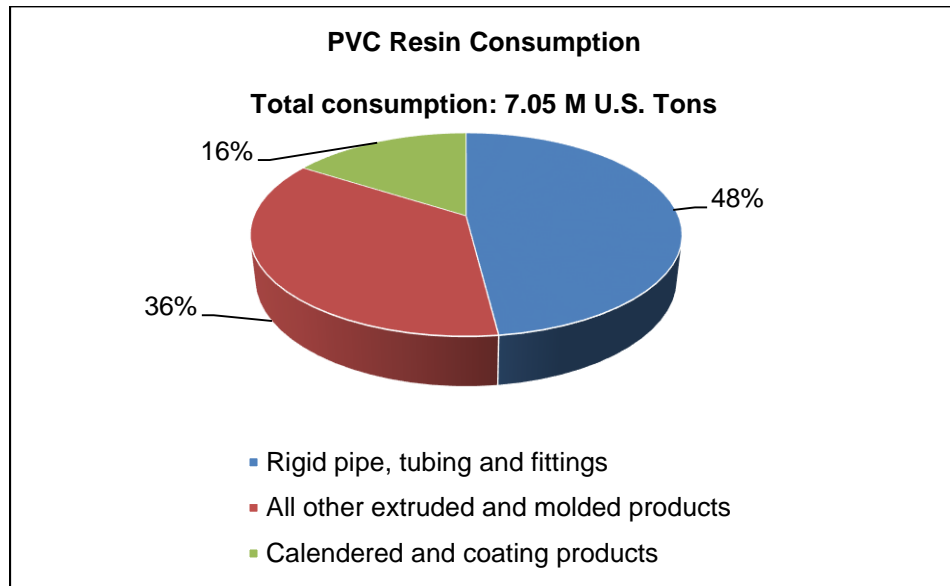


Figure 1-4 PVC Resin Consumption in 2007 in U.S. and Canada
(Source: American Chemistry Council, 2008)

1.4.1 Development of PVC

PVC compound was invented centuries ago by four Dutchmen named Dieman, Trotswyck, Bondt, and Laurverenburg in 1795. The substance was initially called “the oil of the Dutch chemists.” A vinyl-chloride molecule comprised of hydrogen, carbon, and

chlorine is shown in Figure 1-5. Several attempts were made to understand this compound during 19th century. The PVC compound was formally patented in Germany in 1912 (Mulder and Knot, 2001).

PVC was then chlorinated during World War I. Chlorination was an important step in PVC development because it enhanced its processability. After the war, however, the demand for PVC dropped drastically as the material was considered low quality in comparison with other materials. This decline led to its initial downfall with Russia being the first to terminate its production in 1917 followed by Germany in 1925 (Mulder and Knot, 2001).

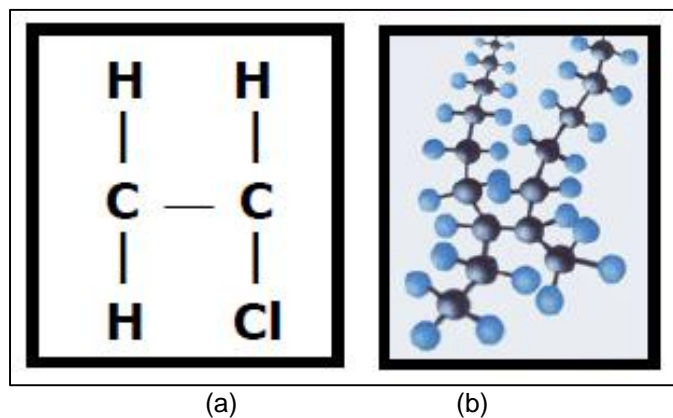


Figure 1-5 (a) Vinyl Chloride Molecule and (b) Molecular Chain in PVC (Rahman, 2004)

Although the production of PVC was completely halted, scientists continued to research PVC fibers. In Germany, the IG Ludwigshafen Laboratory developed the PVC polymerization process. Polymerization reduced the melting temperature of PVC without altering its flexible nature. These polymerizations led to yet another era in PVC development. During 1930's the market flourished with PVC products ranging from cable insulation to tooth brushes and eventually dominated the rubber industry. By the end of the 1930's PVC pipes were manufactured to convey water and other liquids. Table 1-2 illustrates the important milestones of PVC pipe in North America. The flexibility by which

PVC was incorporated into the daily lives of people led to its growing popularity (Meikle, 1995). The performance and cost-effectiveness resulted in PVC becoming the largest volume plastic pipe material in North America. In 2005, PVC sales exceeded \$9.83 billion in North America (Sewer History, 2016). Figure 1-6 illustrates the worldwide growth of the PVC pipe industry from 1970 to 2010 in terms of consumption in billions of lbs.

Table 1-2 Milestones of PVC Pipe in North America (Uni-Bell, 2015)

Year	Milestone
1935	PVC pipes were manufactured in Germany
1936	Installation of PVC pipes for water distribution system
1952	PVC pipe was introduced in U.S.
1955	First PVC pipe for water use was installed
1966	AWWA appointed a committee to study and report on the adaptability of plastic pipe for use in the water industry
1968	The AWWA Standards Committee on thermoplastic pressure pipe was established
1975	First edition of AWWA C900 Standard was published
1980	AWWA published Manual 23 - PVC pipe design and installation
1988	Publication of AWWA C905
1991	Publication of AWWA C901
1994	AWWA approves and publishes C605
1998	Publication of C909

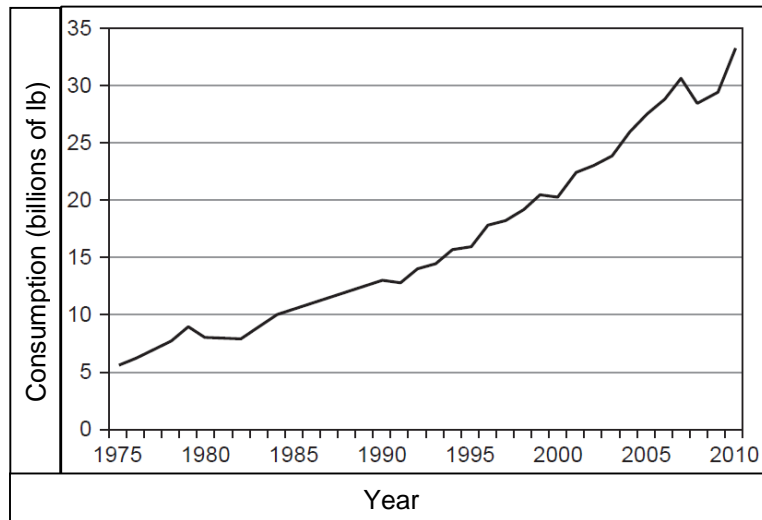


Figure 1-6 PVC Pipe and Fittings Worldwide Consumption (Uni-Bell, 2012)

1.4.2 Manufacturing of PVC Resins

Figure 1-7 illustrates the process used to make PVC at manufacturing plants. The plant consists of batch polymerization reactors, a blow-down vessel, and downstream processing equipment, which includes a stripper, decanters and a fluid bed dryer.

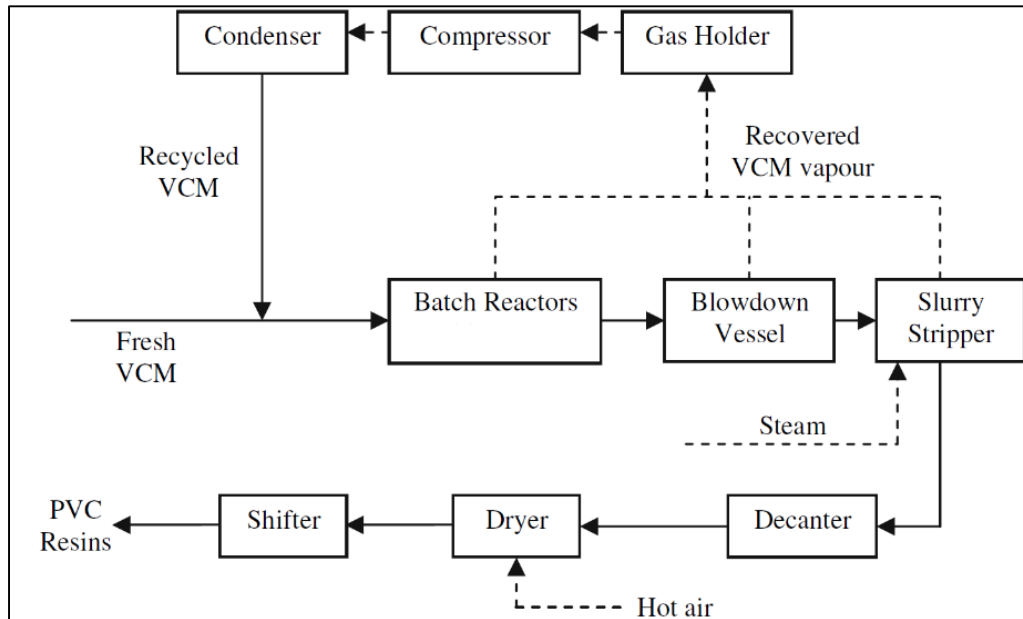


Figure 1-7 Process Flow Diagram for PVC Resin Manufacturing (Chan et al., 2007)

The raw materials used for the polymerization process are demineralized water, a mixture of fresh vinyl chloride monomer (VCM) and recycled VCM (received from blowdown vessel and stripper), initiators and suspending agents. The polymerization process takes place in the batch reactors. The demineralized water along with suspending agents are charged into the reactor followed by initiators. After completion of water charge, the reactor is purged with nitrogen to ensure no oxygen is present in the reactor. The nitrogen is removed from the reactor by vacuuming. After the VCM and water are added to the reactor, the optimum operating temperature and pressure are achieved. The exothermic polymerization process continues for 7.5 hours and the end product is a slurry

consisting mainly of PVC, water and some byproducts such as unreacted VCM, initiators, suspending agent and traces of contaminant (Chan et al., 2007).

The slurry is discharged intermittently from the reactors to the blowdown vessel, which further transfers the slurry to the downstream processing equipment. The blowdown vessel traps the unreacted VCM vapor and compresses it, condenses it into liquid form and sends it back to the reactors for polymerization. The effluent from the blowdown vessel enters the stripper to remove any remaining unreacted VCM from the slurry. Steam is introduced at the end of the stripper to remove the VCM vapors. The stripped slurry then reaches the decanters, which removes approximately 80% of the water from the slurry. Wet cakes are formed after removal of water. They are then dried and transported to the shifter. Fine resins that pass through the shifter are sold as a product and coarse resins sold as low-grade resins (Chan et al., 2007).

1.4.3 Types of PVC Pipe as per Manufacturing Process

PVC is manufactured by integrating PVC resin with stabilizers, pigments, lubricants, and additives and then heating this mixture to 400 °F. The heating causes the components to fuse properly and convert to a malleable state. Further, the material is mechanically extruded in its molten form. After the extrusion, the pipe is allowed to cool. Another method of manufacturing PVC pipe is injection molding. In this process, the molten polymerized polymer is forced into pipe molds and then water cooled (Rahman, 2004).

PVC can be heated and reshaped which is an important property in the beelling operation of the pipe. One end of the pipe is heated and placed in a beelling machine to form the bell end of the pipe along with a groove for a rubber ring. The bell end is then cooled to maintain the shape (Howard, 2015). There are three distinct types of PVC pipes available in worldwide markets: PVC (un-plasticized/ PVC-U, commonly called PVC), PVC-M (modified) and PVC-O (oriented) pipe.

1.4.3.1 PVC-U Pipe

PVC-U (un-plasticized) is also referred as uPVC in some parts of the world. It is referred as PVC in North America. PVC is the most widely used piping material in North America for water applications. The absence of plasticizers in this type of PVC makes it more rigid in nature. The molecules are arranged randomly in long chains and do not display any definite directional orientation. As per AWWA and ASTM standards, PVC pressure pipes must meet or exceed a tensile strength of 7,000 psi, modulus of elasticity of 400,000 psi and have a hydrostatic design basis of 4,000 as per ASTM D2837-13e1 (Najafi and Gokhale, 2005). PVC-U will be referred as PVC throughout this dissertation for simplicity.

1.4.3.2 PVC-O Pipe

Oriented PVC has been manufactured since 1974. PVC-O demonstrates superior performance qualities to standard PVC. The molecular orientation in PVC-O is achieved by increasing the diameter of the conventionally extruded pipe at elevated temperature and then cooling it rapidly. The orientation of molecules is in a circumferential (or hoop) direction along the length of the pipe, which increases the strength of the pipe in the circumferential direction (West and Truss, 2011).

Either inline or offline process is followed to manufacture PVC-O. A rigid small diameter thick-walled PVC pipe called the stock pipe is heated to temperatures between 175 °F to 250 °F in offline process. During the heating, the pipe transits into a rubbery flexible state and then the pipe is inflated within the mold. This process reorients the random molecules in the PVC to align parallel to circumferential direction. The inline process pulls the pipe over a conical die to expand the diameter during the extrusion process of the pipe. The expansion of the pipe reduces the thickness of the wall while increasing the diameter size and reorienting the molecules in circumferential direction. This

process is used in Europe and other parts of the world but is not used in U.S. (Chapman and Agren, 1998).

1.4.3.3 PVC-M Pipe

Modifying the PVC molecular weight and adding an additive (impact modifier) to PVC can yield dramatic changes in the processing characteristics and physical properties of PVC (Tseng et al., 1991). PVC-M is manufactured by adding 'impact modifiers' during the manufacturing process. The impact strength and flexibility of PVC is improved because of the additives. The impact modifiers are either elastomeric or rubbery in nature and have a lower modulus than the PVC. Acrylonitrile butadiene styrene (ABS) and chlorinated polyethylene (CPE) are the two most used impact modifiers to improve regular unplasticized PVC (Plastics Additives and Compounding, 2004). This pipe is mainly used in Europe and Australia. This pipe is not being used in U.S. for buried applications (Najafi and Gokhale, 2005).

1.4.4 *Types of Joints for PVC Pipe*

1.4.4.1 Gasketed Joint

A gasket is compressed between the bell end of one pipe and the spigot end of another pipe around the circumference of the pipe. The gasket acts as a seal to the joint. Gasketed joints are also known as push-on joints or compression joints. Gasketed joints are unrestrained joints because the joint allows movement of one pipe relative to another pipe. The bell end of the pipe faces the direction of laying pipe during installation so that the spigot end of the new pipe is inserted into the bell end of the pipe previously laid. An allowable leakage limit of 10.5 gallons per inch of diameter per mile per day for PVC pipe is mentioned in AWWA C900. Thrust blocks or restraining systems such as the Bulldog™ restraint system (BRS) explained later in this dissertation are necessary to resist the thrust force exerted by the fluid inside the pipe in pressure applications (Howard, 2015).

1.4.4.2 Heat Fused Joint

Heat-fused joints are used with polyethylene pipe and PVC pipe. Alternatively, heat fused joints are also called butt fusion joints. The ends of two pipes are heated and pressed together which forms a solid connection as illustrated in Figure 1-8. A skilled and knowledgeable person is required to execute a heat fused joint. After allowing the manufacturer's recommended minimum time to cool down the joint, the heat-fused joint will achieve a good joint (Howard, 2015).

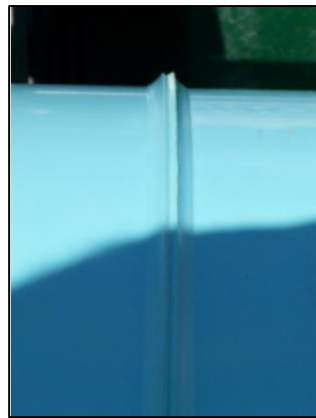


Figure 1-8 Heat Fused Joint Operation for PVC Pipe
(Underground Solutions, 2016)

1.4.5 Current Standards for PVC Pipes

The American Water Works Association (AWWA) has established standards for manufacturing, design, and installation of polyvinyl chloride pressure pipe, fittings and appurtenances for water and other liquids, including:

- AWWA C605 - Underground Installation of Polyvinyl Chloride (PVC) and Molecularly Oriented Polyvinyl Chloride (PVC-O) Pressure Pipe and Fittings
- AWWA C900 - Polyvinyl Chloride (PVC) Pressure Pipe and Fabricated Fittings, 4 in. through 12 in. (100 mm through 300 mm), for Water Transmission and Distribution
- AWWA C905 - Polyvinyl Chloride (PVC) Pressure Pipe and Fabricated Fittings, 14 in. through 48 in. (350 mm through 1,200 mm) for Water Transmission and Distribution
- AWWA C907 - Injection-Molded Polyvinyl Chloride (PVC) Pressure Fittings, 4 in. through 12 in. (100 mm through 300 mm), for Water, Wastewater, and Reclaimed Water Service,
- AWWA C909 - Molecularly Oriented Polyvinyl Chloride (PVCO) Pressure Pipe, 4 in. through 24 in. (100 mm through 600 mm) for Water, Wastewater, and Reclaimed Water Service
- Manual M23 - PVC Pipe - Design and Installation

1.4.6 *Characteristics of PVC Pipes*

1.4.6.1 Lightweight

PVC pipes (smaller diameter < 16 in.) are lightweight and hence are easy to transport and do not take much manpower for installation compared to other pipe materials. Less weight also means cheaper transport because the majority of transport companies charge by weight. This quality makes them not only safe for workers but reduces collateral damage to the actual site of operation. PVC Pipes offer a tremendous weight advantage over alternative piping materials (Think Pipes, Think PVC, 2016).

1.4.6.2 Strength and Flexibility

The ability of a PVC pipe to yield under loading without fracturing gives PVC a performance advantage. It has the ability to withstand soil force and torsion even in places where pressure exists. The modulus of elasticity of PVC reduces the magnitude of pressure surges (water hammer) in pressure applications and hence provides a major advantage for PVC pipes in buried applications (Vinyl Pipes, 2016).

1.4.6.3 Resistance to Corrosion

Corrosion costs more than \$36 billion in losses annually in water and sewer systems throughout U.S. Corrosion is the leading cause of water main breaks in North America with about 300,000 breaks per year. Almost 2.6 trillion gallons of drinking water is lost due to the leaking pipes annually (FHWA, 2002).

PVC pipe material is mostly made from hydrocarbons and some other stabilizers and hence it exhibits an inherent nature of plasticity. That is, unlike its metallic counterparts, it is a poor conductor of electricity. Hence, PVC material is naturally immune to reduction-oxidation reactions caused by acids, bases, and salts leading to corrosion that take place in conductor material such as that of iron or steel. Hence, PVC does not need expensive coatings or liners for protection from corrosion (Uni-Bell, 2012).

1.4.6.4 Resistance to Chemical

PVC pipe is resistant to notable chemicals at temperatures up to 140 °F. Barring a few industrial applications which may require evaluation of chemical resistance such as esters, ketones, ethers and aromatic or chlorinated hydrocarbons, PVC is resistant to most of the chemicals found or used in day-to-day activities. PVC is resistant to many alcohols, fats, oils, common corroding agents including inorganic acids, alkalis and salts. The chemical resistance of PVC also makes it a great protective liner material for other pipe materials (Vinidex, 2013).

1.4.6.5 Joint Tightness

Pipes made from PVC provide optimal and efficient water transport. This is because they provide unhindered joint tightness, thereby preventing water leakage. The types of joint are known as gasketed joints which perform well above standards compared to other pipe materials. The joints are also manageable and easy to fit due to PVC's flexibility (Uni-Bell, 2012). Gasket joints for PVC pressure pipes are designed to withstand 150% of working pressures after installation (Rahman, 2004). Gasket joints have a better record of being leak-free compared to other substitutes and a fusible type PVC has zero joint leakage if the joining process is executed as per specified standard procedure by a skilled labor (Najafi and Gokhale, 2005).

1.4.6.6 Flame-retardant and Insulation Properties

Unless an external ignition source is present, a PVC pipe will not ignite. The spontaneous ignition temperature for PVC is 850 °F. The material is also known to self-extinguish because after combustion takes place in it or near it, the resulting products combine with oxygen and retard the flame (Uni-Bell, 2012). Due to its non-metallic properties, PVC is considered a valuable thermal insulator, mainly in colder temperatures. Hence, PVC can be used as a coating reagent (Deeble, 1994).

1.4.6.7 Simplicity in Manufacturing Processes

As explained earlier, ethylene and chlorine are combined to form ethylene dichloride which forms a vinyl chloride monomer. Then, a polymerization step converts a monomer to a polymer known as polyvinyl chloride (Vinyl Institute, 2016). Because it is easily manufactured and transferred, the average cost for pipe production and disposability are significantly lower than those of other materials (Saeki and Emura, 2001).

1.4.6.8 Prevention from Oxidation

Initially it was determined that extremely high temperature can oxidize the PVC material and cause a reduction in its tensile strength. However, it was recently discovered that adding titanium oxide to the material can hinder the oxidation process and keep the material more durable for longer periods of time. The titanium oxide does so through the following mechanisms (Kim et al., 2008):

- a. The material competes for ultraviolet (UV) light which disallows direct PVC degradation.
- b. Scatters visible light which masks the loss of color and catalyzes surface photo-oxidation.

1.4.7 *Limitations of PVC Pipes*

While PVC is a popular material for pipe construction, it has its limitations. PVC is known to undergo thermal and photo-oxidative degradation. PVC is also prone to fractures due to environmental stress.

1.4.7.1 Photo-oxidative and Thermo-oxidative Degradation

PVC degradation can be classified into two different forms: photo-oxidative and thermo-oxidative. Photo-oxidative degradation occurs when the PVC pipe is exposed to extreme UV radiation from the sun. Thermo-oxidative degradation occurs when PVC pipe is exposed to extremely high temperatures for prolonged periods of time without providing proper protection. Even though the degradations are different in terms of how they are initiated, they undergo degradation due to similar, if not exact, chemical reactions (Burn et al., 2005).

Degradation of the material yields free radical formation which yields hydrochloric acid, and this acid secretion into the environment proves harmful to plants and ecosystem

growth. To prevent this degradation, heat stabilizers and inorganic fillers or UV-protective agents can be used during the manufacturing of PVC pipes (Burn et. al, 2005).

1.4.7.2 Hydrocarbon Compounds and their Effects on the PVC Pipe

PVC pipes are resistant to corrosion, but they are less resistant to certain hydrocarbon compounds. Factory emissions, improper disposal of chemicals and other such pollutants in the environment have created a serious threat to the functionality of PVC pipes. The contamination takes place in a three step process as shown in Figure 1-9:

1. Contaminant makes its way from the source to the soil in which the pipeline rests.
2. Contaminant then diffuses into the PVC pipe through the pipe wall.
3. Through the PVC pipe, contaminant enters the water/material that the PVC pipe carries.
4. If the water carried by the PVC pipe is contaminated, typically, the taste of the hydrocarbons can be detected by the consumer.

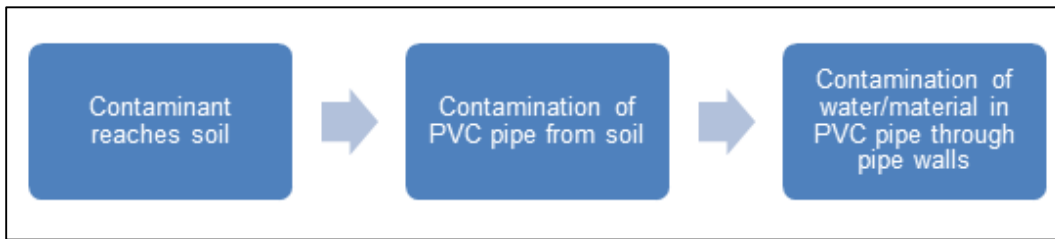


Figure 1-9 Process of Contamination in PVC Pipe
(Ong et al., 2008)

1.4.7.3 PVC Pipe Cracks

PVC pipes can crack during or after installation if they are improperly manufactured. The PVC material is made by melting and it is allowed to reform several times to strengthen individual crystallites into a strong polymer. Hence, hindering this process can alter its brittleness and make it more prone to cracks. Figure 1-10 shows a crack in a PVC pipe caused by stress due to high temperature processing during

manufacturing. PVC pipes undergo blown section failure, which begins initially with a longitudinal split as shown below in Figure 1-11 (Burn et. al, 2005).



Figure 1-10 Crack in PVC Pipe
(Burn et al., 2005)

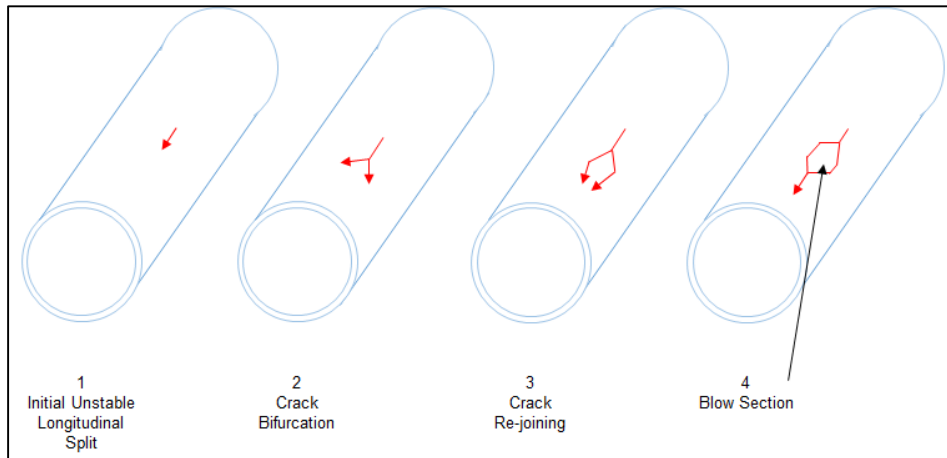


Figure 1-11 Failure Steps Leading to a Blown Section
(Adapted from: Burn et al., 2005)

1.4.7.4 Joint Failures in PVC Pipes

Two types of welded joints (heat fused and solvent cement) are used for connecting two sections of PVC pipes. Welded joints are mainly used in pipes with a

diameter of less than 24 in. Bell and spigot gasketed joints are mainly used in diameters greater than 24 in. Heat fused joints are made by increasing heat and pressure causing the melting of two pipe surfaces together (Rahman and Watkins, 2005). There are several restrained joint systems used to connect PVC pipes. They can be integrated into the pipe or be external parts usually made of ductile iron.

The bell and spigot joints are more common and can accommodate all diameters. The gaskets used for pipe joints are mostly made out of homogenous rubber or an elasticized sealing ring. Today, the current generation of pipe seals use a locked in gasket (Rieber joint). The gasket includes an embedded steel ring, which ensures pipe gasket stability and formidability. The joint is compressed between the spigot (which is at the distal end of a smaller pipe that fits into a bigger component of another pipe to make a pipe joint) and the bell to form a tight seal. Insertion into the spigot disables leakages along the pipe which is explained through Figure 1-12 (Balkaya et.al, 2012).

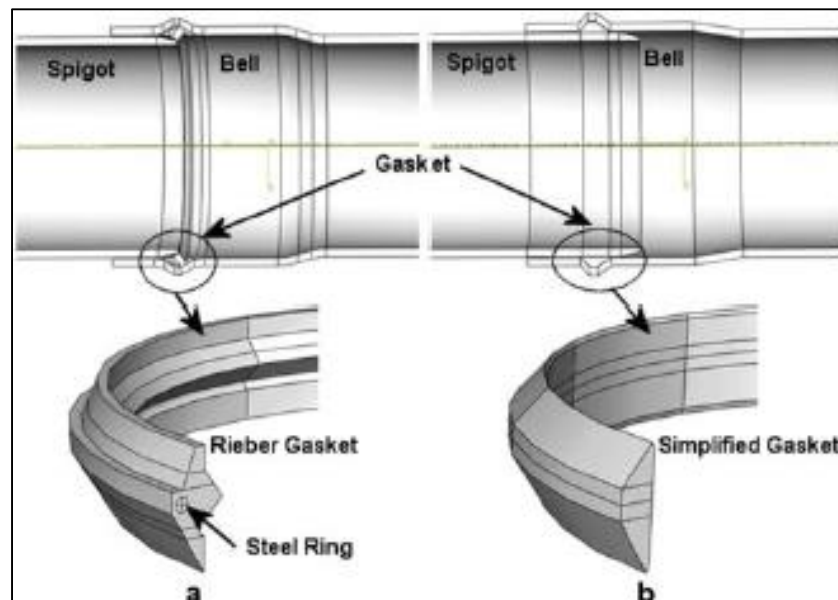


Figure 1-12 (a) New Rieber Type Gasket, and (b) Older Type of Gasket (Balkaya et al., 2013)

Pipe design is based on its ability to withstand the amount of internal fluid pressure as well as the pipe joint systems. If the pipe joint systems are installed incorrectly or contain damage, then fluid can leak out of the pipes resulting in serious repercussions.

Leakage often results as a result of improper installation of gaskets in pipe joints. In order for the pipe to function efficiently, the soil bedding level must be uniform around the joint. If the bedding is not uniform, it can cause pipe bending which can alter the joint tightness (Balkaya et al., 2012).

1.4.7.5 Effects of PVC Resin on Environment

According to Thornton (2002), release of excessive amounts of chlorine during the production and processing of PVC resin may damage the environment if proper disposal methods are not followed by the manufacturer. PVC resin manufacturers faced criticism from environmental groups for the chlorine emissions during manufacturing of PVC resin. Considering the criticism, the industry decided to improve factories' waste management systems. The Netherlands, for instance, improved recycling of PVC products with the goal of drastically reducing chlorine emissions. In other words, their aim was to recycle the damaged products and then reuse it to make new products. In addition to material recycling, burning and chemical recycling processes were also implemented to ensure a drastic reduction in PVC waste production (Mulder and Knot, 2001).

1.4.7.6 PVC Pipe Failure Case Studies

A case study in 2010 involving 16 in. and 24 in. PVC pipes in a service station at an undisclosed location determined various causes of the failures. Firstly, the pipe bedding was uneven leading to an improper installation process which ultimately put unbalanced pressure on the pipe exterior. The continuous pressure led to pipe fatigue which caused the pipe to ultimately fail. Figure 1-13 shows the improper bedding conditions which led to the PVC pipe malfunction (Lackey, 2010).



Figure 1-13 Failure of PVC Pipe due to Improper Bedding Conditions (Lackey, 2010)

According to Long (2012), PVC may undergo rapid crack propagation (RCP). RCP is a rapidly occurring fracture that can impact pipelines over a long distance. The cracks occur when PVC pipes respond to impact behaviors, acid soil surroundings or the inability of bell and spigot joints to attach to each other properly (Long, 2012).

1.4.8 *Installation Requirements for PVC Pipe*

Uni-Bell PVC Pipe Association has developed a guide for installation of PVC considering standards such as AWWA C900, AWWA C905, AWWA C907 and AWWA C909 as mentioned earlier. Figure 1-14 illustrates the various trench terms used during installation of pipe. It is imperative to have proper embedment materials to minimize trench settlement. A foundation might be necessary when the trench bottom is unstable. A bedding of 4 in. to 6 in. is recommended. The initial backfill is placed on the top of the crown for a height of 6 in. to 12 in. Final backfill is generally the material that was excavated originally but is specified by the project engineer based on site design (Uni-Bell, 2013).

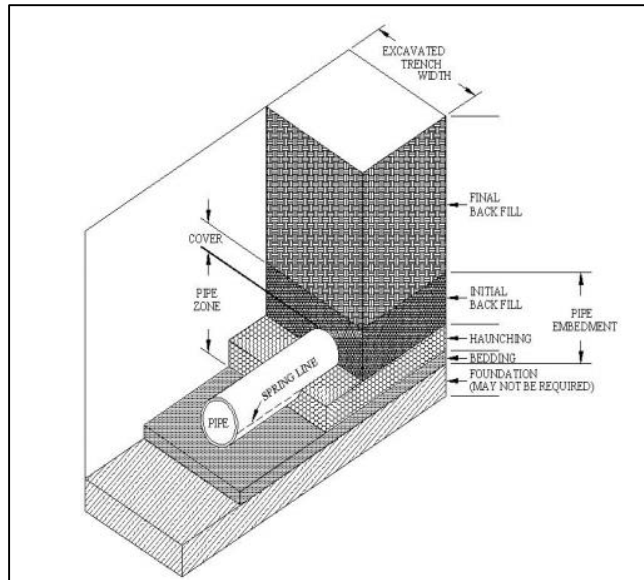


Figure 1-14 Terms used in Pipe Installation
(Uni-Bell, 2013)

The basic steps involved in installation of PVC pipe installation are summarized below:

1. Receiving of pipe
2. Unloading and handling of pipe
3. Storage
4. Trenching
5. Dewatering trench
6. Field cutting of PVC pipe if necessary
7. Lowering of pipe into trench
8. Cleaning and inspection of pipe
9. Lubrication of spigot end
10. Joint assembly
11. Installation of fitting and valves
12. Tracer wire for locating pipe in future

1.4.9 Introduction to iPVC Pipe

American Water, Voorhees, NJ, was approached by Pyungwha Plastic Industry System Inc. (hereafter PPI), a leading PVC pipe manufacturer from South Korea with its possible PVC pipe product. The product is known as iPVC pipe and is available in 4, 6, 8, 10, 12, 16, and 24 in. diameter size and with dimension ratios of DR 14, DR 18 and DR 25.

Currently, iPVC pipe is manufactured in South Korea (operating out of three plants in South Korea and one plant in China) and marketed in Japan, China and South Korea. The iPVC pipe is manufactured using the extrusion process. The high strength resin is produced by mixing raw material in different proportions along with additives during the polymerization process. Figure 1-15 illustrates the molecular structure snapshot of a regular PVC (C900) and iPVC pipe from scanning electron microscope (SEM).

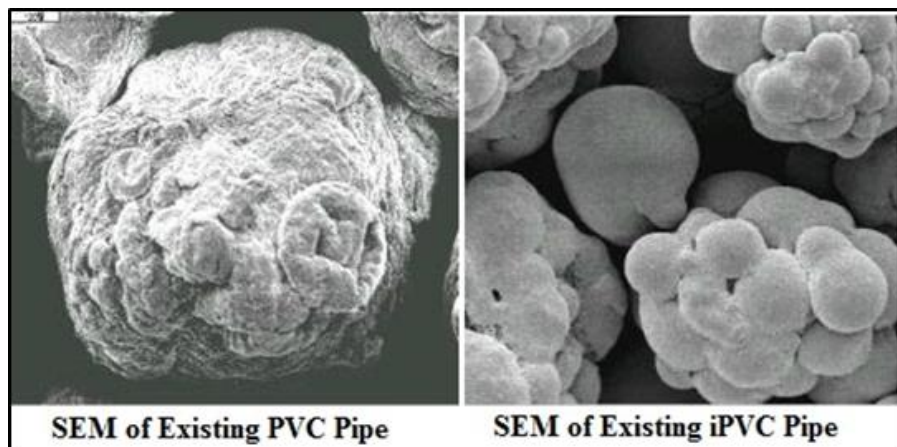


Figure 1-15 PVC and iPVC pipe Structure under SEM
(Source: AW and PPI, 2015)

1.5 Introduction to iPVC Pipe Project

The iPVC pipe evaluation project was a tailored collaboration between Water Research Foundation and American Water. American Water elected to evaluate the capability of the iPVC pipe and pursued and secured funding from the Water Research

Foundation to support testing by CUIRE at the University of Texas at Arlington, Arlington, TX and Microbac Laboratories, Denver, CO. The performance evaluation in the field was conducted by installing the iPVC pipe by American Water in St Louis County, Missouri. This dissertation is part of this research project.

1.6 Research Needs

The innovative iPVC pipe offers some unique strength features. iPVC pipe is expected to provide an alternative to the current pipe materials available for water applications. The engineering properties and strength characteristics of iPVC pipe are expected to exceed the AWWA standards requirements set for PVC pipes. There is a significant gap in the awareness of water utilities about this PVC alternative. This research is needed to introduce iPVC pipe to U.S. water utilities.

1.7 Research Objectives

The main objectives of this dissertation parallels the goal of the research project with Water Research Foundation to evaluate a new structurally enhanced iPVC pipe for water applications. Specifically, this dissertation will evaluate the following properties to further develop and market iPVC pipe:

- Engineering properties
- Strength characteristics
- Behavior of iPVC pipe installation in native clayey soils
- Comparison of iPVC pipe with conventional PVC, ductile iron and HDPE pipe materials

1.8 Research Methodology

As stated previously, this project was funded by the Water Research Foundation and American Water. This dissertation research is a subpart of the iPVC pipe research project. The tasks accomplished under this project include a complete assessment of

tensile performance, pipeline bedding needs, fatigue resistance, impact resistance, pipe stiffness and short-term burst pressure test on the iPVC pipe to evaluate performance characteristics of iPVC pipe. The impact tests, stiffness tests, and tensile tests were performed by Microbac. CUIRE performed the bedding test in the field, fatigue test, tensile test and the hydrostatic short-term burst pressure test. The installation of iPVC pipe was performed by Missouri American Water in St. Louis County. As a part of the research project, iPVC pipe was analyzed based on the test results and further compared to other available competitive pipe materials. Conclusions and recommendations are presented at the end of this dissertation report along with recommendations for future research. Figure 1-16 presents a methodology flow chart for this iPVC pipe project. The testing conducted at CUIRE along with the analysis in Chapter 5 for all the tests is the focus of this dissertation.

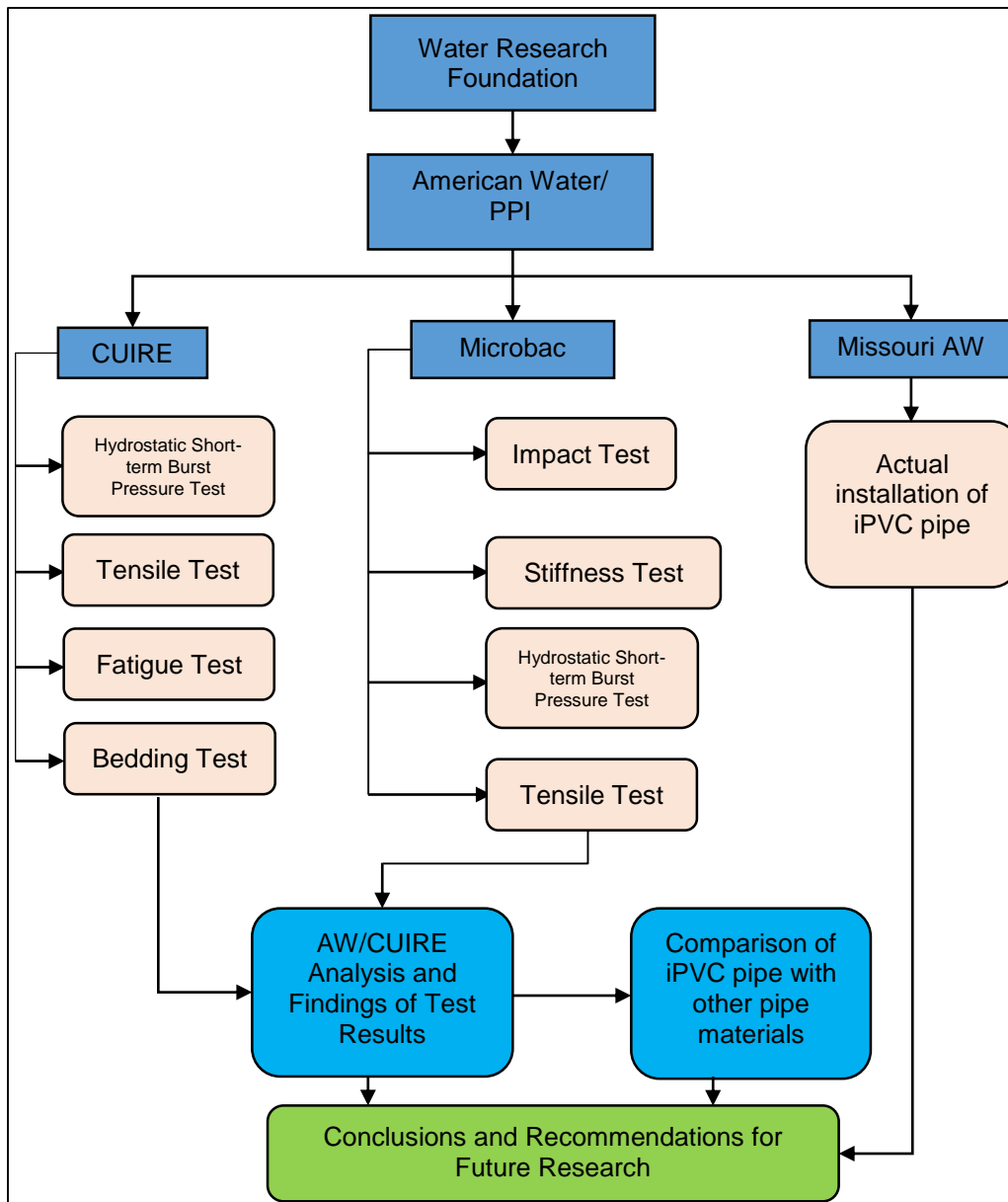


Figure 1-16 Project Methodology Overview
 (Source: Adapted from WRF Report No. 4650, 2016)

1.9 Expected Outcome

The expected outcome of this dissertation is to establish a new PVC product for water application which is expected to be more sustainable and efficient in installation

compared to other similar pipe materials. The testing carried out in this dissertation study provides analysis and test results on iPVC pipe material characteristics.

1.10 Dissertation Organization

Chapter 1 presents an overall idea of the whole research. It contains the history of pipelines, classification of pipes, types of pipe materials, introduction to polyvinyl chloride (PVC), advantages and limitations of PVC, introduction to iPVC pipe, research needs and objectives, methodology and expected outcome of this dissertation. Chapter 2 provides a literature review on PVC pipe, previous tests conducted on iPVC pipe and case studies discussing performance of PVC pipes. Chapter 3 explains the methodology used for this dissertation in detail by outlining a step by step description of the research performed. Chapter 4 outlines results of the research. Chapter 5 analyzes the results achieved in this dissertation. Chapter 6 draws conclusions and offers recommendations for further study. Appendices and references are provided at the end of this dissertation.

1.11 Chapter Summary

This chapter discussed the history of pipelines, types of pipe materials followed by an introduction to PVC pipe. Development of PVC resin, types of PVC pipes, types of joints used for PVC pipes, current standards for PVC pipes, characteristics and limitations of PVC pipes and an introduction to iPVC pipe were presented. Additionally, this chapter reviewed the research needs and objectives, methodology and expected outcome of this dissertation.

Chapter 2

Literature Review

2.1 Introduction

Chapter 1 discussed the history of pipeline and introduced different types of pipe material available in the market, followed by introduction to PVC resin and pipe, iPVC pipe project, research needs and objectives, methodology and expected outcome of this dissertation. This chapter consists of a detailed review of findings from an extensive literature search. The literature search was used as one of the tools to understand more about PVC behavior and the behavior of other pipe materials for different experimental tests. The subjects covered in this chapter include previous experimental studies conducted on pipe materials and their results, as well as previous testing conducted on iPVC pipe.

2.2 Hydrostatic Short-term Burst Pressure Test

This test method was used to determine the resistance of pipe material to hydraulic pressure in a short period of time. The standard used for this testing was the ASTM D1599-14 "Standard Test Method for Resistance to Short-Time Hydraulic Pressure of Plastic Pipe, Tubing, and Fittings." This test method could be used to establish laboratory testing requirements for quality control purposes or for procurement specifications in future iPVC pipe projects.

Bai and Bai (2014) conducted a study to analyze the burst strength of reinforced thermoplastic pipe (RTP) as the use of RTP is increasing due to its cost effectiveness, corrosion resistance and ease of installation. RTP consists of one polyethylene liner, two layers of reinforced tape overwrapping the liner, and one outer polyethylene coating as illustrated in Figure 2-1. The inner liner pipe and outer coating pipe are made of HDPE.

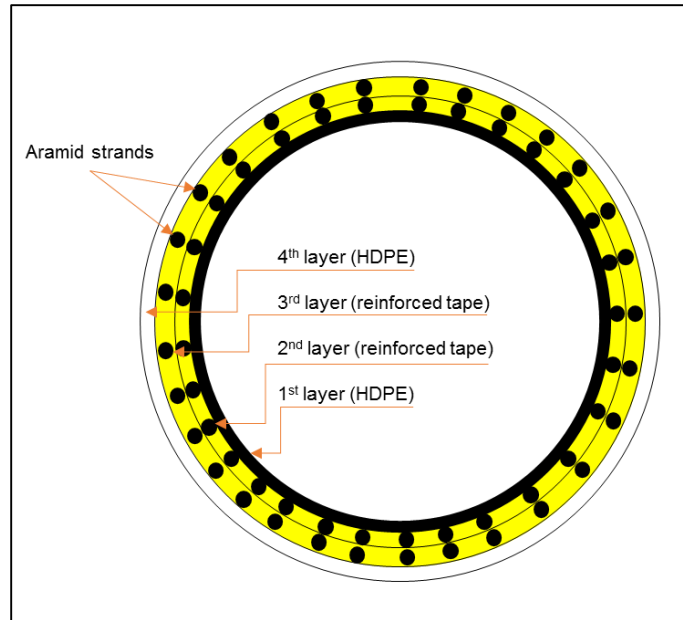


Figure 2-1 Cross-section of RTP
(Adapted from: Bai and Bai, 2014)

In this study, RTP was considered a thick cylinder, and the stress distribution was characterized as a generalized plane strain. An assumption of uniform stresses through the thickness of the two layers was made to simplify the analysis. It was assumed that the strains in the reinforcing layers are equal to the strains in the isotropic material. The fiber failure and the matrix failure, the two failure modes used as the failure criterion, were used to determine the failure pressure of RTP. A 3D finite element RTP model was established to evaluate the relationship between the mechanical properties and the final failure pressure. The failure pressure was calculated using both the finite element method and the theoretical method so the methods could be compared based on the experimental burst pressure of RTP.

Burst tests were carried out according to the ASTM D1599-14 procedure A. A short-time loading process was applied, such that the time to failure for all the specimens was between 60 and 70 seconds. The RTP samples used were 30 in. long and terminated

by steel swage fittings. The pressure applied to the internal pressure of RTP was increased uniformly and continuously until the specimen failed. The experimental temperature was controlled at 73–75 °F. A total of five specimens were tested and the observed burst pressures are summarized in Table 2-1.

Table 2-1 Measured Burst Pressure of RTP Samples
(Bai and Bai, 2014)

Specimen No.	Time to Failure (min)	Burst Pressure (psi)
1	31	5,366
2	30	5,395
3	28	4,670
4	31	4,858
5	27	5,351
Average	-	5,128
Standard Deviation	-	303

The calculated values from analytical and finite element analyses were in agreement at low pressures but the values started to deviate from each other as the internal pressure in RTP increased. The authors believe that the reason for the deviations could be due to the assumptions used in analytical analysis, and different boundary conditions in the finite element analyses. The burst pressure from the finite element analyses was 6,062 psi whereas that from the analytical analysis was 6,483 psi.

Law and Bowie (2007) conducted a study on a high yield-to-tensile strength ratio linepipe. This study predicted the failure pressures for a number of burst tests to explore the performance of high yield-to-tensile strength ratios for linepipe. Twenty-three methods for predicting the burst pressure were compared and the best method was documented as per the results. This study was performed in Australia.

Twenty equations and two other methods were used to predict the burst pressure. Figure 2-2 illustrates the equations used as well as the nomenclature for the prediction of burst pressure test.

ASME [1]	$P_{\max} = \sigma_{\text{TS}} \left(\frac{k-1}{0.6k+0.4} \right)$	Marin [2]	$P_{\max} = \frac{2}{\sqrt{3}} \frac{\sigma_{\text{TS}}}{(1+\epsilon_u)} \ln(k)$
Barlow OD, ID, or flow,	$P_{\max} = \sigma_{\text{TS}} \frac{2t}{D_o}, \sigma_{\text{TS}} \frac{2t}{D_i}, \text{ or } \sigma_{\text{flow}} \frac{2t}{D_i}$	Marin (3) [3]	$P_{\max} = \frac{2t}{(\sqrt{3})^{(n+1)}} \frac{\sigma_{\text{TS}}}{R_i}$
Bailey-Nadai [4]	$P_{\max} = \frac{\sigma_{\text{TS}}}{2n} \left(1 - \frac{1}{k^{2n}} \right)$	Max. shear stress [5]	$P_{\max} = 2\sigma_{\text{TS}} \left(\frac{k-1}{k+1} \right)$
Bohm [6]	$P_{\max} = \sigma_{\text{TS}} \left(\frac{0.25}{0.227+\epsilon_u} \right) \left(\frac{e}{\epsilon_u} \right)^{\epsilon_u} \frac{2t}{D_i} \left(1 - \frac{t}{D_i} \right)$	Nadai [7]	$P_{\max} = \frac{2}{\sqrt{3}} \sigma_{\text{TS}} \ln(k)$
DNV [8]	$P_{\max} = \sigma_{\text{Flow}} \frac{2t}{D_{\text{ave}}}$	Nadai [9]	$P_{\max} = \frac{\sigma_{\text{TS}}}{\sqrt{3}n} \left(1 - \frac{1}{k^{2n}} \right)$
Faupel [10]	$P_{\max} = \frac{2}{\sqrt{3}} \sigma_{\text{YS}} (2 - YT) \ln(k)$	Soderberg [11]	$P_{\max} = \frac{4}{\sqrt{3}} \sigma_{\text{TS}} \left(\frac{k-1}{k+1} \right)$
Fletcher [12]	$P_{\max} = \frac{2t\sigma_{\text{flow}}}{D_i(1-\epsilon_u/2)}$	Svenson [13]	$P_{\max} = \sigma_{\text{TS}} \left(\frac{0.25}{0.227+\epsilon_u} \right) \left(\frac{e}{\epsilon_u} \right)^{\epsilon_u} \ln(k)$
Margetson [14]	$P_{\max} = \frac{4t}{D_i\sqrt{3}} \sigma_{\text{YS}} \exp \left(-2\epsilon_u \frac{(1+\nu_{\text{secant}})}{\sqrt{3}} \right)$	Turner [15]	$P_{\max} = \sigma_{\text{TS}} \ln(k)$
Marin [16]	$P_{\max} = 2.31(0.577)^n \frac{\sigma_{\text{TS}}}{D_i}$	Zhu and Leis [17]	$P_{\max} = \left(\frac{2+\sqrt{3}}{4\sqrt{3}} \right)^{(1+0.239(1/YT)-1)^{0.596}} \frac{4t\sigma_{\text{TS}}}{D_{\text{ave}}}$
Nomenclature		<ul style="list-style-type: none"> n strain hardening exponent, $n = \exp(1 + \epsilon_u)$ R_o, R_i outer radius, inner radius $\sigma_{\text{YS}}, \sigma_{\text{flow}}, \sigma_{\text{TS}}$ yield, flow, and tensile strength ν Poisson's ratio ν_{secant} failure secant Poisson's ratio = $0.5 - (0.5 - \nu)$ YT $\sigma_{\text{TS}}/(\epsilon_u E)$ YT yield-to-tensile ratio 	
$D, D_i, D_o, D_{\text{ave}}$	diameter, inner, outer, average		
t	wall thickness		
e	2.718, etc.		
E	Young's modulus		
ϵ_u	uniform strain		
k	R_o/R_i		

Figure 2-2 Equations for Predicting Burst Pressure
(Law and Bowie, 2007)

The burst test specimen was made by welding endcaps to the pipe. The testing results as well as the predicted results are illustrated in Figure 2-3. Figure 2-3 presents the values of predicted burst pressure for linepipe calculated using the equations in Figure 2-2. The equations which predicted the burst pressure closer to the burst pressure obtained by actual testing were CIS-full, Fletcher, Bohm, and Bailey-Nadai, Barlow ID, ASME, and the maximum shear stress equations. The results verify that the actual material property variations cannot be fully quantified. The results show a rapid reduction in failure strain with yield-to-tensile ratio (Y/T). Although the average strain values at failure are low, all pipes burst at high pressure (28% higher than specified minimum yield strength, and 8% higher than actual yield strength).

	X42 ex-mill	X65 aged	X70 aged	X80 ex-mill	X80 aged
Test result	15.75	36.33	30.53	27.44	27.8
ASME	17.23	35.19	31.06	27.38	26.88
Barlow OD	16.98	34.45	30.52	26.96	26.46
Barlow ID	17.61	36.35	31.91	28.04	27.53
Barlow flow	14.81	34.29	30.48	25.95	26.64
Bayley–Nadai	17.19	35.26	31.14	27.40	26.94
Bohm	16.28	36.02	32.72	28.29	28.24
CIS-full	16.38	37.76	31.75	29.39	29.53
CIS-A	16.45	37.76	32.06	29.92	29.98
CIS-B	16.53	38.15	32.14	29.85	29.86
DNV	14.54	33.37	29.80	25.44	26.12
Faupel	17.94	40.33	35.74	31.04	31.04
Fletcher	16.58	35.87	31.40	27.20	27.59
Margetson	14.05	36.06	33.32	27.63	28.23
Marin	12.23	34.07	31.29	25.23	27.86
Marin(2)	16.45	37.55	34.04	29.07	29.15
Marin(3)	18.62	40.53	35.94	30.85	30.97
Max shear	17.29	35.38	31.20	27.49	26.99
Nadai	19.97	40.86	36.03	31.74	31.16
Nadai(2)	19.85	40.72	35.96	31.63	31.11
Soderberg	19.96	40.85	36.03	31.74	31.16
Svensson	16.89	37.98	34.20	29.42	29.37
Turner	17.29	35.38	31.21	27.49	26.99
Zhu–Leis	13.88	33.27	29.92	25.13	26.47

Figure 2-3 Burst Pressure Results and Predictions in MPa
(Law and Bowie, 2007)

Netto et al. (2005) studied the effect of corrosion on the burst pressure of pipelines. The corrosion of pipelines could lead to a reduction in the structural integrity and eventually cause the pipe to fail. The failure could lead to economic consequences such as reduced operating pressure, loss of production due to downtime, repairs, or replacement which can be severe and, in some cases, not affordable. This study examines the effects of corrosion defects through a nonlinear numerical model based on the finite element method. This study investigates the factors governing the behavior of corroded pipelines subject to internal pressure through combined experimental and numerical efforts. The model determined the burst pressure as a function of material and geometric parameters of different pipes and defects.

The residual strength of pipelines with single longitudinal corrosion defects was evaluated initially by performing a series of small-scale experiments. A total of seven small-scale steel specimens were tested. One specimen was without any damage and the other six had induced defects. Table 2-2 presents the burst pressure results for the tested specimens. Figure 2-4 illustrates the test specimen after the burst test.

Table 2-2 Burst Pressure Results for Small-scale Steel Specimens
(Adapted from: Netto et al. 2005)

Specimen	Burst Pressure (psi)
1 (Intact Specimen)	8,310
2	5,370
3	6,475
4	4,710
5	5,990
6	3,880
7	5,010

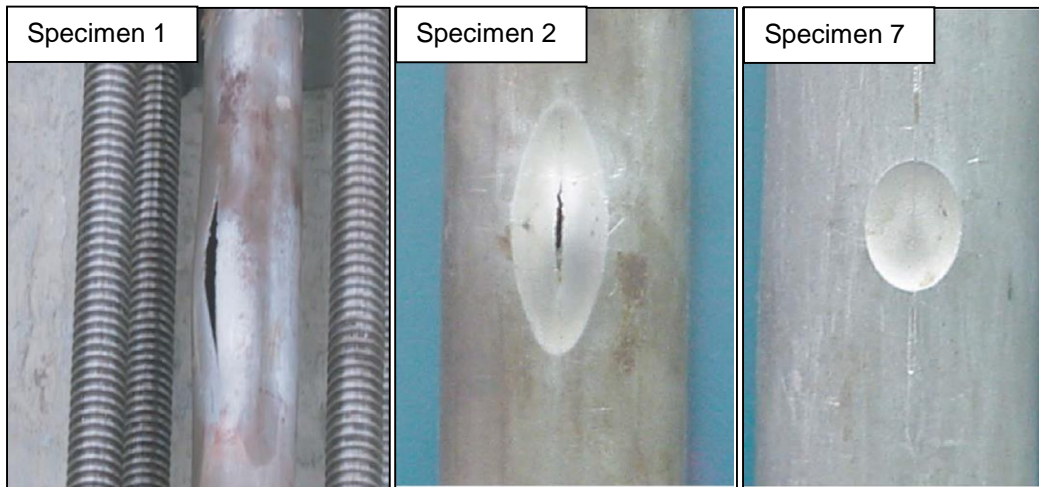


Figure 2-4 Test Specimens after Burst Test
(Netto et al. 2005)

A three-dimensional nonlinear finite element model was developed to predict the burst pressure of intact and corroded pipes. The model was first validated by reproducing numerically the physical experiments performed and was subsequently used to carry out an extensive parametric study. The predicted burst pressures set the finite element (FE)

model values lower than the experimental values because the depth of the defect simulated in the FE model led to lower burst pressure values. More material was removed from the pipe in the FE analysis as compared to the actual defects induced on the test specimens. The data set was then reduced to a simple curve that related the main geometric parameters of the pipe and defect to its residual pressure capacity. A comparison of codes currently used in practice was made with both experimental and numerical results.

2.3 Impact Test

This test is to evaluate the impact resistance of thermoplastic pipe and fittings under specified conditions of impact by means of a tup (falling weight). The impact resistance of thermoplastic pipe and fittings is related to the suitability for service and to the quality of processing. Impact resistance may also provide a relative measure of a material's resistance to breakage during handling and installation and, for non-buried applications, to in-service breakage. The standard used for this testing is the ASTM D2444-99 "Standard Test Method for Determination of the Impact Resistance of Thermoplastic Pipe and Fittings by Means of a Tup (Falling Weight)." Following are a few case studies for previous impact testing conducted on pipes:

Gabet et al. (2011) conducted a small and full scale testing of flexible pipe in an Arctic environment where oil and gas has been transported through flexible pipes for more than 30 years. The use of flexible pipes needs to be evaluated at colder temperatures as the Arctic regions are emerging as significant oil and gas provinces, and the different regions' options are continuously being explored. This study reviews the technical challenges of the Arctic environment, dealing with the suitability of flexible pipe materials in cold environment. This study describes the small and full scale tests performed by a company Flexi France/Technip in France.

The tests performed in this study analyzed the potential brittle behavior of some materials at low temperatures. Mechanical tests have been performed at a laboratory scale down to $-76\text{ }^{\circ}\text{F}$. Test Results on polymers and carbon steels (wires and forgings) were obtained via several tests such as impact, tensile, and fatigue tests as well as defects propagation and other tests.

The impact test was performed as per ASTM D2444-99 on 3 in. polymer tubes to determine the low temperature impact properties of the polymer material. An 11 lb spherical tup was dropped from a height of 16 ft with an impact energy of 176 foot-pounds. Figure 2-5 presents the experimental setup used in this test. The polymer tubes successfully passed the impact test at $-58\text{ }^{\circ}\text{F}$ without any failure on the 20 tubes that were tested.



Figure 2-5 Small Scale Impact Test Setup
(Gabet et al. 2011)

A full scale impact test was also performed on flexible pipes. The experimental setup is presented in Figure 2-6. A hammer of a given weight, positioned at the end of an arm of a given length drops at a given angle that varies between 14.7° and 33.6° , depending on the desired impact energy (between 1,475 foot-pounds and 7,375 foot-

pounds). The plain steel bar of 4 in. diameter located on the front face of the hammer then strikes the flexible pipes maintained in front of it. Visual observations are then made to determine if the external sheath is broken or not. The structures were kept at -85°F for at least 24 hours before the test was performed.

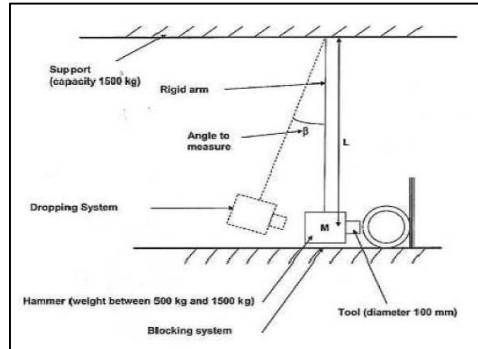


Figure 2-6 Full Scale Impact Test Setup
(Gabet et al. 2011)

Two flexible pipes were tested in the full scale setup. The first pipe had an inner diameter of 2.5 in., and the body was made of austenitic stainless steel. The pressure sheath was made of Polyamide 1 (PA1), the armor wires were made of medium strength (MS) wires and the external sheath is a polyethylene (PE) one. The other pipe had an inner diameter of 4 in., and the body was made of austenitic stainless steel with a pressure sheath of Polyamide 1 (PA1). The armor wires are High Strength (HS) wires and the external sheath is a Polyamide 2 (PA2). The pipes were tested at 1,475 foot-pounds and 3,680 foot-pounds impact energy successfully and had no failure of the sheath.

2.4 Stiffness Test

Plastic pipe stiffness is the measurement of the load capacity of the pipe itself subjected to loading conditions. Pipe stiffness is a function of the material type and the geometry of the pipe wall. Plastic pipe stiffness can be determined using the ASTM D2412-11 “Standard Test Method for Determination of External Loading Characteristics of Plastic Pipe by Parallel-Plate Loading” test shown in Figure 2-7. The pipe stiffness (PS) is defined as the ratio of applied force (F) in pounds per linear inch over the measured change of pipe inside diameter (Δy). Pipe stiffness can also be defined as the slope of the load-deflection diagram. The stiffness factor (SF), which is the value of the pipe modulus multiplied by moment of inertia is defined as shown in Equation 2.1 (ASTM D2412-11). The pipe stiffness at 5% vertical deflection, i.e., the change in vertical pipe diameter divided by the original pipe diameter, is typically used as the design value of stiffness. This represents the secant pipe stiffness at 5% deflection. ASTM D2412-11 stated that the stiffness of pipes with larger sizes made from relatively low modulus material may be affected by creep due to the time taken to reach the 5% deflection. Both pipe stiffness and stiffness factor are highly dependent on the degree of deflection. Plastic pipe stiffness is strain rate and time dependent.

$$SF = EI = (0.0186) \frac{F}{\Delta y} D^3 \dots \text{Eq. 2.1}$$

where,

E = Flexural modulus of elasticity (psi)

I = Moment of inertia

D = Mean diameter (in.)

F = Load applied to the pipe ring (lbs-in.)

Δy = Measured change in inside diameter in the direction of applied load (in.)

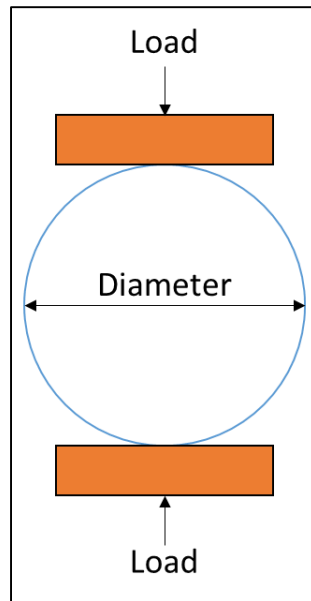


Figure 2-7 Parallel Plate Load Test

Schluter and Shade (1999) reported the parallel plate tests performed at three different loading rates using PVC and HDPE pipes. These rates were 0.05 in./min, 0.5 in./min, and 5 in./min. Changing the loading rate by a factor of 100 resulted in a 6.5% stiffness change in PVC pipes and 56% in HDPE pipes. This study stated that the ASTM D2412-11 deflection rate of 0.5 in./min does not relate to the real-world deflection rate and that a deflection rate of 0.05 in./min is more realistic. It was concluded that both laboratory measurements and theoretical calculations of ASTM D2412-11 are too simplistic and that the deflection rate effect on PVC pipes is minor but has a great influence on HDPE stiffness.

Another study by Sargand et al. (1998) tested and evaluated PVC and HDPE pipes using a variable rate parallel plate test at two different rates of 0.5 in./min and 0.05 in./min. Figures 2-8 and 2-9 show the load per unit length (lb/in.) versus the vertical deflection percent results of variable loading rate parallel plate tests performed on 18 in. PVC and HDPE pipes, respectively. The pipe stiffness calculated using Equation 2.1 is summarized

in Table 2-3. These results showed that the loading rate has little effect on the PVC pipe stiffness, while HDPE material is more sensitive to the loading rate. The reduction of pipe stiffness was 3% to 6% for PVC and 25% for HDPE pipes. This study results clearly show that special treatment needs to be considered when dealing with HDPE pipe properties.

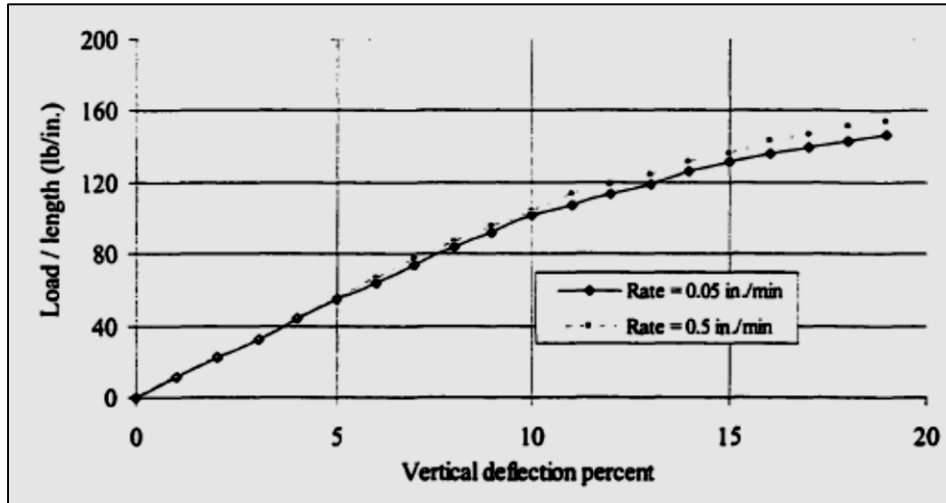


Figure 2-8 Parallel Plate Test for 18 in. PVC Pipe (Sargand et al., 1998)

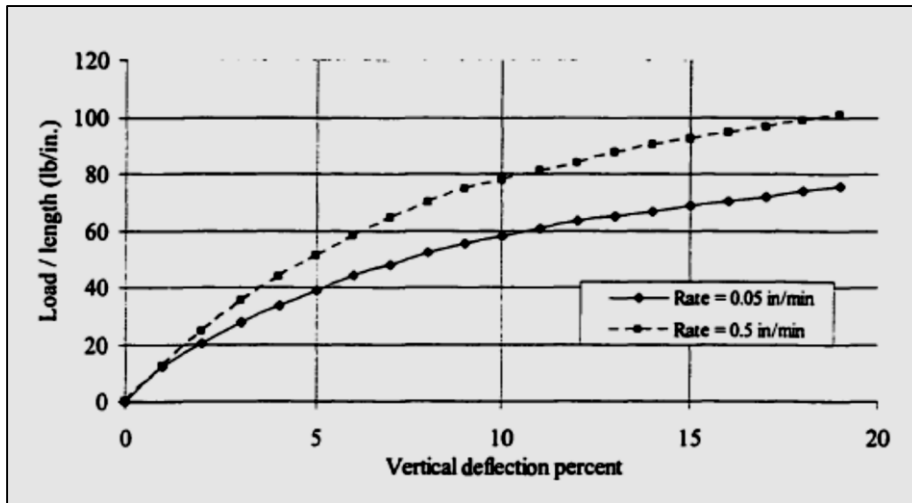


Figure 2-9 Parallel Plate Test for 18 in. HDPE Pipe (Sargand et al., 1998)

Table 2-3 Pipe Stiffness of Parallel Plate Test at Two Different Loading Rates
 (Adapted from: Sargand et al., 1998)

Pipe Material	Loading Rate (in./min)	Pipe Stiffness (lb/in.) at Percent Deflection			
		5%	10%	15%	19%
PVC	0.5	62	57.9	50.8	45
	0.05	60.5	55.6	48.4	42.5
HDPE	0.5	56.2	44.8	34.7	23.9
	0.05	42.5	33.2	25.9	22.3

The authors studied the stress relaxation of PVC and HDPE pipes using the parallel plate test. A variable load was applied over a period of one hour to maintain three different vertical deflection percentages of 5%, 10%, and 15%. Figure 2-10 illustrates the stress relaxation results for PVC pipes, while Figure 2-11 illustrates the stress relaxation of HDPE pipes. The time was extrapolated to estimate the pipe stiffness at 50 years. The percent reduction in stiffness was dependent on the percent deflection for PVC pipes with a range of percent reduction between 12% and 32%. The percent reduction in pipe stiffness is greater for HDPE pipes but it is less dependent upon the vertical deflection percent. The percent reduction in stiffness for HDPE pipes was between 75% and 82%. Table 2-4 summarizes the results of both tests.

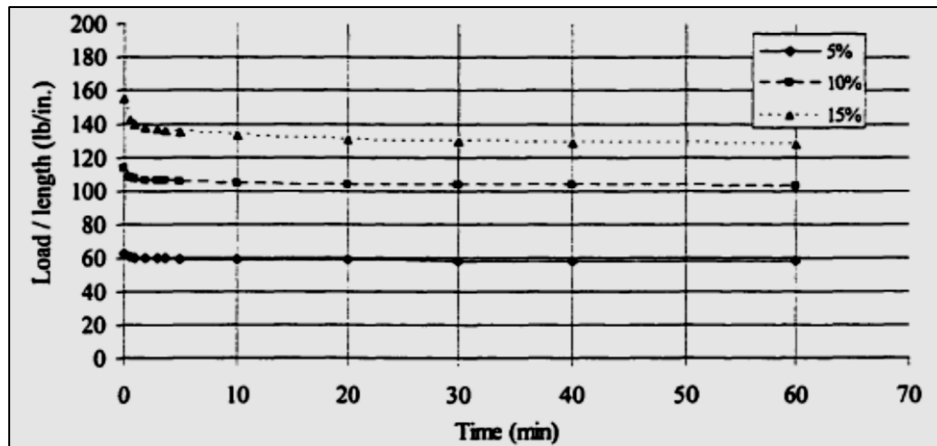


Figure 2-10 Stress Relaxation of PVC Pipe
 (Sargand et al., 1998)

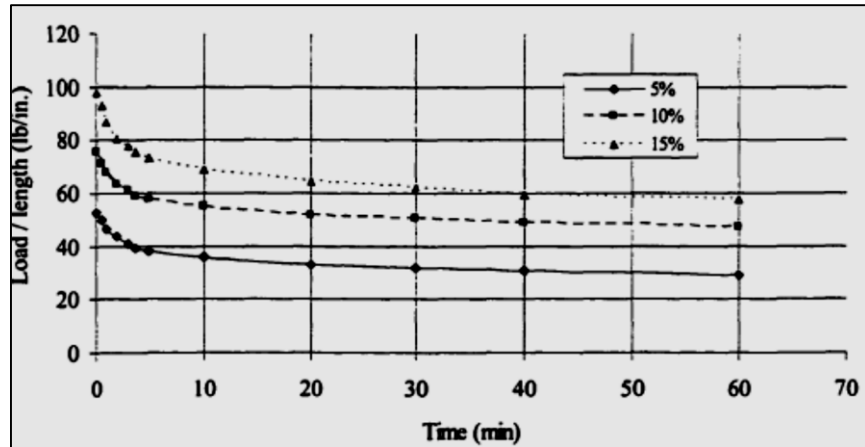


Figure 2-11 Stress Relaxation of HDPE Pipe
(Sargand et al., 1998)

Table 2-4 Pipe Stiffness Results of Stress Relaxation Tests
(Adapted from: Sargand et al., 1998)

Pipe Material	Time	Pipe Stiffness (lb/in.) at Percent Deflection		
		5%	10%	15%
PVC	1 min	60.3	107.7	140.6
	50 years	52.6	88.7	95.7
HDPE	1 min	46.8	67	88.1
	50 years	8.4	16.3	16.2

2.5 Tensile Test

Tensile tests are conducted to study the tensile strength of materials. This test used dumbbell shaped test specimens mentioned in ASTM D638-14. It is important to maintain the conditions of the sample before and during the testing. The temperature, humidity, and testing machine speed must be maintained as well. The data obtained from this testing could be used for qualitative characterization and for research and product development.

A study by Bazoune (2012) evaluated the effect of dry heat on tensile properties of chlorinated PVC pipe (CPVC). CPVC pipes are used extensively for water supply pipes, wastewater, and gas distribution. Their quick installation, durability and strength, heat resistance and flexibility for welding and bending make CPVC a popular choice amongst

utilities. Its utilization in harsh environmental conditions requires an understanding of how weather affects its mechanical properties. This study documents the effect of dry heat on the tensile properties of CPVC under artificial weathering procedures. CPVC specimens were prepared according to ASTM D638-14 and exposed to accelerated dry heat temperature to simulate natural weathering effects of long-term outdoor exposure.

Tests were performed at two different temperatures, 104 °F and 158 °F, for a duration of up to 3,000 hours. Stress-strain curves were plotted and weathering effects on the tensile strength, modulus of elasticity and strain at fracture were obtained. Test results show that the ultimate tensile stress and the fracture stress exhibited a slight increase over the period of the exposure. The modulus of elasticity was not affected by the exposure while the fracture strain decreased slightly at the beginning of the exposure and remained constant for the remaining period of the exposure.

Neelam and Kalaga (2002) studied the elastic properties of PVC pipes. The yield strength (σ_y), yield strain (ϵ_y), percentage elongation, initial modulus of elasticity (E_i), and increase in axial strain, i.e., Poisson's ratio (ν), are the material properties used to describe the physical nature of PVC. This study reports the results of the tensile tests conducted on dogbone shaped PVC pipe specimens 8 in. diameter with a wall thickness of 3.5 and 5.5 mm. The tests were performed as per ASTM D638-14. The dogbone specimens were obtained from the longitudinal direction of the pipe. An extensometer was used to measure the axial strain during the test. Strain in the specimen was measured with the help of strain gauges. The test was performed at a loading rate of 5mm per min. The test was stopped when the specimen was fractured and the fracture load, ultimate load and final gauge length were recorded. The elastic parameters determined from the testing are summarized in Table 2-5. The modulus of elasticity results in this study were slightly higher than those mentioned in the 'Handbook of PVC Pipe Design and Construction' standard by Uni-Bell

which should test out at 400,000 psi. But, on the contrary, the tensile strength was lower than the expected tensile strength as per the standard which is 8,000 psi. The discrepancy of results is not explained by the authors in this study.

Table 2-5 Elastic Parameters for PVC Pipe
(Adapted from: Neelam and Kalaga, 2002)

Parameter	Results
Tensile Strength (σ_y)	7,520 psi
Modulus of Elasticity (E)	507,000 psi
Shear Modulus (G)	195,200 psi
Poisson's Ratio (ν)	0.31

2.6 Fatigue Test

Pressure surges are the result of a rapid change in liquid velocity within a pipeline which causes the stored energy in the flowing fluid to be converted to pressure energy, caused for example by rapid valve closure or a pump tripping. The resulting pressure changes, commonly referred to as transients, hydraulic surges, hydraulic transients, and water hammer, are an important consideration in the design of water transmission and distribution systems (Brad, 2009).

Occasional pressure surges and recurring pressure surges are the two types of surges considered while designing. Occasional pressure surges can be defined as the peak pressure surges caused by events outside normal operations of a pipeline (e.g., power outage causing tripping of all system pumps), and recurring pressure surges are peak pressure surges caused by normal pipeline operation (e.g., pumps turned off and on, valves opening and closing) occurring at a frequency of more than once per day (Oliphant et al. 2012).

Metallic pipes have a much higher modulus of elasticity (more rigid and less flexible) than PVC pipe. According to AWWA C150/C151, the nominal surge allowance for ductile iron pipe is 100 psi which is 3 times more than the AWWA standards recommended

for PVC pipes, which shows the relative ability of a PVC pipe to manage surge. However, this does mean that the PVC is essentially absorbing the energy of the surge which calls into question how the PVC material holds its strength particularly if subjected to cyclic surge stresses. Hence, to study the surge effects on iPVC pipe, a testing protocol was developed and executed at CUIRE.

Several studies have provided PVC ability to handle desired surges generated from the operating pressure. Burns et al. (2005) studied PVC fatigue resistance by conducting rotational bending tests on the pipe. From the test results, PVC-U used in North America offers slightly more resistance to fatigue as compared to PVC-M and PVC-U used in in European and Australian markets. PVC-O used in North America exhibits highest resistance to all the material tested for fatigue.

Petroff (2013) conducted an experimental study to determine the effect of flow velocity on surge pressure. Petroff suggested that as the flow velocity increases, lower dimension ratio (thicker wall) pipes may be required to handle the surge pressure. A reasonable flow velocity recommended for design is 5 fps or higher based on the American Water Works Association Research Foundation (AwwaRF) report, 'Guidance Manual for Maintaining Distribution System Water Quality (2000) which helps in removal of biofilm, assists in scouring and removal of deposits as well as reduces disinfection. He predicted the number of cycles required to fail HDPE pipe is based on the following equations:

$$Number\ of\ Cycles = 10^{\frac{1.708 - \text{Log}\left(\frac{Peak\ Stress}{145}\right)}{0.101}} \dots\dots\dots Eq. 2.2$$

$$Peak\ Stress = (P_{pumping} + P_{Surge}) \times \frac{(DR-1)}{2} \dots\dots\dots Eq. 2.3$$

A study was conducted by Vinson (1981) to predict failure in PVC pipes. He studied the response of 6-in. diameter PVC pipes exposed to repeated large pressure surges with a base hoop stress of 400 to 500 psi to various peak hoop stresses. Before the study by

the Utah State University, the approach developed by Herbert W. Vinson was used to predict the fatigue failure in PVC pipes. Vinson cycled the pipe from a base hoop stress between 400 and 500 psi up to various peak hoop stresses. Based on his experiments, he developed an equation for predicting cycles to failure from a peak hoop stress (Vinson, 1981):

$$C = (5.05 \times 10^{21}) \times S^{-4.906} \dots\dots\dots \text{Eq. 2.4}$$

where,

C = number of surges to failure

S = peak hoop stress, psi

Shigley and Mischke (1989) explained that fatigue is a function of stress amplitude and mean stress. Although this study was conducted for steel, a similar study was necessary for PVC as limited testing had been performed on PVC to predict crack initiation due to fatigue. Shigley and Mischke believed fatigue in a member is due to the large number of times that stress occurs (i.e., stress cycles). The plastic nature of PVC pipes will tend to promote crack growth when it is subjected to erratic pressure variations while in service (Burns et al, 2005). The resistance to crack initiation can be assessed by conducting fatigue tests on the pipe. The higher the fatigue resistance is, the lower the risk of crack initiation.

A few other studies were conducted by Hucks (1972), Bowman (1990) and Marshall et al. (1998) to predict the fatigue life of PVC pipes. Moser (2001) examined all these previous studies and conducted his own tests. He determined that the previous tests were inadequate and concluded that the way to predict failure of PVC would be to use two independent variables, stress amplitude and mean stress together. Figure 2-12 presents the S-N plot (Stress-Number of Cycles to Failure) developed by Moser.

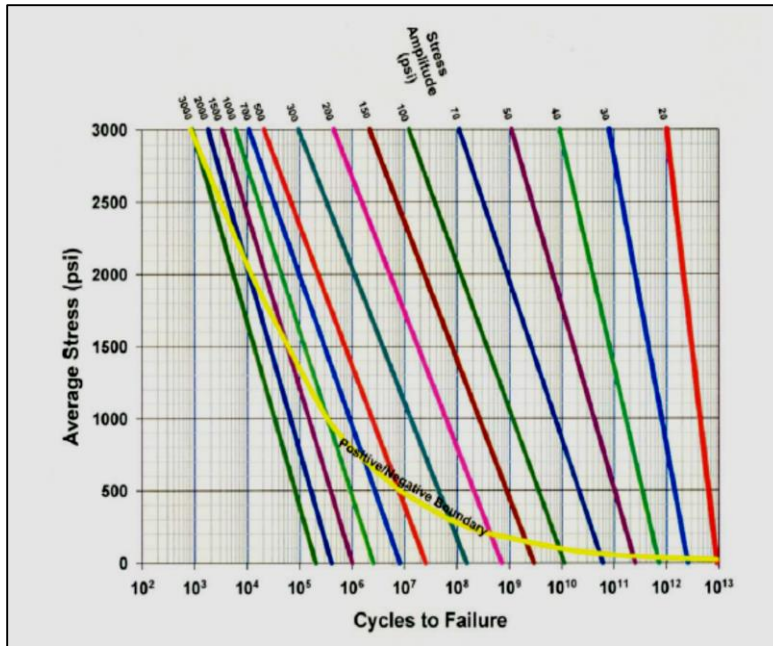


Figure 2-12 Moser's S-N Plot
(Jeffrey et al., 2004)

A fatigue study (cyclic test) on 6 in. C900 PVC pipe was performed by Utah State University to validate failure models. The cyclic study was performed in two phases: Phase I was conducted on 10 pipe sections predicted to fail at 322,000 cycles to validate Vinson's equation that predicted the pipe to fail after 322,000 cycles; Phase II was conducted for 10 million cycles on five pipe samples to validate Moser's methodology for predicting failure time.

Jeffrey (2002) discusses the three important parameters while studying fatigue. These parameters are as follows:

Stress Range (σ_{range}):

$$\sigma_{range} = \sigma_{max} - \sigma_{min} \dots \dots \dots \text{Eq. 2.5}$$

Stress Amplitude (σ_{amp}):

$$\sigma_{amp} = \frac{(\sigma_{max} - \sigma_{min})}{2} \dots \dots \dots \text{Eq. 2.6}$$

Mean Stress (σ_{mean}):

$$\sigma_{mean} = \frac{(\sigma_{max} + \sigma_{min})}{2} \dots\dots\dots \text{Eq. 2.7}$$

The stress is calculated based on the water pressure the pipes are subjected to using thin wall theory (Gere and Timoshenko, 1997).

$$\sigma = \frac{Pr_{mean}}{t} \dots\dots\dots \text{Eq. 2.8}$$

where,

σ = circumferential or hoop stress

r_{mean} = mean radius and

t = minimum wall thickness

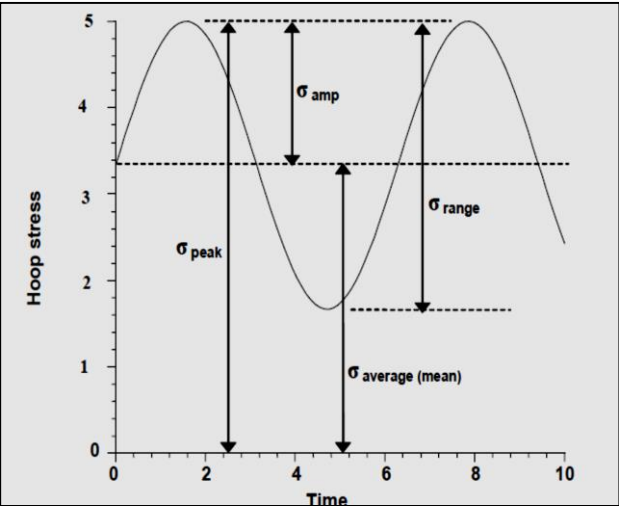


Figure 2-13 Illustration of Stress Terms (Jeffrey et al., 2004)

The testing continued to 10 million cycles without any failure. Jeffrey (2002) predicted the number of cycles for failure would be at around 20M cycles. He verified and confirmed that the mean stress and mean amplitude have direct influence on the fatigue of the PVC pipe. The testing by Jeffrey (2002) to validate Moser’s idea that mean stress and stress amplitude together influence PVC fatigue determined that stress amplitude primarily

influences the fatigue in PVC and mean stress plays a small role. As the amount of fatigue failure data was limited in the testing, Jeffrey recommends to use the Moser's plot only as a guide (Jeffrey, 2002).

2.7 Bedding Test

Bedding tests do not have a specific standard and hence an overall approach was developed to perform a bedding test on a pipe to study the deflection behavior of the pipe. A procedure was developed as a part of this dissertation for the testing which included use of sensors such as displacement sensors to measure the deflection of pipe, strain gauges to study the strains and earth pressure cells to measure the stress experienced by the pipe. A detailed procedure of the testing is explained in Chapter 3.

Alam and Allouche (2010) conducted an experimental investigation of pipe soil friction coefficients for direct buried PVC pipes. The structural performance of flexible buried pipes is greatly influenced by the interaction between pipe and the soil envelope surrounding it. A schematic diagram of a buried pipe is given in Figure 2-14. The pipe is subjected to thrust forces due to changes in flow direction, cross-sectional area, pipeline terminations, and/or thermal expansion/contraction. Use of concrete reaction blocks as a way to restrain the pipe systems is on a rise, which helps reduce the amount of thrust.

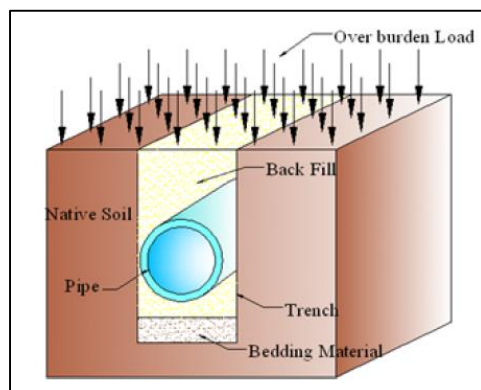


Figure 2-14 Schematic Diagram of Buried Pipe
(Alam and Allouche 2010)

An experimental testing program using an 8 in. diameter, 14 ft long PVC pipe was performed using silty sand, moist silty sand, graded gravel, silty clay and moist silty clay as bedding materials. The experimental work on the buried pipe covered a wide-range of soil types, pressures and moisture contents. The experiment investigated the soil-pipe friction coefficients of a direct buried, restrained, PVC pipe under controlled laboratory conditions. The force needed to overcome friction between pipe and its surrounding bedding, total pipe movement along its longitudinal axis, rigid body movement, and elongation of pipe under applied axial force were measured during the testing.

The PVC pipe was installed in a soil chamber and a circular opening to the end of the soil chamber was used to bolt the front-end of the pipe with a control actuator. The actuator was used to apply an axial tensile load to the pipe. A linear variable differential transformer (LVDT) was placed on the rear-end cap of the pipe to measure the rigid body movement of the pipe. Strain gauges were mounted on the top of the crown to measure the elongation of the pipe under the applied axial load. Four earth pressure cells were used to measure the soil pressure during the test.

The experimental results of the friction forces from the test were compared with the calculated results using three different approaches. The first approach utilizes Coulomb's equation along with modifiers suggested by Potyondy (1961) for the cohesion and soil friction angle coefficients. This first approach assumes that the behavior at the pipe-soil interface is similar to that at a soil-soil interface and calculates the frictional force accordingly.

The second approach for calculating the friction force utilized a modified Coulomb's equation. In the second approach, the authors developed a semi-empirical expression that accounts for the stiffness of the pipe, overburden pressure, and the nature of the bedding material. The third approach was based on the experimental data. It

calculated the friction force by using an average friction force per unit of surface area of the pipe (lb/sq ft) per psi of overburden (or foot of soil cover) backfill. Predictions from the three approaches were compared and the first approach was found to be in fair agreement with the test data, slightly over-predicting the friction force for fine grain soils and under-predicting it for gravelly soils.

The friction force results can be used by designers for calculating the minimum embedment (around the pipe) length needed to minimize the thrust experienced by the pipe and eliminate the requirement for thrust blocks for a given project.

Another study by Kawabata et al. (2006) studied the behavior of buried pipe under high fills and the design implications of high fills. The design guidelines for installation of flexible pipes are suitable for a cover depth of 33 ft (10 m) or less in Japan. There is a need for installation of pipelines at a depth of 66–99 ft (20–30 m) due to development in infrastructure, residential and industrial developments and use of difficult terrains. The authors monitored a fiberglass reinforced plastic mortar (FRPM) pipe in Japan. The earth pressures, deflections, and strains in the pipe were measured over a period of 1 year which was installed at a depth of 155 ft (47.1 m). This study proposed a revised vertical and lateral earth pressure diagram for flexible pipes having a cover of > 66 ft (> 20 m).

A 13 ft (4 m) long section of the 36 in. (900 mm) diameter and wall thickness of 0.71 in. (18 mm) FRPM pipe was instrumented to measure earth pressures, pipe deflections and strains in the pipe. A standard gravel 0-1 in. (0-25 mm) was used to backfill around the pipe and was compacted with the help of 176 lbs (80 kg) tamping rammer. A mixture of gravels and sands obtained from the natural ground (volcanic gravel tuff) was used to fill above the pipe.

The instruments for measuring the earth pressures, pipe deflections and strains in the pipe were located on the pipe. The vertical stresses were measured using three force

transducers and another one was used to measure the lateral pressure at the springline. Vertical and lateral deflections of the pipe wall were measured using two linear variable differential transducers (LVDTs) which were installed inside the pipe. Strain gauges at 12 locations on the outside of the pipe were installed to measure the circumferential strains. The measurements were taken at 16.4 ft (5 m) height interval until the fill reached the final height of 155 ft (47.1 m).

The vertical earth pressure had a concave distribution with the pressure at the center being 0.9 times and at the edges of pipe being 1.1 times the average vertical pressure for the whole test. The lateral earth pressure measured at the springline was 1.4 times the average vertical earth pressure across the top of the pipe. The results suggested that the triangular lateral pressure distribution recommended by the Japanese Sewage Works Association [JSWA] (1999) will be overly conservative and uneconomical for high fills whereas Spangler's analysis will not be conservative. Kawabata et al. (2006) proposed a modified design diagram which was a combination of the existing methods by Spangler (1941) and JSWA (1999) to design the earth pressure presented in Figure 2-15. The proposed design could be useful in examining pipe behavior under high fills in future installations.

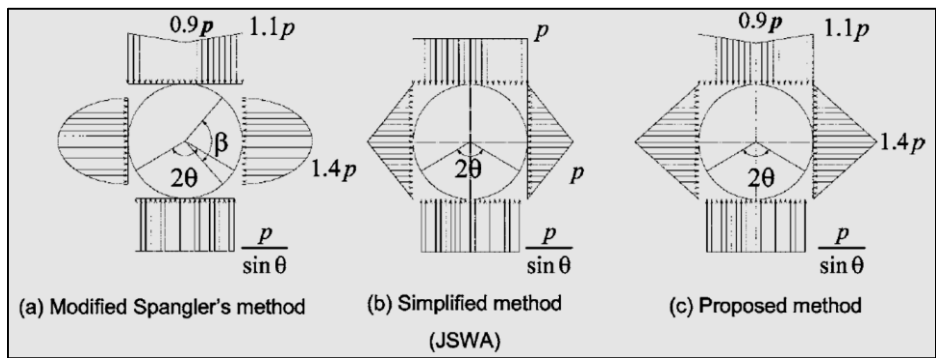


Figure 2-15 Earth Pressure Diagrams for: a) Spangler's Analysis, b) Simplified Analysis by JSWA and c) Proposed Analysis for High Fills (Kawabata et al., 2006)

Although there are many developments in the design of buried flexible pipes, issues such as three-dimensional soil-pipe interactions and pipe behavior in terms of deflections and strain limits of pipe wall sections are still unclear. Faragher et al. (2000) performed a controlled field test to study the behavior of embedded flexible pipes under repeated loadings and reported that the vertical deformation of pipe increased rapidly initially when the loads were applied and the rate of deformation was reduced as the test progressed and further loads were applied.

Terzi et al. (2010) studied the behavior of a single 4 in. (100 mm) diameter, 0.4 in. (10 mm) thick and 20 in. (500 mm) long HDPE pipe with a series of tests to help understand the soil-pipe interaction. The tests were performed to evaluate the impact of backfill properties and installation quality on pipe behavior. The tests were carried out in a laboratory test box with the pipe buried in sand backfill material with different relative densities subjected to surcharge loads.

The above test setup included a test tank, pluviation system, data acquisition system and instrumentation on the pipe. The test tank was a rigid steel box with 1.7 ft (500 mm) in length, 3.3 ft (1000 mm) in height and 2.3 ft (700 mm) in width. The backfill material used for this study was Sile sand (fine sand) which was washed and dried before use. The pluviation system was used to distribute the Sile sand uniformly in the test box to obtain the expected relative density. They used LABVIEW data acquisition system software to measure deformations and strains in the pipe wall.

Two linear-position transducers (LPTs) were attached to the pipe wall to detect the vertical and lateral deflections on the pipe wall. Biaxial strain gauges at eight locations measured the circumferential and axial strains. The photogrammetric method was used for deformation measurements. The photogrammetric method provided three-dimensional measurements at any point on the pipe and there was no need to install instruments on

the surface of the pipe. At each step of adding of load on the pipe, the motion at the marked points on the pipe was tracked and the magnitude and direction of motion was determined with the photogrammetric method. The behavior of shoulders, haunches, springlines, crown, and invert of the pipe were determined using a close-range image processing technique. The measurements from the LPTs and the photogrammetric method were acquired simultaneously.

The test results displayed that the pipe wall shrank vertically and elongated horizontally under the increasing vertical surcharge loading. The maximum deflection of the pipe was observed at the vertical axis (pipe invert). Depending on the backfill conditions, the deflections of the pipe wall were different with 0.071 in. (1.8 mm) in loose conditions, 0.055 in. (1.4 mm) on medium and 0.024 in. (0.62 mm) in dense conditions. It is important to have a well compacted dense backfill as this study results showed the flexible pipe installed in loose backfill had more deflection in the pipe wall than the pipe installed in dense backfill conditions.

Based on the bending moment distribution diagrams and the deflections observed in the testing, the stresses on the pipe wall were more in loose backfill embedment because of the lack of soil reinforcement around the springline of the HDPE pipe. This resulted in an increase in the vertical stress and a decrease in the horizontal support to the pipe wall resulting in a soft response and large deflection in the pipe. This study concluded that increasing the backfill quality would offer more protection to the pipe in terms of bending moment distribution and maximum circumferential strain.

A study by Zhan and Rajani (1997) evaluated the benefits of use of controlled low strength material (CLSM) as a trench backfill over the traditional backfill materials such as sand and clay for a PVC pipe under traffic loading. It studied the influence of CLSM on the behavior of buried pipes. This study aimed to determine the sensitivity of load transfer from

truck loads to buried pipes with different trench backfill materials, pipe burial depths and pipe materials using finite element modeling and to compare the finite element results with the field results.

CLSM is a flowable, cementitious mixture of Portland cement, aggregate, fly ash, and water. CLSM is easy to place in the trench and there are no long-term settlement problems, requires minimum inspection and no compaction; hence, CLSM has started to gain wide acceptance in North America for trench reinstatement. CLSM has higher strength and higher elastic modulus than sandy, clayey and native soils.

The National Research Council of Canada (NRCC) along with city of Edmonton, Alberta have undertaken field studies since 1993 to study the behavior of PVC water mains in different trench backfills and to examine the pipe-soil interaction. These studies have evaluated the thermal performance of the backfill materials which could be used to minimize the risk of freezing water in the mains. As a part of this initiative by NRCC, two PVC water mains of 8 in. (200 mm) diameter were installed parallel at different depths (8.2 ft and 3.3 ft) in the trench and were monitored. The trench was divided into seven sections of 66 ft (20 m) length each and each section was backfilled with different backfill materials such as native clay, sand (with and without insulation layers), CLSM, expanded shale lightweight aggregate, thermal Crete (biomass), and bottom ash. The bypass main installed at a depth of 3.3 ft (1.0 m) was studied for the truck load in this paper.

Strain gauges were installed in 3 of the 7 sections of backfill materials with native clay, clean sand and CLSM. The strain gauges were installed to measure the circumferential (hoop) as well as longitudinal strains (axial). Three earth pressure cells were used to measure the earth pressures on the pipe. The test instrumentation setup for this study is presented in Figure 2-16.

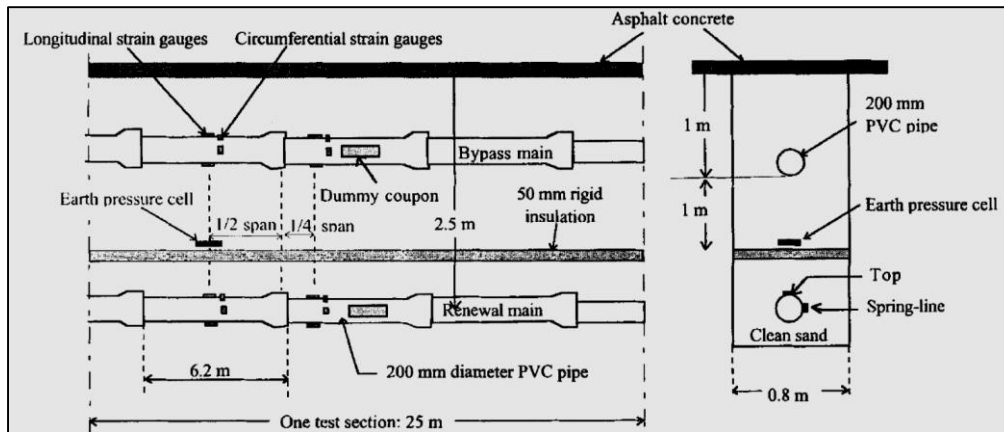


Figure 2-16 Typical Section of Renewal and Bypass Mains in Edmonton, Canada (Zhan and Rajani, 1997)

In 1995, the 3 sections of backfill with the strain gauges and earth pressure cells were subjected to truckloads of 45,000 lbs (200 KN) truck weight, 5,620 lbs (25 KN) for each front tire and 8,430 lbs (37.5 KN) in each of the four rear tires. Each section was subjected to loading and the truck remained stationary at each location for 5 minutes while the data for strain and pressure was collected. While the field testing was performed, another analysis with the help of finite element modeling was done to validate the field results and conduct sensitivity analyses to understand the importance of burial depth on the water pipes in the three different backfills.

The hoop strains estimated from the finite element analyses and from the field truck loads were significantly less on pipes in the section of the trench with CLSM as the backfill material as compared to those from sand and clay backfill sections. The sensitivity analyses on an 8 in. (200 mm) PVC and ductile iron pipe were performed buried at various depths and in different backfills. The value of hoop strain or stress in the pipe wall illustrated the effectiveness of the backfill material—the lower the value, the better the backfill material.

Test results determined the external hoop stresses for clay and sand backfills were 68% and 127% higher, respectively, at springline as compared to external hoop stress in CLSM backfill. The external hoop strain at springline in sand backfill was 92% higher than in clay backfill, while it was negligible in CLSM backfill. This study concluded that the CLSM backfill is a better alternative to sand and clay backfills for PVC pipes. CLSM protects the buried pipe from traffic loads better than sand and clay.

Balkaya et al. (2012) evaluated the stresses and the deformations in a buried PVC water pipe with bell-and spigot joints. Pipe joints greatly affect the performance of the pipe, and defects at the joint could lead to pipe failure. Leakage at joints could lead to erosion of the soil materials around the pipe creating voids under the pipe. The creation of voids leads to a non-uniform bedding at the joints. The pipe considered in this study is unsupported at the invert and haunches as voids are created to simulate non-uniform bedding while performing the finite element analyses. The changes in the stresses and deformations were determined based on the geometry of the voids.

While pipe design is based on its ability to withstand the amount of internal fluid pressure as well as external loads acting on the pipe, it is also partially determined by pipe joint systems. If the pipe joint systems are installed incorrectly or contain damage, then fluid can leak out of the pipes resulting in serious repercussions. Leakage is an extremely common problem caused by improper installation of pipe joints. Leakage can cause serious damage to public water systems resulting in drinking water contamination if sewage enters the water pipe by groundwater infiltration. Pipe leakage can cause chemicals to seep into the soil leading to hazardous levels of erosion. This erosion can alter the soil quality exerting pressure on the pipe system and causing pipe failure. In order for the pipe to function efficiently, the soil bedding level must be uniform around the joint. If the bedding is not uniform, it can cause pipe bending which can alter the joint tightness.

The finite element modeling in this study illustrates that an increase in void length under the pipe leads to an increase in vertical displacements with the lowest increase at the crown and maximum at the invert of the pipe. If the void angle (width of invert without soil support) is small the factor of safety drops significantly. If the voids under the invert have a larger angle and the pipe is unsupported from the haunches, more soil load is distributed through the soil resulting in less stress on the pipe.

Highest stresses were observed when the voids were directly under the joints. The vertical displacement observed for PVC pipes was more in loose silty sand as compared to medium-dense sand. This study aimed to focus on non-uniform bedding conditions while considering future pipe products and pipe joints, and emphasizes the potential effects of joint leakage and soil erosion (Balkaya et al., 2012).

Balkaya et al. (2013) studied the non-uniform bedding support conditions under continuous PVC water distribution pipes. The purpose of this study was to understand the effect of non-uniform bedding support on the stability of buried PVC pressure pipes and study the longitudinal soil-pipe interaction. This study aimed to develop a better understanding of longitudinal bending as a result of voids under the invert of buried PVC pipes. The performance of the buried pipe depends on the relative stiffness of the soil and the pipe. The structural performance of the pipe depends on the structural characteristics of the soil and the pipe. ASTM D2321-14e1 (2005) lists various factors such as method and extent of compaction of embedment materials, types of embedment, water conditions in the trench, pipe stiffness, uniformity on embedment support, and installation practice that affect the deflection of the pipe. Ideally, a uniform bedding is important to provide a uniform support along and around the pipe.

Due to factors such as unstable bedding materials, uneven settlement due to angular distortion between individual segments of the pipeline, over-excavation and non-

uniform compaction of the bedding soil, a pipe will have a non-uniform bedding support. The non-uniform bedding could result in longitudinal and circumferential cracks and joint openings, which will lead to leakage and ultimately failure of the pipe. Hence, it is imperative to understand the effects of non-uniform bedding on longitudinal bending in buried PVC pipes.

A PVC water pipe with a 6 in. (150 mm) outside diameter and thickness of 0.19 in. (5 mm) was studied for both uniform and non-uniform bedding conditions. The pipe was installed on a soil layer of 3.3 ft (1 m) depth and a bedding of 9 in. (0.225 m) depth and then covered with overburden soil to a depth of 8.2 ft (2.5 m). Voids of varying sizes were created to make the bedding non-uniform with the effect of voids located under the invert and around the haunches of PVC pipe studied for this paper.

The finite element analyses indicates that the increase in void length will increase the stresses on the pipe walls considering other variables remain constant. The results from this study illustrate that the pipes with non-uniform bedding conditions experience peak tensile wall stresses from 37% to 69% higher than those pipes with uniform bedding for medium dense sand and 45% to 95 % higher than dense sand.

Najafi et al. (2011-a) at the Center for Underground Infrastructure Research and Education (CUIRE) at the University of Texas at Arlington (UTA) was involved with Tarrant Regional Water District (TRWD) and the Dallas Water Utilities (DWU) as part of a design project for a major raw water transmission project entitled "Integrated Pipeline (IPL)." The project consisted of approximately 155 miles (250 km) of large diameter [54 in. to 108 in. (1372 mm to 2743 mm)] pipes to meet future water demands of the TRWD and DWU service areas. The IPL project transmits raw water from Lake Palestine, Richland Chambers Reservoir and Cedar Creek Reservoir to Dallas and Tarrant Counties. The testing of steel pipe considered for the transmission of water was performed at CUIRE

laboratory at UT Arlington in order to observe the behavior of steel pipe embedded in native soil under static loads (Najafi et al. 2011-a).

Five tests on large diameter steel pipe were conducted at the Center for Underground Infrastructure Research and Education (CUIRE) laboratory at UTA. The tests were conducted on a 19.75 ft long, 72 in. nominal diameter bare steel pipe with a DR of 230. The embedment soils included clayey soils obtained from the Integrated Pipeline (IPL) project site in Texas in both natural and lime treated forms, crushed limestone and their combinations. Clayey soils were compacted by using tamping foot compactors, while crushed limestone was compacted using a vibratory plate compactor.

Peaking deflections or vertical elongations of steel pipe were observed in each of the tests during embedment construction. Static cover loads of pea gravel were placed over the embedded pipe. Pipe deflections and pipe wall strains were measured during and after placement of cover load construction using convergence meters and strain gauges. Lateral earth pressures at pipe springline and load cell wall, and vertical loads at the top and bottom of each pipe were measured.

Peaking deflections are defined as diametric changes due to vertical elongation during the embedment process. Peaking of flexible pipe is illustrated in Figure 2-17. The tests on large diameter steel pipe analyzed deflection ratios (ratio of horizontal to vertical deflection), bedding angles, and moduli of soil reactions which are important factors to consider in the design of flexible pipe and soil systems. The results provided insight into construction loads and peaking deflections as well as pipe behavior in mixed embedment conditions (Najafi et al. 2013).

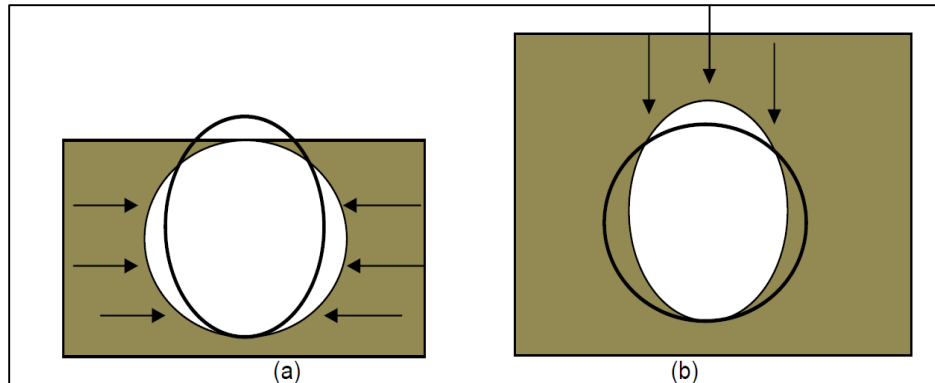


Figure 2-17 (a) Peaking Load due to Lateral Forces of Embedment and (b) Deflection due to Backfill Cover (Najafi et al. 2013)

Another study by Najafi et al. (2011-b) was conducted to study the applicability of The Bulldog™ restrained joint system (BRS) in PVC pipe. The BRS is comprised of a gasketed bell and spigot integrated into PVC pipe during manufacturing. The current version is designed for integration into pipes manufactured to AWWA C900 standard, diameters 4 in. (100 mm) through 12 in. (300 mm). A schematic drawing of the joint components is shown in Figure 2-18. The horizontal directional drilling (HDD) installation of gasketed bell and spigot pipe has the benefit of joining pipe sections while HDD pullback operation is in process. This is compared with fusible joints where a long string of pipe must be ready to be pulled back, thereby occupying space and possibly closing driveways and intersections.

The advantages and limitations of each pipe type and joining method must be evaluated based on the project requirements and site conditions. CUIRE developed a formal testing program in order to establish the performance limits for the BRS product when installed by HDD. The tensile testing conducted by CUIRE on the PVC pipe employing the BRS demonstrated that these products have the tensile strength needed for HDD applications. The testing proved that two different HDD pulling-head designs are

capable of achieving the full joint tensile strength of the BRS joint. For trenchless applications, it is important to know about behavior of joints under a combination of tensile and bending loads (Najafi et al. 2011-b).

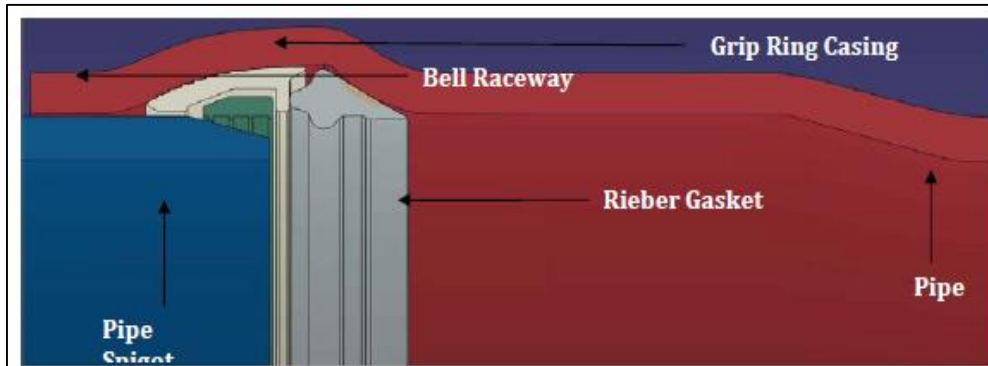


Figure 2-18 Bulldog™ Restrained Joint Pipe Components
(Najafi et al. 2011-b)

A comprehensive study on PVC pipe longevity was conducted by Folkman (2014) at Utah State University's Buried Structures laboratory. This research demonstrated that the PVC pipe has the lowest rate of main breaks of pipe materials considered in this study which includes ductile iron, cast iron, steel, concrete, and asbestos cement. This study was conducted on in-service pipes with operational conditions. The tests at Utah State included pipe dimensions, acetone immersion, and pressure tests. The test results in the U.S. and around the world indicate that PVC pipe can be expected to provide reliable service in excess of 100 years. PVC pipes excavated showed a high degree of resilience in freezing conditions, met all applicable standards, and had no change in mechanical properties and strength. The Water Research Foundation reported that 100 years is a conservative estimate for a properly designed and installed PVC pipe. This study concluded that if a pipe fails in less than 100 years, it either has a manufacturing defect, was installed improperly, was part of a poorly designed or maintained system, or was the wrong material selected (Folkman 2014).

During the installation of flexible and rigid pipe, backfilling procedure of soil is important to transfer loads into the bedding. The soil load results in the deflection of the flexible pipe walls. Deflection is defined as the change inside the diameter that results when a load is applied to a flexible pipe. In pipe design, it is the vertical dimension that is usually of more concern. Vertical deflection is usually limited to 7.5% of the base inside diameter; the inside diameter of the base is the nominal diameter less manufacturing and out-of-roundness tolerances inherent to the manufacturing process (Uni-Bell, 2012).

Beamer et al. (2009) at the Calleguas Municipal Water District in Southern California performed laboratory tests to find out the cause of the 16 in. PVC transmission main failures experienced by the water district. One of the tests performed was the Acetone Immersion test. A coupon was cut from the pipe and subjected to acetone immersion in accordance with ASTM D2152-13, which is a requirement of AWWA C905-88. This test is intended to confirm the quality of the extrusion. The results showed that the pipe material did not comply with the minimum requirements. It was concluded that the central part of the PVC pipe wall was incompletely fused (Beamer et al. 2009).

2.8 Previous Tests on iPVC Pipe

The product studied for this dissertation is an innovative iPVC pipe. The manufacturer of iPVC pipe, PPI (a company registered in South Korea) conducted several tests on iPVC pipe before the pipe was studied for the first time in U.S. The iPVC pipe has the same thickness as standard PVC (see Figure 2-19). These experimental results were published in metric system (Korea uses metric system) and in compliance with ASTM/ISO standards. Table 2-6 summarizes the test results for iPVC pipe performed by PPI.



Figure 2-19 9 in. OD DR 18 iPVC pipe Thickness
 (Source: AW and PPI, 2015)

Table 2-6 iPVC pipe Test Results by PPI
 (Source: AW and PPI, 2015)

Test Description	iPVC pipe Pressure Class 235	AWWA Standards Requirements
Tensile Strength (psi)	7,780	7,000
Impact Strength (ft-lb/in.)	1.26	0.65
Modulus of Elasticity (psi)	Min – 438,000; Max – 485,000	400,000
Vice Flattening Test	No Cracks	-
Long Term Pressure Test (1000 hrs.) 73 °F at 500 psi	No Failure	-
Short Term Burst Test (5 sec)	Pass	-
Acetone Immersion Test	Pass	-
Hydrostatic Burst Test	Pass	-
Elongation at Break (%)	574	>400
Compression Set Test (%)	14	20 (Max)
Short Term Burst Pressure Test (psi)	899	>755
Water Pressure at 6,090 psi at 73 °F	18 hrs.	1 hr.
Deflection Temperature Test (°F)	76 °F	70 °F
Flammability Test (ASTM D635-14)	<10 mm	<25 mm

The earlier test results as per Table 2-6 display that iPVC pipe exceeds AWWA C900 and C909 criteria. The impact load, hydrostatic burst pressure, tensile strength and weight for iPVC pipe is higher than the recommended AWWA requirements for standard

PVC. PVC and iPVC pipe has been tested under low temperature (-4°F) for impact resistance. PVC pipe failed from a drop height of 4.9 ft whereas iPVC pipe only had a scratch on the surface even when the load was dropped from a height of 16.4 ft. Figure 2-20 displays the results of the impact of the dropped load from a height.



Figure 2-20 PVC and iPVC pipe Impact Test Results
(Source: AW and PPI, 2015)

PPI has performed practical demonstrations to display the strength and flexibility of the iPVC pipe. The iPVC pipe sample was tested by freezing the water contained in the pressurized iPVC pipe. The freezing resulted in the expansion of the pipe material but without any failure in the pipe. In another test, a full size excavator passed over the pipe (crawl test) as well as the bucket end of the excavator, which was used to pinch the pipe with maximum load on the pipe (bucket test). In both instances, the pipe was squeezed (by 80% for crawl test and 90% for bucket test) and retained its original dimensions without damaging the pipe after the loads were released. Only a few scratches were observed on the external surface of the pipe. Figures 2-21, 2-22 and 2-23 illustrate the freezing water test, crawl test and bucket test conducted on iPVC pipe by PPI.

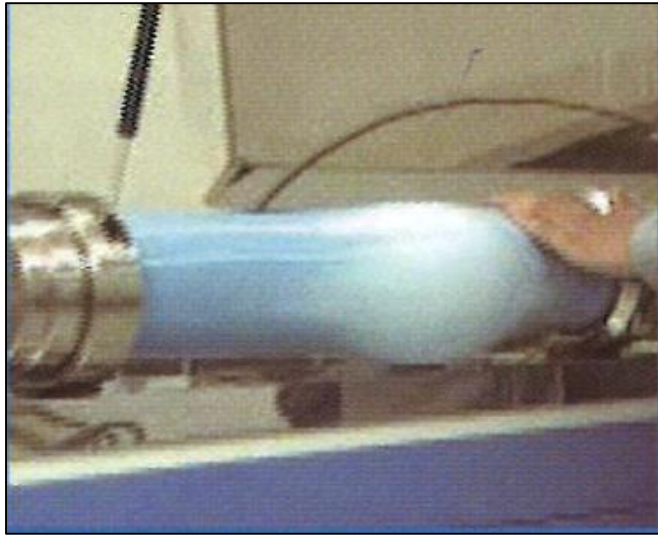


Figure 2-21 iPVC pipe Pressurized with Freezing Water
(Source: AW and PPI, 2015)



Figure 2-22 Crawl Test
(Source: AW and PPI, 2015)



Figure 2-23 Bucket Test
(Source: AW and PPI, 2015)

2.9 Chapter Summary

This chapter reviewed the existing literature on the various tests that could be performed on flexible pipes. The tests discussed in this chapter included hydrostatic short-term burst pressure test, impact test, stiffness test, tensile test, fatigue test and bedding test. Also, the previous tests conducted on iPVC pipe were discussed in this chapter.

Chapter 3

Testing Methodology

Chapter 2 discussed the previous available literature on the tests performed in this dissertation research. This chapter discusses the methodology for the testing conducted on iPVC pipe. The testing protocol for the iPVC pipe research project was developed by AW. Meanwhile, CUIRE and Microbac were hired to perform the tests by AW. The research testing was funded by WRF. This testing methodology follows WRF Project Report No. 4650 entitled “An Evaluation of the Value of Structurally Enhanced PVC Pipe (2016).”

3.1 Introduction

The iPVC pipe research project was divided into six different tests based on the testing protocol developed by American Water as follows:

1. Hydrostatic Short-term Burst Pressure Test
2. Impact Test
3. Stiffness Test
4. Tensile Test
5. Fatigue Test
6. Bedding Test

Hydrostatic short-term burst pressure test, tensile test, fatigue test and bedding test were performed by CUIRE as a part of this dissertation author’s project tasks, and hydrostatic short-term burst pressure test, tensile test, impact test and stiffness test was performed by Microbac on iPVC pipe specimen. The following sections explaining the purpose, detailed test procedure, and the expected outcome from these six tests are based on the WRF Project Report No. 4650 entitled “An Evaluation of the Value of Structurally Enhanced PVC Pipe.”

3.2 Hydrostatic Short-term Burst Pressure Test (Adapted from WRF Report No. 4650, 2016)

3.2.1 Purpose

The purpose of the hydrostatic short-term burst pressure test as per ASTM standards is to determine the resistance of either thermoplastic or reinforced thermosetting resin pipe, tubing, or fittings to hydraulic pressure in a short time period. For iPVC pipe project, the test was conducted to determine the burst pressure of iPVC pipe and compare the test results to the AWWA standards requirement of burst pressure which is 755 psi for a PVC pipe.

3.2.2 Procedure

Procedure A of ASTM D1599-14 is used to determine burst pressure of a specimen if the mode of failure is to be determined. Procedure B of ASTM D1599-14 is used to determine that a specimen complies with a minimum burst requirement. In simple terms this is a burst test in which the test specimen is subjected to an increasing level of internal pressure until failure occurs. Failure is defined as the first weep or leaking of fluid. The minimum allowable time to failure is 60 seconds; however, the failure time may be extended beyond 60 seconds for a more conservative result. The length of the samples tested at CUIRE was 30 in. Microbac conducted the burst test on samples longer than CUIRE. The length of the samples at Microbac was 42 in. for each sample.

3.2.3 Expected Outcome

Data obtained by this test method are generally used in predicting the behavior of pipe, tubing, and fittings under conditions of temperature, time, method of loading, and hoop stress similar to those used in the actual test. For iPVC pipe project, the test determined the burst pressure of iPVC pipe which helped in calculating the hoop stress and evaluate the performance of iPVC pipe as compared to the AWWA standards requirement of 755 psi for a PVC pipe.

3.2.4 *Benefit to the Industry*

The current test results will provide the maximum pressure capacity and maximum hoop stress induced in the iPVC pipe when subjected to uniform internal pressure.

3.3 Impact Test (Adapted from WRF Report No. 4650, 2016)

3.3.1 *Purpose*

The purpose of the impact test is to follow ASTM D2444-99 and determine the impact resistance of thermoplastic pipe and fittings under specified conditions of impact by means of a tup (falling weight).

3.3.2 *Procedure*

The standard test procedure by ASTM requires testing 125 specimens, out of which 25 specimens shall be used as preliminary test samples to calculate the approximate drop height and weight of the tup. The preliminary test is carried out, by trial and error, or judgment, by estimating the drop height at which 85 % of the specimens will pass. During the testing, the 100 samples are divided into two sets of 50. The first set of 50 specimens is tested using the height obtained during the preliminary test to pass at least 85% of the specimens. The next set of 50 is tested on samples by increasing height or weight of the tup to achieve 85% of specimens to fail. The value of the mass is recorded at tup, the drop height, and the number of passes. The test continues until failure in the test specimens through shattering or any crack or split created by the impact can be seen by the naked eye. The PPI Korea already tested and qualified the iPVC pipe per ASTM D2444-99. The sole objective of retesting the impact study was to estimate the maximum impact energy of iPVC pipe. Hence, the current impact test was modified, to align with the research objective by AW. Although the standard test procedure requires testing 100 specimen, in the current research study 70 specimens were tested. To eliminate the preliminary testing, previously studied impact results were provided to the lab. But, the samples that passed

the test without any failure were re-tested again. Initially, the samples were tested at 73 °F and then the re-tests were performed at 32 °F as the samples failed to break at 73 °F and the impact strength of iPVC pipe is reduced at colder temperatures.

3.3.3 *Expected Outcome*

Considering the demonstrations of iPVC pipe resilience by PPI, it is expected that the breaking of iPVC pipe samples would be a challenge. The impact resistance of iPVC pipe is determined by the test.

3.3.4 *Benefit to the Industry*

The impact resistance of thermoplastic pipe and fittings relates to suitability for service and to the quality of processing. Impact resistance may also provide a relative measure of a material's resistance to breakage during handling and installation. The testing aims to provide impact resistance for iPVC pipe which could be used by the industry while comparing with other pipe materials a performance evaluation parameter.

3.4 Stiffness Test (Adapted from WRF Report No. 4650, 2016)

3.4.1 *Purpose*

The purpose of this test as per ASTM is to determine the load-deflection characteristics such as pipe stiffness, the stiffness factor, and load at specific deflections of plastic pipe under parallel-plate loading. For iPVC pipe project, the purpose of the testing was to see the load resistance of iPVC pipe as well as understand the deformation of iPVC pipe under the load.

3.4.2 *Procedure*

The ASTM D2412-11 test procedure was followed for this test. Measure the specimen used for testing 1 mm (1/32 in.) from the top as well as the outside diameter to the nearest 0.2 mm (0.01 in.). After the measurements, locate the pipe section with its longitudinal axis parallel to the bearing plates and center it laterally in the testing machine.

Bring the upper plate into contact with the specimen with no more load than what is necessary to hold it in place. This establishes the beginning point for subsequent deflection measurements.

Further, compress the specimen at a constant rate of 0.50 ± 0.02 in. (12.5 ± 0.5 mm)/min. Start recording the load-deflection measurements continuously or intermittently to the relative movement of the bearing plates. If the load on the specimen fails to increase with increasing deflection or if the specimen reaches 30% of the average inside diameter or the required maximum deflection, stop the test.

3.4.3 *Expected Outcome*

The expected outcome of this test is to provide the pipe stiffness and pipe deflection of iPVC pipe under load applied. At every 5% reduction in the OD of the iPVC pipe (95%, 90%, 85%, 80%...20%), the pipe stiffness, pipe deflection and the load applied is recorded.

The value obtained by dividing the force per unit length of specimen by the resulting deflection in the same units at the prescribed percentage deflection is referred to as Pipe Stiffness (PS) and the product of PS and $0.149r^3$ is known as the stiffness factor (SF) of the pipe. The PS determined by this test method can be used to calculate approximate deflections under earth load. Accordingly, the following modified Spangler equation is one available expression that can be used to give approximations of deflections occurring in plastic pipe under earth load and earth load plus live load:

$$\% \text{ Deflection} = \frac{D_e K (W' + P) 100}{0.149 PS + 0.061 E'} \dots\dots\dots \text{Eq. 3.1}$$

where:

% Deflection = predicted percentage of diametric deflection

D_e = deflection lag factor (unitless),

K = bedding constant (unitless), dependent upon the support the pipe received from the bottom of the trench

W' = live load (psi), pressure transmitted to the pipe from traffic on the ground surface

P = prism or dead load (psi), pressure acting on the pipe from the weight of the soil column above the pipe

PS = pipe stiffness (psi), flexible pipe's resistance to deflection in an unburied state

E' = modulus of soil reaction (psi), stiffness of the embedment soil

3.4.4 *Benefit to the Industry*

PS relates to handling and installation characteristics of a pipe during the early stages of soil consolidation around the pipe. For PVC pipes, the minimum requirement for pipe stiffness is 364 psi set by AWWA M23 Manual. The Spangler equation will provide the theoretical percent deflection experienced by iPVC pipe under loading which could be further compared to the AWWA maximum allowable limit of 5% for flexible pipes. The deflection of pipe under loads is used by designers while evaluating the pipe materials.

3.5 Tensile Test (Adapted from WRF Report No. 4650, 2016)

3.5.1 *Purpose*

The purpose of the tensile test as per ASTM is to determine the tensile properties of unreinforced and reinforced plastics in the form of a standard dumbbell-shaped test specimens when tested under defined conditions of pretreatment, temperature, humidity, and testing machine speed. For iPVC pipe project, the testing was performed to evaluate iPVC pipe for its tensile behavior and to provide information about the tensile strength and modulus of elasticity of iPVC pipe.

3.5.2 *Procedure*

Measure the width and thickness of each specimen to the nearest 0.025 mm (0.001 in.) using the applicable test methods in ASTM D5947-11. Measure the width and

thickness of flat specimens at the center of each specimen and within 5 mm of each end of the gauge length. Place the specimen in the grips of the testing machine, taking care to align the long axis of the specimen and the grips with an imaginary line joining the points of attachment of the grips to the machine.

Tighten the grips evenly and firmly to the degree necessary to prevent slippage of the specimen during the test, but not to the point where the specimen would be crushed. Set the speed of testing at the proper rate as required in ASTM D638-14, and start the machine. Record the load-extension curve of the specimen. Record the load and extension at the yield point (if one exists) and the load and extension at the moment of rupture.

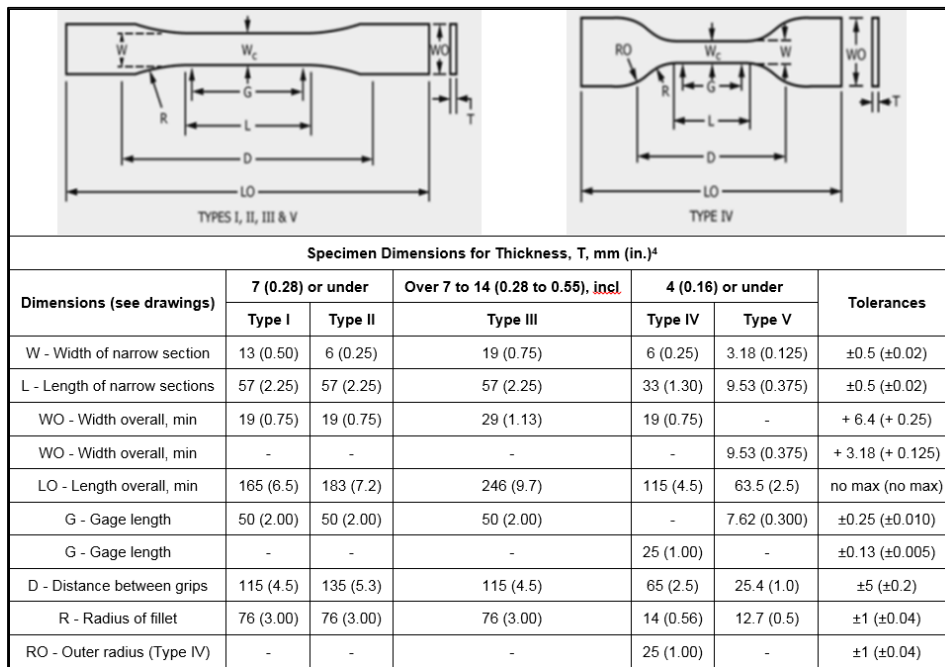


Figure 3-1 Specimen Dimensions (ASTM D638-14, 2010)

3.5.3 Expected Outcome

This test method is designed to produce tensile property data for the control and specification of plastic materials. These data are useful for qualitative characterization and

for research and development. The modulus of elasticity and dimension ratio (OD/t) of iPVC pipe obtained from the testing could be used to predict the expected deflection in the pipe under earth and other loading conditions using Eq. 3.2 as follows:

$$\% \text{ Deflection} = \frac{(D_e K P + K W t) 100}{\{2E/[3(DR-1)^3]\} + 0.061E'} \dots \text{Eq. 3.2}$$

where:

E = Modulus of elasticity of pipe (psi)

DR = dimension ratio (OD/t)

3.5.4 *Benefit to the Industry*

Tensile properties provide useful data for plastics engineering design purposes. Test data obtained by this test method have been found to be useful in engineering design.

3.6 Fatigue Test (Adapted from WRF Report No. 4650, 2016)

3.6.1 *Purpose*

The objective of the experimental fatigue test task at CUIRE was to conduct a high pressure cyclic loading fatigue test on a 8 in. DR18 10 ft long iPVC pipe delivered by PPI. The test determines whether the iPVC pipe can withstand cyclic surge loading that are 1.5 times higher than the operating pressure rating (150 psi for DR 18 iPVC pipe) of the pipe for an extended period of time of 2 million surge cycles.

3.6.2 *Procedure*

The experimental setup consists of a 450-gallon water reservoir tank, a multi-stage centrifugal pump (15 HP), a data acquisition system, a control board, several pressure transducers, a DC power supply, one specimen (9 in. OD and 10 ft long), and control valves including one back-flow pressure valve, two solenoid/pressure ball valves, and two butterfly valves. A galvanized steel pipe system with pipe diameters of one in. and 2-in. connects the equipment.

The back-flow pressure control valves in the test setup protects the pump from excessive water pressure due to water hammer and controls the excessive pressures from the pump at the inlet control valve, which cannot sustain excessive pressures. Back-flow pressure control valve reduces the pressure by assimilating the water head from the multi-stage pump and reduces the surge on the inlet valve. When the pump is powered and the control board is connected to the valves, the inlet valves open and let water run into the specimen. The inlet solenoid valve opens and induces pressure inside the specimen to reach 225 psi, while the outlet solenoid valve reduces the pressure inside the specimen to 150 psi. The control board signalizes both inlet and outlet solenoid valves to open and close.

Further, a pressure transducer is used in the test setup to convert water pressure in the pipe into an analog electrical signal. The transducer is connected to the oscilloscope, which converts the output signal of pressure transducer to a waveform pattern in terms of voltage. The oscilloscope receives a signal from the pressure transducer and demonstrates the pressure waves on a desktop monitor screen. Figure 3-2 and Figure 3-3 presents the schematic diagram and the actual fatigue test setup at CUIRE.

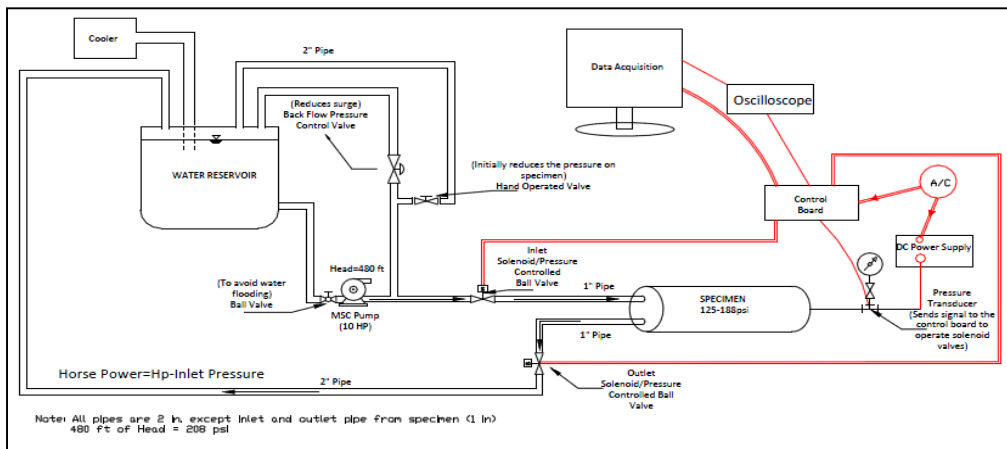


Figure 3-2 CUIRE Fatigue Test Schematic Diagram (Divyashree et al. 2015)



Figure 3-3 CUIRE Fatigue Test Experiment Setup

3.6.3 *Expected Outcome*

This experiment will help in evaluating the reliability and durability of the pipe under surge pressures and predict the approximate service life of the iPVC pipe. The failure of the pipe under fatigue could be evaluated. The rate of expansion of the pipe and dimensional changes could be measured based on the continuous impact of the surges. The results of the tests will be validated with manufacturing specifications (in particular to pressure ratings of the pipes), compared with previous studies and design information of the pipe materials.

3.6.4 *Benefit to the Industry*

There is no known ASTM Standard to evaluate the performance of iPVC pipe under cyclic loads to investigate recurring surge pressures and, hence, this test will act as a performance indicator of iPVC pipe under surge pressures.

3.7 Bedding Test (Adapted from WRF Report No. 4650, 2016)

3.7.1 *Purpose*

To understand pipe deformation pipe under soil loading conditions, outside the AWWA C605 backfilling requirements.

3.7.2 Procedure

The bedding test was performed at the laboratory facility of CUIRE at UTA. Figure 3-4 presents the location of the CUIRE lab and the test location. AW advised UTA to conduct a test similar to the University of Kansas study on SRHDPE (Khatri, 2014).



Figure 3-4 Bedding Test Location

3.7.3 Test Pit

Two test pits were excavated for the bedding test. The trenches were 30 ft long, 32 in. wide and 5 ft deep. Figure 3-5 presents the test pit for the two tests. Figure 3-6 illustrates the installation details for the second bedding test. The type of soil used was lean clay for backfill and embedment.

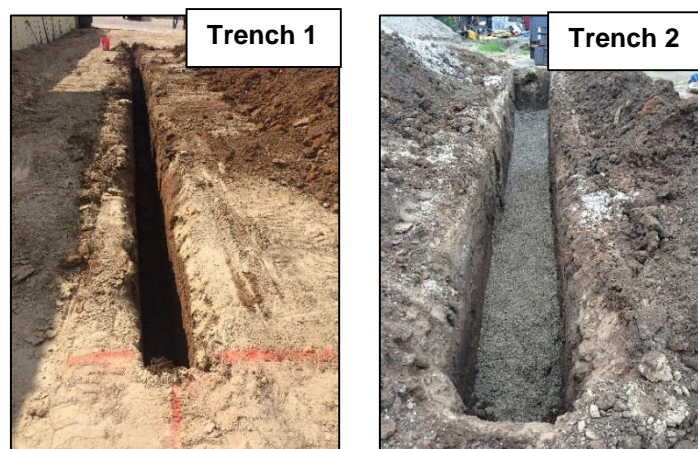


Figure 3-5 Trench 1 and Trench 2 Pit

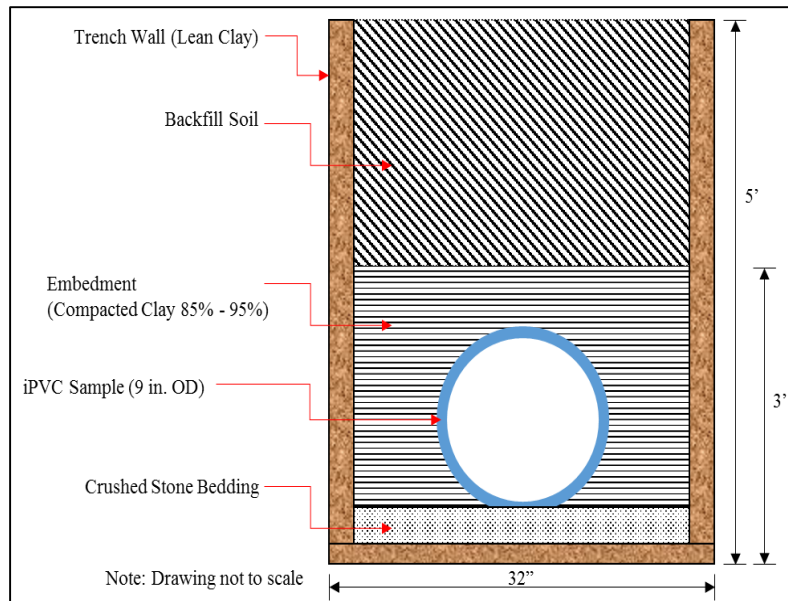


Figure 3-6 Cross Section of Bedding Test 2 Setup

3.7.4 Test Pipe

The two test pipes for the bedding test were provided by PPI and were shipped directly from South Korea to the UTA CUIRE. The 9 in. OD, half in. thick test pipe measured 20 ft with a bell and spigot joint in the middle (at 10 ft). The joints were pre-assembled in South Korea and shipped to UTA for the experimental study on the iPVC pipes.

Two bedding tests were conducted as a part of the testing. The first test (round 1) was piloted in the trench 1 with single joint on a 20 ft length pipe. Due to the pre-assembled joints and smaller pipe diameter, the installation of sensors at the vicinity of joints was not achievable during the first test. To ensure comprehensive research, a second bedding test (Round 2) with an additional joint for the second 20 ft pipe sample was conducted. To accommodate the additional joint, AW, our research associate in Voorhees requested its Missouri counterpart to cut a 10 ft pipe section with bell joint and have it shipped to UTA. The 10 ft section from Missouri American Water was received and the additional sensors were installed.

Before achieving the new joint, the second pipe sample (20 ft length, joint at 10 ft) was curtailed to 12 ft long pipe with a joint at 10 ft. The longer section of the 12 ft pipe became the new spigot end for the Round 2 pipe. The sensors were installed in the vicinity of the new bell and new spigot, and the end of the pipe. The new pipe length for Round 2 measured, 22 ft long with a joint at 10 ft and 20 ft.

3.7.5 *Instrumentation*

Several instruments were deployed to measure the deformation and stress caused due to the movement of soil and simulated load on the test pipes. Instruments such as earth pressure cells, displacement sensors (deflectometers) and strain gauges were deployed to acquire stress, strain and deflection experienced by the test pipes due to the movement of the soil and simulated loads. These instruments were connected to the data loggers and the data loggers were connected to the computer for data recording. Network cables were used to connect the sensors to the data loggers and a total of about 3,000 ft of network cables were required for the experiment.

3.7.5.1 Earth Pressure Cells

Geokon™ Model 4810 vibrating wire earth pressure cells illustrated in Figure 3-7 were used for measurement of horizontal and vertical earth pressures. These sensors are made up of two stainless steel plates welded together around their periphery with a narrow gap in between filled with hydraulic fluid. The external pressures experienced by the two plates squeezes them together creating equal pressure in the internal fluid. A length of stainless steel tubing connects the fluid filled cavity to a pressure transducer that converts the fluid pressure into an electrical signal transmitted by a cable to the data logger. The range of the pressure cells used was 51 psi with an accuracy of 0.1%. The earth pressure cells were used only in the second test. The details and specifications for the sensor are presented in Appendix B.



Figure 3-7 Earth Pressure Cells used in Test

3.7.5.2 Displacement Sensors

Vishay micro-measurements cable-extension displacement sensors (Model CDS-05) were used to measure the horizontal and vertical pipe deflections. The sensor delivers a voltage signal linearly proportional to the extension of a retractable stainless steel cable. The base of the sensors are attached to the pipe surface and the string cable is attached to a hook to the opposite end on the pipe surface. An electrical wire from the sensors is connected to a data logger which is further connected to the computer for data collection. Two sensors were used for Test 1, and four sensors were used for Test 2 to measure the deflections. Figure 3-8 presents the displacement sensors (CDS) used for the tests. The details and specifications for the sensor are presented in Appendix B.

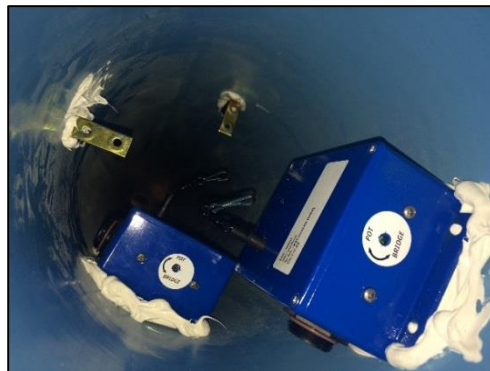


Figure 3-8 Displacement Sensors Attached to iPVC pipe for Round 2 Test

3.7.5.3 Strain Gauges

The strain gauges were deployed to measure the strain on the pipes due to external loads. The experiment uses the gauges manufactured by Tokyo Sokki Kenkyujo Co., Ltd. (Model FLA-6-11) uniaxial strain gauges for the measurement of strains. The strain gauges were used only in Round 2. The installed strain gauge on the pipe is illustrated in Figure 3-9. The details and specifications for the sensor are presented in Appendix B. Installation of strain gauges is a delicate process and the following steps summarize the installation procedure:

- i. First step of strain gauge installation is to prepare the surface for the attaching of the strain gauge.
- ii. An iPVC pipe sample was prepared to attach the strain gauges as below:
 - The surface of the iPVC pipe sample was cleaned where the gauge was supposed to be placed. Sandpaper was used to increase the surface area for contact of strain gauge with iPVC pipe.
 - The conditioner provided by Vishay Micro-measurements was applied to the iPVC pipe sample to clean the surface thoroughly.
 - Neutralizer was applied to the iPVC pipe sample to remove any remaining dust particles on the surface.
 - Catalyst provided by Vishay Micro-measurements was applied to the surface of the iPVC pipe sample. This helps in reducing the time required for the strain gauge to bond with the sample.
 - M-Coat A adhesive was applied on the strain gauge and then the strain gauge was attached to the iPVC pipe sample. Pressure was applied for two minutes on top of the strain gauge to develop a proper bond between the gauge and iPVC pipe.

- Further, M-Coat JA-1 was applied on top of the strain gauge for extra protection to the gauges.
- The wire from the strain gauge is further connected to the Vishay™ System 7000 data logger similar to the displacement sensors, and the data is collected on a computer.



Figure 3-9 Strain Gauge attached to iPVC pipe

3.7.5.4 Data Loggers

Separate data loggers were used to accrue data from the attached pipe.

i. Data Logger - Earth Pressure Cells

Geokon™ 8002-16 (LC-2 x 16) was used to collect and record data from earth pressure cells. The data logger consists of 16 channels out of which eight channels are used for eight earth pressure cells. Figure 3-10 illustrates the data logger used in the second round test. The data logger was connected to a desktop computer and data was retrieved by using Geokon™ Logview software. The details and specifications for the data loggers are presented in Appendix B.

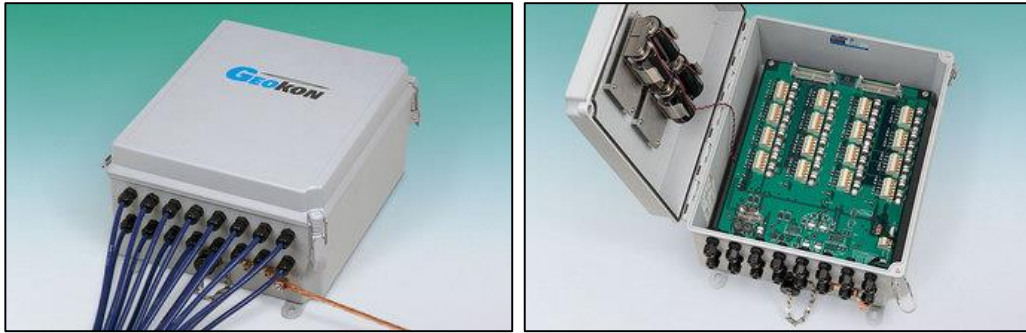


Figure 3-10 Geokon™ 8002-16 (LC-2 x 16) Data Logger used in Test 2 (Geokon 2016)

ii. Data loggers for Displacement Sensors

A 4 channel P3 model from Vishay™ was used for Test 1 to collect the deflection readings from the two sensors used for the test with the help of a software specific for this data logger. Figure 3-11 illustrates the P3 data logger.

iii. Data Loggers for Strain Gauges

A Vishay™ System 7000 32 channel scanner was used to collect and record data from displacement sensors and strain gauges in Test 2. The scanner was connected to desktop computer for data logging. Strain Smart™ software was used to collect the data recorded by the scanner. Figure 3-11 presents the scanner used in the Test 2. The details and specifications for the sensor are presented in Appendix B.



(a)

(b)

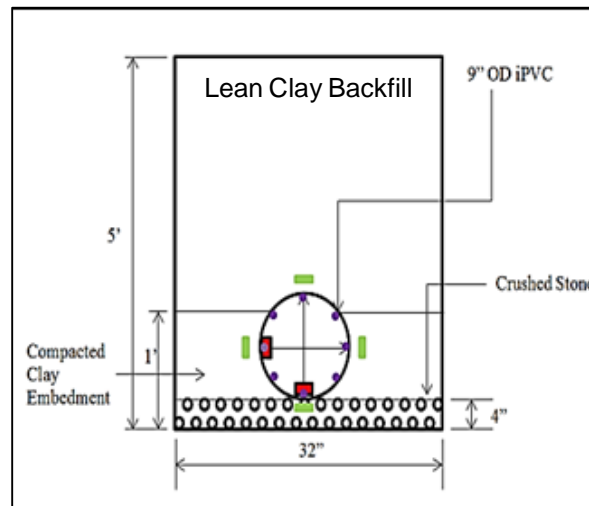
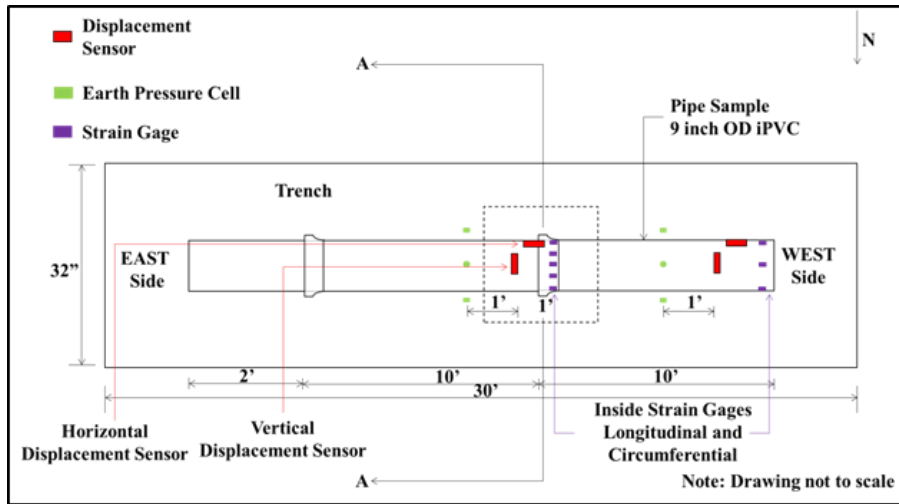
Figure 3-11 (a) P3 Data Logger for Test 1, (b) System 7000 Data Logger for Test 2

3.7.5.5 Installation of the Sensors

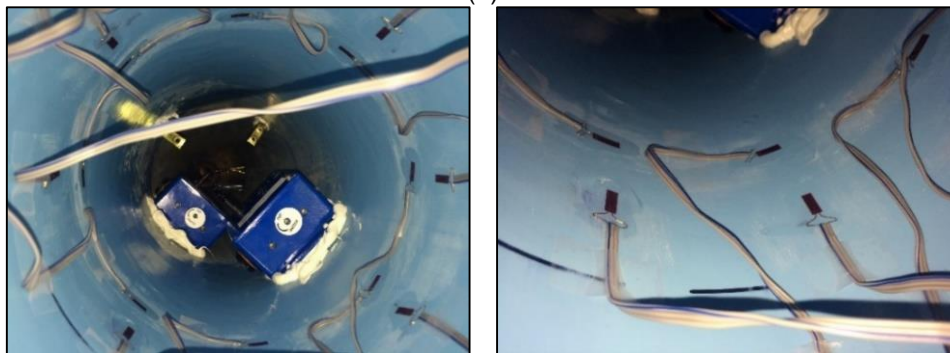
The Round 1 test was completed by installing two displacement sensors each at the end of the test pipe to measure the vertical deflection. Further, for the Round 2 test, it was deemed necessary to have more comprehensive research. Hence, the second test setup was designed with AW consultation and pursued an approach studied at the University of Kansas, to test steel reinforced high density polyethylene (SRHDPE) pipe (Khatri, 2014).

The second pipe sample was instrumented with four displacement sensors, 20 strain gauges, and eight earth pressure cells. Two displacement sensors, 16 strain gauges and four earth pressure cells are placed at the joint of the pipe and the remaining two displacement sensors, four strain gauges and four pressure cells are placed 2 ft from the end of the pipe. The displacement sensors will provide the deformation in the horizontal and vertical directions, in the pipe wall at the joint and at the end of pipe due to the load experienced by the pipe.

The strain gauges will provide the strain experienced by the pipe walls longitudinally and circumferentially at the gauge mounted locations. The use of earth pressure cells allows to measure the load experienced by the pipe walls due to the soil as well as any external loads exerted on the pipe. The location of sensors is of great significance in this test. Figure 3-12 presents the locations of the pressure cells, displacement sensors as well as the strain gauges.



(a)



(b)

Figure 3-12 (a) Schematic diagram showing location of instruments, (b) Actual photographs for displacement sensors and strain gauge location

3.7.5.6 Nomenclature

It was important to mark the location of sensors on the pipe as well as use proper nomenclature to collect data. The pipe was identified based on the Figure 3-13.

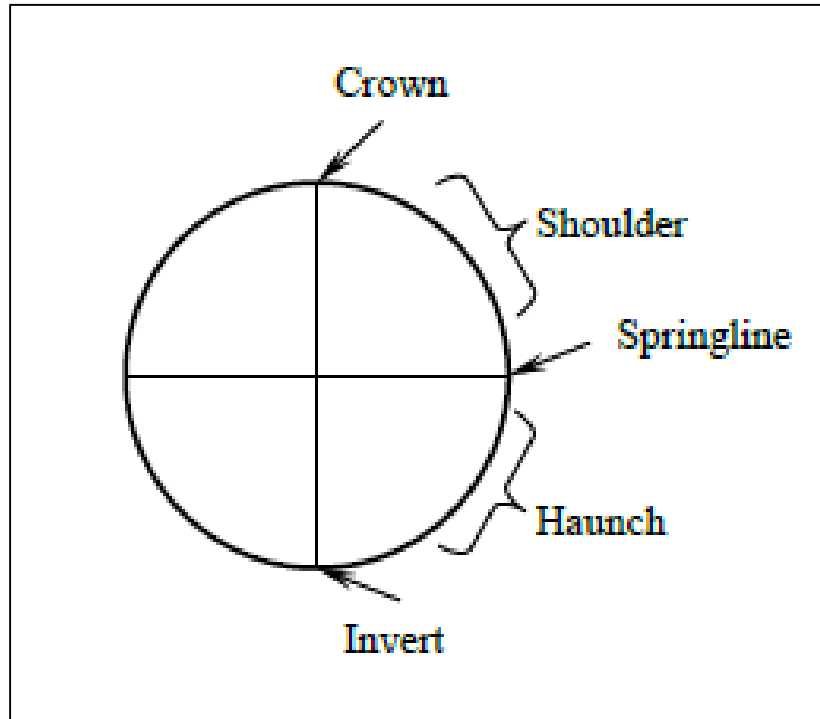


Figure 3-13 Sectional View of a Typical Pipe

The sensors were abbreviated as SG for strain gauges, CDS for displacement sensor, and EPC for earth pressure cells. The direction of measurements used were circumferential (C), longitudinal (L), vertical (V), and horizontal (H). The load measured from the EPC was either a vertical load (VL) or side load (SL). Further, a nomenclature system was developed as illustrated in Figure 3-14. Table 3-1 presents the sensor details as per location, direction of measurement, and the code used in this test.

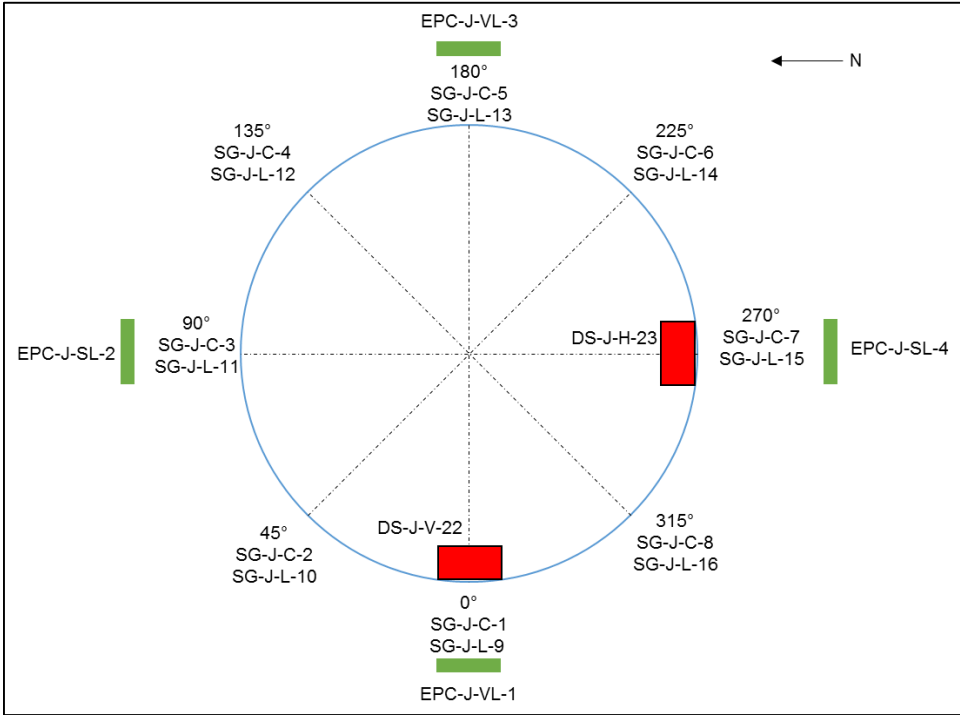
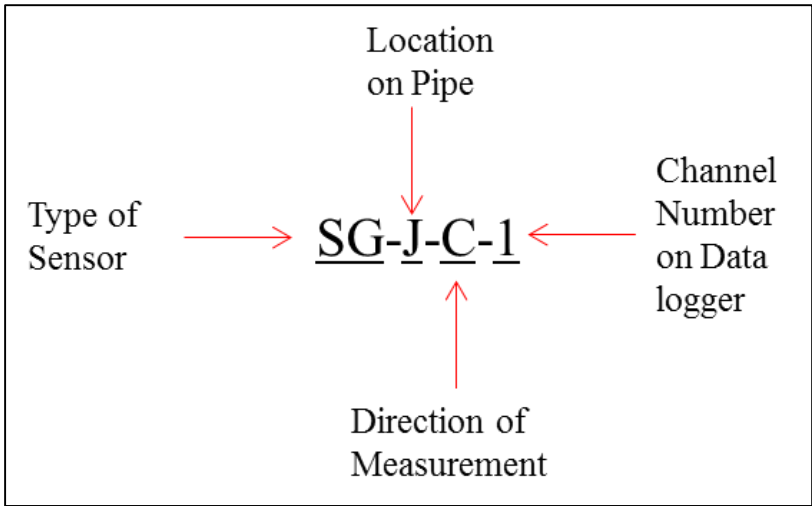


Figure 3-14 Nomenclature Used for Sensors in Bedding Test 2

Table 3-1 Details of Sensors used for Bedding Test 2

Sr. No.	Code	Sr. No.	Code	Abbreviations
1	SG-J-C-1	19	EPC-J-VL-1	SG - Strain Gauge DS - Displacement Sensor EPC - Earth Pressure Cell
2	SG-J-C-2	20	EPC-J-SL-2	
3	SG-J-C-3	21	EPC-J-VL-3	
4	SG-J-C-4	22	EPC-J-SL-4	
5	SG-J-C-5	23	EPC-J-VL-5	
6	SG-J-C-6	24	SG-E-C-18	J - Joint
7	SG-J-C-7	25	SG-E-C-19	E - End of Pipe
8	SG-J-C-8	26	SG-E-C-20	
9	SG-J-L-9	27	SG-E-C-21	V – Vertical
10	SG-J-L-11	28	SG-E-L-27	H – Horizontal
11	SG-J-L-12	29	SG-E-L-28	
12	SG-J-L-13	30	SG-E-L-29	C – Circumferential
13	SG-J-L-14	31	DS-E-V-24	L - Longitudinal
14	SG-J-L-15	32	DS-E-H-25	VL - Vertical Load
15	SG-J-L-16	33	EPC-E-VL-6	SL - Side Load
16	SG-J-L-17	34	EPC-E-SL-7	
17	DS-J-V-22	35	EPC-E-VL-8	
18	DS-J-H-23	36	EPC-E-SL-9	

3.7.5.7 Data Collection and Monitoring

The data from the first test is collected in the P3 model data logger from Vishay™. The two sensors from the test pipe are connected to the P3 with the help of two Ethernet cables. The P3 is further connected to the computer which records the deflection data for the test pipe every day and the data is displayed on the computer with the help of a software specific to the P3 data logger.

The data collection for the second test was more complicated and involved the use of two different software programs. The earth pressure cell readings were collected with the help of Geokon™ 8002-16 (LC-2 x 16) data logger and Geokon™ Logview software. The deflection readings and the strain gauge readings were collected using Vishay™ System 7000 32 channel data logger and Strain Smart™ software. The data was collected every day since installation of the pipe and the whole setup of data collection was monitored once or twice a week to ensure that the data was being recorded and the

sensors were working correctly. The data collected from the sensors is exported to Microsoft Excel and stored in a compiled data file for all the readings.

3.7.5.8 Sign Conventions

Measurement of pipe deflections (changes in horizontal and vertical diameters), and pipe wall strains require establishment of a sign convention for collecting the results. Thus any decrease in diameter is reported as negative deflection and any increase in diameter is reported as positive deflection. Likewise, when pipe wall strains are reported, compressive strains will be reported as negative (–) and tensile strains (+) will be reported as positive.

3.7.6 *Pipe Installation*

A 4 in. trench bottom was prepared using crushed stone before iPVC pipe was installed in the trench. The round 2 installation of iPVC pipe was carried out on February 12 and 13, 2016. Figure 3–15 presents the installation work of iPVC pipe. Before installation, the pit was marked for locations of pressure cells around the pipe. The pressure cells were protected with a thermo-ply sheet to avoid any damage as well as it helps in locating the pressure cells after completion of the testing. The backfilled soil was compacted (85% - 95% compaction was achieved) around the pipe for a height of 3 ft from the bottom of the trench. Remaining 2 ft of trench was backfilled with the lean clay. Extra soil and gravel was added on the surface of the trench to apply more load on the pipe.



Figure 3-15 iPVC Pipe Installation

3.7.7 Live Load Simulation

A truck was used to create a live load simulation on top of the trench. A 20 ton truck was loaded with gravel with a total combined weight of truck and gravel of 50,000 lbs.

The truck was driven on the top of the trench along the length of the pipe to exert load on the whole iPVC pipe sample. The truck was driven for 2 hours and then it was halted on top of the trench for another 2 hours.

3.8 Pipe Modeling using Finite Element

To evaluate the deflection of pipe under the soil and live loads similar to the experimental bedding test, finite element (FE) model was prepared using PLAXIS 2D and ABAQUS 6.14-3 software. For modeling purposes, standard boundary conditions were considered as illustrated in Figure 3-16. Although bedding was provided in the experimental test, FEA was performed for worst conditions of pipe installation i.e. without any bedding support to get the maximum deflection iPVC pipe could experience in PLAXIS 2D. ABAQUS model considered the standard conditions of bedding to represent the conditions similar to the bedding test.

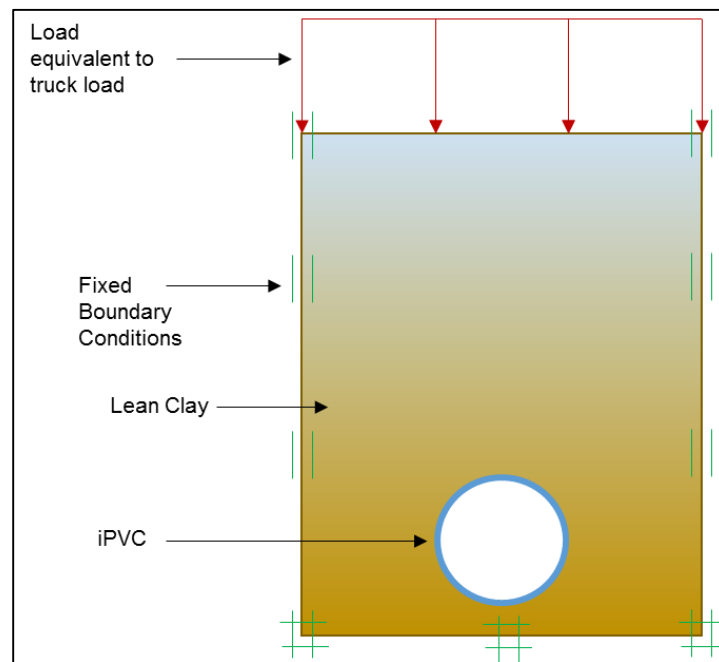


Figure 3-16 Boundary Conditions

The soil characteristics used for the analysis were considered from a previous research by Sharma (2013) which studied the soil at CUIRE for another testing. The same soil was used for the bedding test performed in this dissertation. A detailed analysis, assumptions in the FEA, and the simulation results are presented in Chapter 5.

3.9 Chapter Summary

This chapter discussed the various test procedures performed for the iPVC pipe project. Hydrostatic short term burst pressure test, impact test, tensile test, stiffness test, fatigue test and the bedding tests performed by CUIRE and Microbac as a part of this dissertation as well as the iPVC pipe project were discussed in detail. The purpose of testing, procedures, expected outcomes and benefit to the industry were described. This chapter is an adaptation of the WRF Report No. 4650 (2016) entitled “An Evaluation of the Value of Structurally Enhanced PVC Pipe.”

Chapter 4

Research Results

Chapter 3 discussed in detail the testing methodology for the iPVC pipe testing developed by AW and performed by CUIRE and Microbac. This chapter presents the testing results from CUIRE and Microbac performed under the supervision of AW conducted as a part of the WRF Project Report No. 4650. These results have been divided according to tests performed on iPVC pipes.

4.1 Hydrostatic Short-term Burst Pressure Test

This test was conducted first by CUIRE and then Microbac to determine the ultimate burst pressure of the iPVC pipe and to study the way this pipe might fail in the field. The testing was performed as per ASTM D1599-14. Ductile and brittle failures were observed in iPVC pipe in this test. Brittle failure could be defined as the bursting of pipe throughout the circumference with broken pieces whereas ductile failure could be defined as the failure of pipe with pressure loss, ballooning of pipe and pin hole leak observed in pipe samples. All the samples at CUIRE experienced brittle failure of iPVC pipe. Six samples at Microbac experienced brittle failure and four samples experienced ductile failure. Figure 4-1 (a) illustrates a typical brittle failure observed during testing of iPVC pipe at CUIRE and (b) illustrates the ductile failure that was observed at Microbac for an iPVC pipe specimen. Table 4-1 presents test results.

The average pressure at failure for this was 1,065 psi with average time of 84 seconds (CUIRE) and 1,033 psi with 123 seconds (Microbac). The average failure pressure is 40% higher than the AWWA C900 requirement for DR 18 pipe (755 psi) and the average failure time is 76% more than maximum 70 seconds taken to reach 755 psi. The rate of application of pressure, i.e., the time taken to increase the pressure inside the iPVC pipe sample was longer in the testing at Microbac as compared to CUIRE. This does not mean

that the pipe failed earlier than expected at CUIRE. The settings on the equipment for burst pressure were different. CUIRE decided to apply pressure at a faster rate as compared to Microbac (WRF Report No. 4650, 2016).

Data obtained from this test method can be used to predict the behavior of pipe and the failure mode under high hoop stress. Figure 4-2 summarizes the hydrostatic burst pressure test results for iPVC pipe in a graphical chart.



(a) (b)
 Figure 4-1 iPVC pipe Failure in Short-term Burst Pressure Test:
 (a) Brittle Failure and (b) Ductile Failure
 (Source: WRF Report No. 4650, 2016)

Table 4-1 Short-term Burst Pressure Test Results from Microbac and CUIRE

Sample No.	Failure Pressure (psi)	Failure Time (seconds)	Failure Mode
1	1,070	127	Brittle
2	1,050	112	Brittle
3	1,020	122	Brittle
4	1,050	101	Brittle
5	1,010	113	Brittle
6	1,030	116	Brittle
7	1,030	150	Ductile
8	1,010	145	Ductile
9	1,035	126	Ductile
10	1,020	121	Ductile
11	1,065	56	Brittle
12	1,060	59.7	Brittle

Table 4-1 — *Continued*

Sample No.	Failure Pressure (psi)	Failure Time (seconds)	Failure Mode
13	1,060	139	Brittle
14	1,075	80	Brittle
Average	1,042	112	-
Std. Dev.	21	27	-

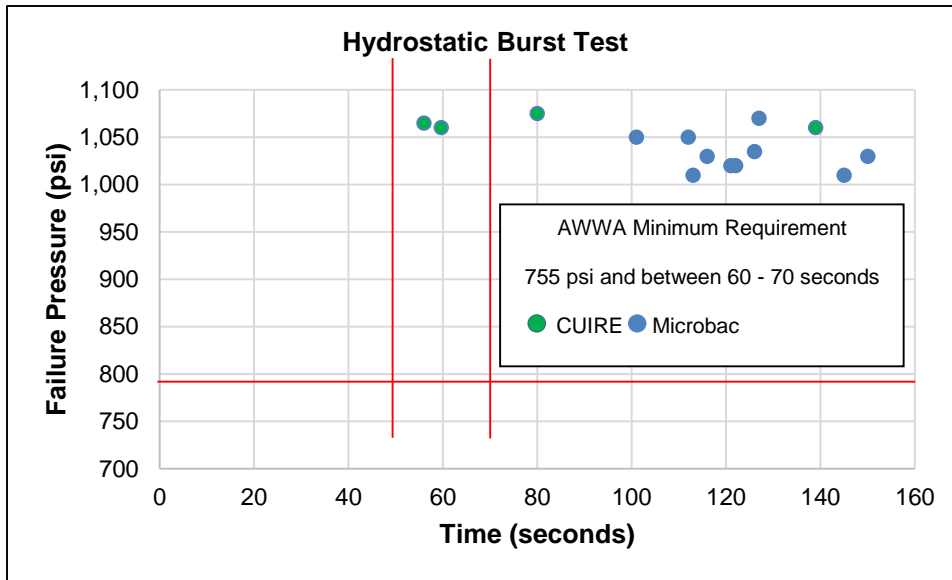


Figure 4-2 Graphical Illustration of Hydrostatic Burst Test Results (WRF Report No. 4650, 2016)

4.2 Impact Test

The impact test was performed in accordance with ASTM D2444-99 standards on partial number of samples at 73 °F with standard tup A (cone-shaped, see Figure 4-3 a) as the falling weight, weighing 100 pounds with a drop height 12 ft (maximum height at the lab). The TUP was able to generate maximum impact energy of 1,200 foot-pounds with this height and weight combination. The test was performed on 35 pipe samples with this configuration, and the maximum impact of the apparatus did not break, but only dented the surface of the pipe samples at 73 °F (see Figure 4-3 b).

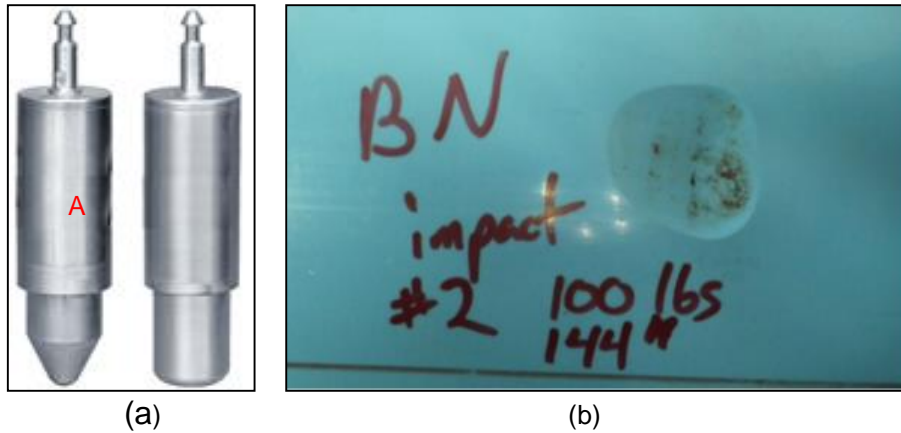


Figure 4-3 (a) Falling Weight TUP A and (b) Impact Test Results at Microbac

In order to test the material to failure in some way, AW decided to test the pipe samples at a colder temperature (32 °F) which could be readily achieved at the Boulder, Colorado laboratory in January. The samples were conditioned at 32 °F for 16 hours and impacted within 1 minute of removal from sub-ambient temperature. This test resulted in the breaking of the pipe sample at 1,050 foot-pounds (dropping the 100 pound tup from a drop height of 10.5 ft). Table 4-2 and Table 4-3 summarizes the partial test results for the impact test at 73 °F and at 32 °F (WRF Report No. 4650, 2016).

Table 4-2 Impact Test Results at 73 °F at Microbac for Partial Number of Test Samples

Specimen	Weight of Tup	Height of Drop	Impact Energy	Results
	lbs	ft	ft-lbs	
AV	30	10	300	Pass
AB	30	10	300	Pass
Z	35	10	350	Pass
N	40	10	400	Pass
T	40	11.8	470	Pass
BP	50	12.3	613	Fail
Q	60	12.3	737	Pass
K	60	12.3	737	Pass
BS	65	12.3	799	Pass
L	65	12.3	799	Pass
AJ	70	12.3	860	Pass
AB	100	12	1200	Pass
BN	100	12	1200	Pass

Table 4-3 Impact Test Results at 32 °F at Microbac for Partial Number of Test Samples

Specimen	Weight of Tup	Height of Drop	Impact Energy	Results
	lbs	ft	ft-lbs	
BO	40	10.8	433	Pass
AO	40	11.1	443	Pass
BN*	20	11.8	237	Pass
AB*	40	11.8	473	Fail
AJ*	40	10.8	433	Pass
BS*	40	11.3	453	Fail
Q*	40	11.1	443	Fail
N*	40	11.1	443	Fail
K*	40	11.1	443	Pass
L*	40	11.3	453	Pass
AV*	50	11.8	588	Pass
Z*	50	12.3	613	Pass

Note: * Specimen tested at 73 °F earlier

The partial impact test results at 73 °F were better than expected; hence, retesting the samples that did not fail was undertaken with an increased weight of tup and increased drop height to evaluate the performance of the iPVC pipe with further details. Table 4-4 presents the impact test results at 32 °F for the samples that were tested earlier at 32 °F and did not fail (WRF Report No. 4650, 2016).

Table 4-4 Impact Retest Results at 32 °F at Microbac for Partial Number of Test Samples

Specimen	Weight of Tup	Height of Drop	Impact Energy	Results
	lbs	ft	ft-lbs	
L	40	11.6	463	Pass
AO	40	11.8	473	Pass
BO	50	12.3	613	Fail
K	50	11.3	563	Pass
AJ	50	11.8	588	Pass
BN	50	12	600	Pass

Table 4-4 — *Continued*

Specimen	Weight of Tup	Height of Drop	Impact Energy	Results
	lbs	ft	ft-lbs	
Z	55	12.3	674	Pass
AV	55	12.3	674	Pass
BN	65	12.3	796	Pass
K	75	12.3	919	Pass
AO	85	12.3	1041	Pass
AJ	85	12.3	1041	Pass
L	85	12.3	1046	Fail
AJ	85	12.3	1046	Pass
AV	85	12.3	1046	Fail
Z	85	11.8	1004	Fail

The impact resistance of thermoplastic pipe such as iPVC pipe is a function of the material, the quality of extrusion or molding, geometry and dimensions of the test specimen and of testing variables such as temperature, tup nose geometry, tup weight, specimen support, and height of drop. As all of these factors play a role in the impact strength of iPVC pipe, impact tests are mainly used for quality control and comparative purposes (WRF Report No. 4650, 2016).

4.3 Stiffness Test

The third test performed by Microbac was the stiffness test per ASTM D2412-11. This test is critical to determine the deflection and vertical load resistance of the pipe, considered a key design element for pipe installation. The maximum allowable design deflection for PVC pipe is 5% as per AWWA M23 standards. In this test, pipe sample was placed between two parallel plates of machine and a controlled load was applied on 8 in. long pipe samples. The behavior of pipe was studied at 5% decrements from 95% of the pipe diameter through 20% or until the inner walls of pipe are in contact (see Figure 4-4). The pipe deformed beyond 20% and the average load at 20% was about 7,500 psi without

cracking and the average load beyond 20% was about 10,500 psi (WRF Report No. 4650, 2016).

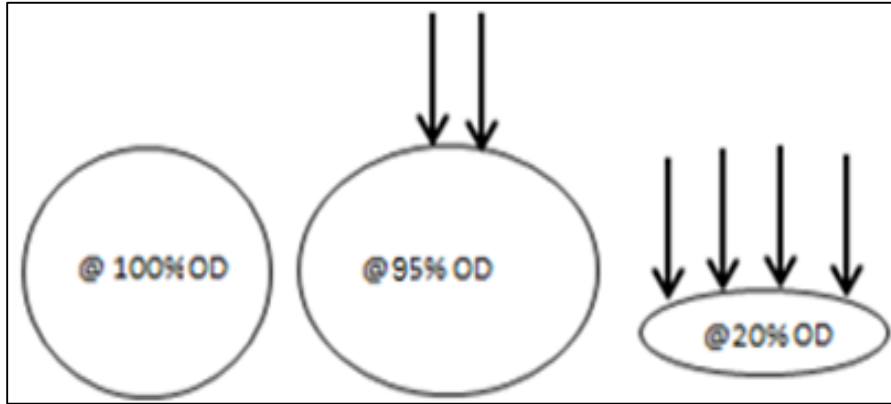


Figure 4-4 Deflection of Pipe during Stiffness Test
(Source: WRF Report No. 4650, 2016)

Pipe stiffness (PS) is the inherent resistance of flexible pipe to deflect under load.

PS is defined by the following Equation 4.1 as per ASTM D2412-11:

$$PS = \frac{F}{\Delta Y} \dots\dots\dots \text{Eq. 4.1}$$

Where:

PS = pipe stiffness, psi

F = force, lb/in. of sample length,

ΔY = vertical deflection, in.

Sample Calculation:

For sample R in Table 4-5,

Load = 1,508 lbs

Length of sample = 7.87 in.

$F = 1,508/7.87 = 191.6 \text{ lbs/in.}$

$\Delta Y = \text{OD} - 95\% \text{ of OD} = 9 \text{ in.} - 8.6 \text{ in.} = 0.4 \text{ in.}$

$$PS = \frac{F}{\Delta Y} = \frac{191.6}{0.4} = 479 \text{ psi}$$

Ten samples were tested and the average pipe stiffness at 95% deformation was 479 psi. This exceeds the minimum AWWA requirements of 364 psi at 95% deformation (AWWA M23 Manual, Table 4-2, Pg. 26). The partial stiffness test results are presented in Table 4-5. Figure 4-5 illustrates the load versus deflection of all the pipe samples (WRF Report No. 4650, 2016).

Table 4-5 Partial Stiffness Test Results for iPVC pipe at Microbac

Specimen	Load @ 95 % OD	F @ 95% OD	Pipe Stiffness @ 95% OD	Load @ 20% OD	F @ 20% OD	Pipe Stiffness @ 20% OD
	lbs	lbs/in.	psi	lbs	lbs/in.	psi
R	1,508	191.6	479	7,701	978.5	153
Y	1,468	184.8	462	7,517	946.3	148
W	1,540	193.6	484	7,650	961.7	150
U	1,490	190.8	477	7,502	960.7	150
V	1,521	192.8	482	7,628	966.9	151
AS	1,509	192.4	481	7,477	953.3	149
AP	1,553	195.6	489	7,759	977.2	153
AQ	1,448	186.4	466	7,276	936.3	146
AU	1,548	196.4	491	7,663	972.2	152
Average	1,509	191.6	479	7,575	961.5	150
Std. Dev.	36	4	10	147	13	2

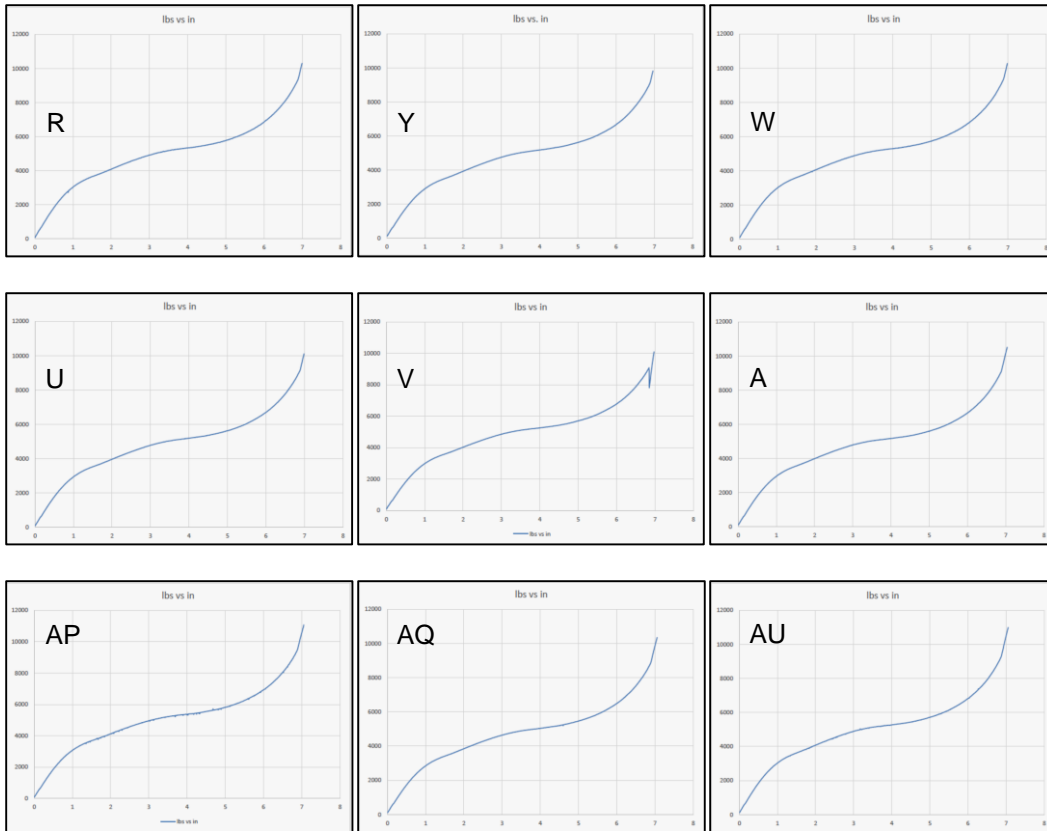


Figure 4-5 Load vs. Deflection in Stiffness Test
(Source: Microbac)

4.4 Tensile Test

Microbac conducted tensile tests per ASTM D638-14, type I and type III tensile samples and UTA conducted test with type III tensile samples. Initial tensile test was conducted by UTA using type III samples, the type III samples are full walled samples (thickness = 0.5 in.). To validate the UTA results, 10 type III samples were provided to Microbac to conduct the tensile test. According to AWWA, the ASTM D1784-11 Cell Classification 12454-B PVC material must be tested for type I sample preparation. Each type I sample was prepared by trimming the mid-wall section of the pipe in the form of standard dumbbell-shape as per ASTM D638-14. Each Type III sample was prepared with

full section of the pipe wall. Each pipe sample was tested under defined conditions of pretreatment, temperature, humidity, and testing machine speed within the ASTM requirements resin (see Figure 4-6).



Figure 4-6 Type I Tensile Test (Mid-wall) in Action at Microbac

The average tensile strength observed for the type I test was 7,930 psi with a modulus of elasticity of 461,000 psi, exceeding the preliminary results provided by PPI testing. The testing results exceeded the AWWA C900 pipe requirement by 13% in the tensile strength (7,000 psi) and the modulus of elasticity (400,000 psi) by 15%. Table 4-6 summarizes the test results from the Microbac for type I pipe samples. Figure 4-7 and Figure 4-8 presents a graphical summary of tensile strength and modulus of elasticity values of the type I iPVC pipe samples (WRF Report No. 4650, 2016).

Table 4-6 Type I Mid-wall Pipe Sample Tensile Test Results at Microbac

Specimen	Width (in.)	Thickness (in.)	Tensile Strength (psi)	Modulus of Elasticity (psi)
A-1	0.498	0.130	8,030	459,000
A-2	0.499	0.130	8,010	424,000
A-3	0.498	0.130	7,880	455,000
A-4	0.498	0.129	7,890	499,000
A-5	0.498	0.130	7,970	448,000
A-6	0.498	0.130	7,920	501,000
A-7	0.499	0.130	7,880	559,000
A-8	0.499	0.131	7,800	401,000
A9	0.499	0.129	7,900	420,000
A-10	0.501	0.131	8,020	448,000
Average	-	-	7,930	461,400
Std. Dev.	-	-	75	46,755

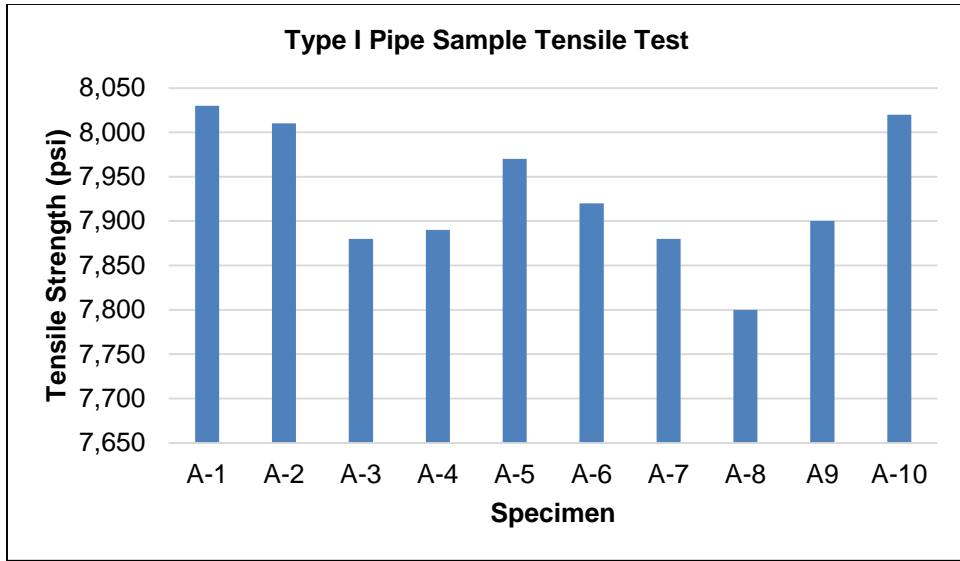


Figure 4-7 Tensile Strength of Type I iPVC pipe Specimen
(Source: WRF Report No. 4650, 2016)

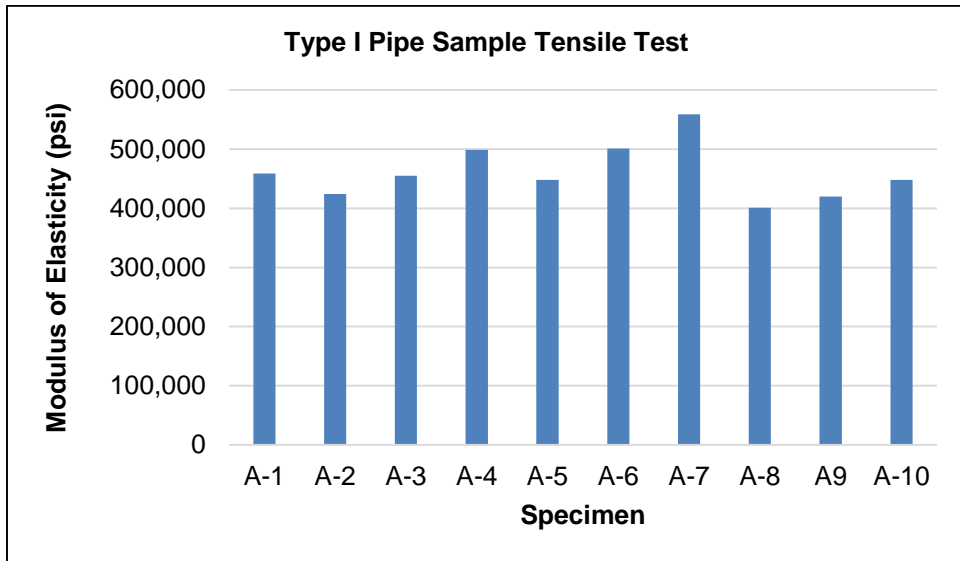


Figure 4-8 Modulus of Elasticity of Type I iPVC pipe Specimen
(Source: WRF Report No. 4650, 2016)

Tensile test was performed on 16 type III samples (full-wall) per ASTM D638-14 (see Figure 4-9). The average tensile strength reported for these test samples was 7,920 psi. The results are summarized in Table 4-7. Figure 4-10 and Figure 4-11 presents a

graphical summary of tensile strength and modulus of elasticity values of the type III iPVC pipe samples (WRF Report No. 4650, 2016).



Figure 4-9 Tensile Test Type III (Full-wall) Testing at CUIRE

Table 4-7 Type III Full-wall Pipe Sample Tensile Test Results at Microbac and CUIRE

Specimen	Width	Thickness	Tensile Strength	Tensile Modulus (Tangent)
	in.	in.	psi	psi
DB	0.749	0.540	7,840	396,000
DC	0.750	0.528	7,870	382,000
DD	0.747	0.528	7,820	394,000
DE	0.747	0.536	7,820	389,000
DF	0.751	0.535	7,810	383,000
DQ	0.749	0.536	7,790	389,000
DH	0.749	0.524	7,830	400,000
DI	0.751	0.536	7,770	404,000
DK	0.749	0.541	7,810	396,000
DN	0.753	0.530	7,810	420,000
DG	0.748	0.531	8,322	-
DJ	0.749	0.531	8,385	-
DL	0.748	0.531	9,149	-
DM	0.75	0.541	6,825	-
DPP	0.747	0.531	7,518	-
DU	0.748	0.541	8,328	-
Average	-	-	7,920	395,300
Std. Dev.	-	-	470	10,570

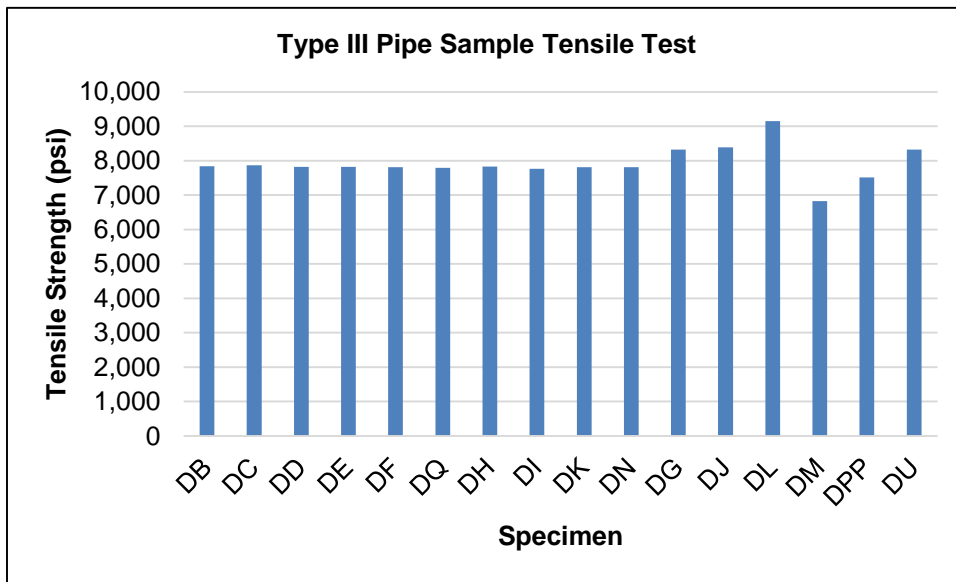


Figure 4-10 Tensile Strength of Type III iPVC pipe Specimen

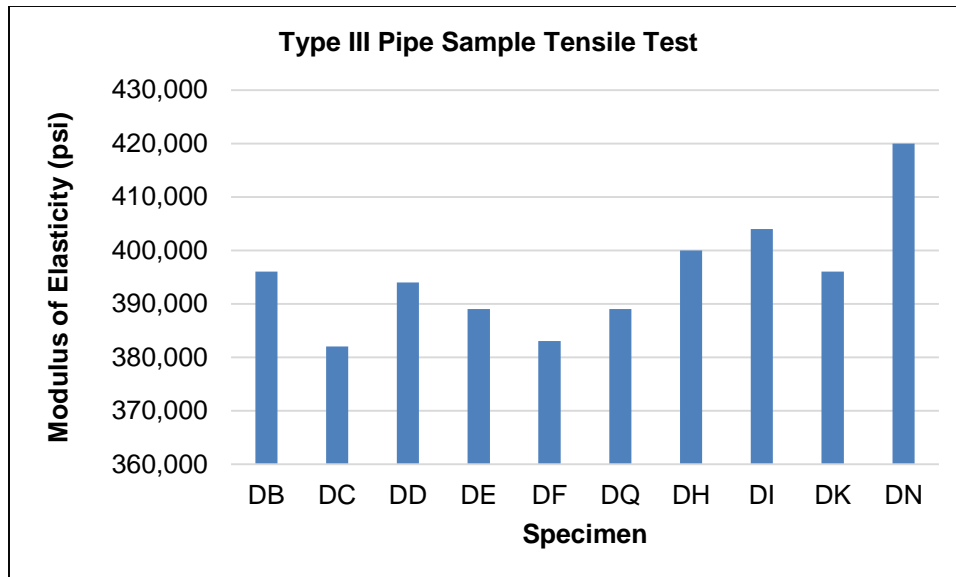


Figure 4-11 Modulus of Elasticity of Type III iPVC pipe Specimen

A few anomalies were reported in the testing results while testing at CUIRE at UTA. The reasons for these anomalies could be improper conditioning of pipe samples before the testing, samples tested under higher capacity MTN machine, inaccurate placement of samples on the testing machine or improper grips to secure the samples (WRF Report No. 4650, 2016).

4.5 Fatigue Test

The objective of this test was to trigger continuous high pressure cyclic loading to determine whether the 9 in. OD DR 18 iPVC pipe can withstand the induced cyclic loads of 1.5 times higher than the operating pressure rating of the pipe (150 psi) for 2 million cycles. The water pressure inside the pipe sample was varied between 150 psi to 225 psi in 10 – 12 seconds per cycle (at the rate of 5 – 6 cycles per minute). Initially, the pipe was marked to measure the circumference at three locations, then the project team decided to measure the pipe at as many locations as possible. The 10 ft pipe was marked longitudinally at 15 locations (A through O) and the increment in the circumference was

measured at regular intervals as the test progressed (see Figure 4-12). The temperature of water was maintained at 60 °F throughout the test using coolers attached to the reservoir.

The first set of readings were reported after the completion of 40,000 cycles. There was marginal increment of 2 mm in circumference of pipe at six locations. The research team suspected the increment in the circumference of the pipe, might have increased due to initial pressurization of the pipe, as they remain constant afterwards. To validate this assumption, the test was stopped intentionally after completion of half a million cycles and readings were obtained. The pipe sample regained its original dimensions at all the 15 points, validating the cause of circumferential changes was due to the internal pressure exerting hoop stress in the pipe. 14 locations out of 15 marked on the pipe witnessed negligible change (-2 mm to 3 mm) in the circumferential variations. The test was stopped after completing 2.3 million cycles (on June 8, 2016).

After stopping the test, the maximum circumferential change observed was 3 mm at locations A, B, C, D, F, G, H, I, J, K, L, M, N, and O. One week after stopping the test, the circumference regained its original dimensions at 14 out of the 15 locations. The results achieved were for a 9 in. OD DR 18 iPVC pipe and it is likely that the results would vary for iPVC pipe based on the diameter size as well as the DR. The change in circumference as the test progressed is illustrated in Figure 4-13. This test will help in evaluating the reliability and durability of the iPVC pipe (WRF Report No. 4650, 2016).

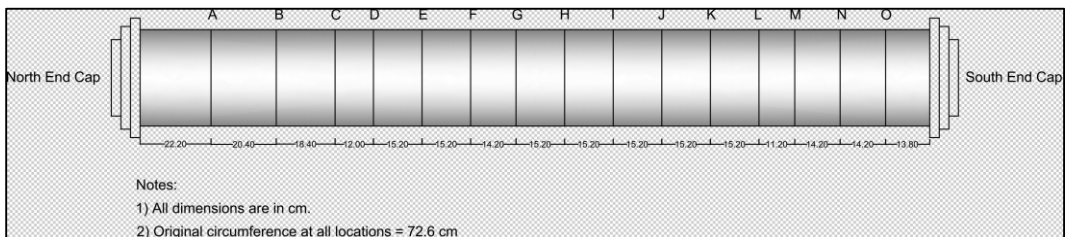


Figure 4-12 Change of Pipe Circumference Measurement Locations on iPVC pipe

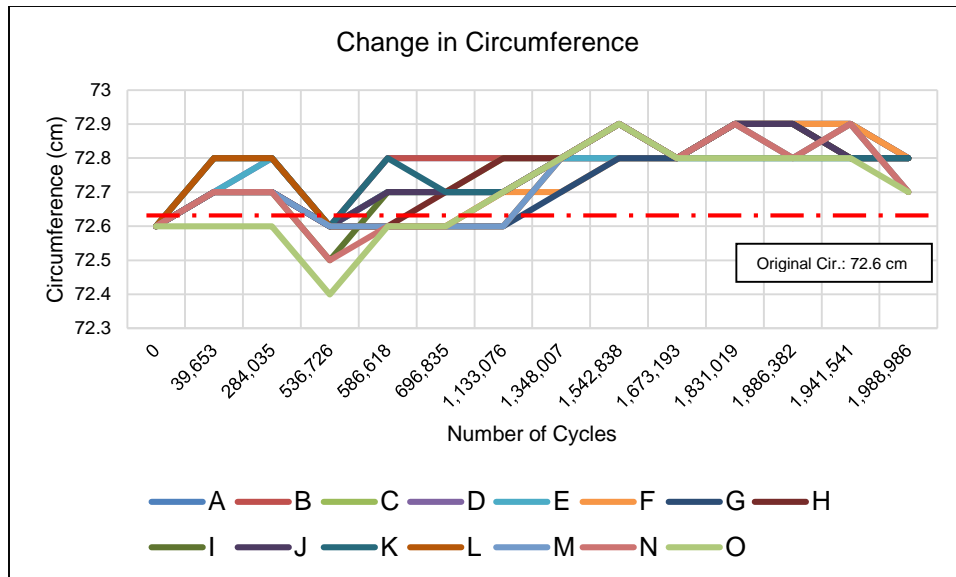


Figure 4-13 Change in Circumference at Various Stages

4.6 Bedding Test

The first round bedding test results were not considered in this dissertation as the sensors installed on the first iPVC pipe sample were insufficient to provide enough data for analysis. Only two displacement sensors were installed in the first round test without strain gauges or pressure cells. Under the guidance of AW and based on the report by Khatri (2014), second bedding test was conducted with sufficient sensors for data collection. The data collection for second round bedding test started from February 1, 2016 when the pipe installation was under progress. Since the pipe joint is more critical in terms of deflection, more sensors were installed at the pipe joint compared to the end of the pipe. The earth pressure data was collected from four pressure cells at the joint of the pipe. One pressure cell (EPC-J-VL-5) stopped working after the trench was backfilled; hence, that cell was not considered in the experimental results. The circumferential strain data at the joint of the pipe was collected with the help of eight strain gauges, longitudinal strain data at the joint

of the pipe was collected with the help of seven strain gauges as one strain gauge (SG-J-L-12) was damaged during the installation of the joint of the pipe.

Similarly, four earth pressure cells were collecting data at the end of the pipe. During the testing, one pressure cell (EPC-E-SL-7) at the north springline of the pipe stopped functioning. Two circumferential strain gauges (SG-E-C-18, SG-E-C-20) stopped functioning and, hence, data from only five strain gauges (two circumferential and three longitudinal) were collected. The displacement sensors were collecting the vertical and horizontal deflections of iPVC pipe at the pipe joint as well as at end of the pipe.

4.6.1 Effect of Only Earth Load on iPVC Pipe

Pipe deflections observed at the joint and end of the pipe are summarized in Table 4-8. Only a few points of data are mentioned in the table for simplicity purpose. Figure 4-14 and Figure 4-15 illustrate the graphical presentation of deflection of iPVC pipe under earth load at the joint and end of the pipe, respectively. Horizontal and vertical deflections were relatively closer in absolute values throughout the testing.

Table 4-8 Pipe Deflection at Joint and End of Pipe due to Earth Load

Date	Joint of Pipe		End of Pipe	
	Deflection (mm)		Deflection (mm)	
	Vertical	Horizontal	Vertical	Horizontal
February 16, 2016	-0.114	0.144	-0.165	0.142
February 23, 2016	-0.084	0.134	-0.359	0.240
March 1, 2016	-0.292	0.298	-0.736	0.466
March 8, 2016	-0.228	0.222	-0.780	0.430
March 15, 2016	-0.186	0.201	-0.512	0.392
March 22, 2016	-0.288	0.276	-0.707	0.357
March 29, 2016	-0.266	0.254	-0.735	0.555
April 5, 2016	-0.273	0.250	-0.789	0.501
April 12, 2016	-0.426	0.396	-0.609	0.386
April 19, 2016	-0.392	0.472	-0.516	0.406
April 26, 2016	-0.110	0.200	-0.653	0.395

Table 4-8 — Continued

Date	Joint of Pipe		End of Pipe	
	Deflection (mm)		Deflection (mm)	
	Vertical	Horizontal	Vertical	Horizontal
May 3, 2016	-0.253	0.241	-0.596	0.486
May 10, 2016	-0.184	0.164	-0.493	0.343
May 17, 2016	-0.485	0.515	-0.628	0.364
May 24, 2016	-0.100	0.111	-0.676	0.464
May 31, 2016	-0.283	0.307	-0.647	0.463
June 7, 2016	-0.554	0.580	-0.707	0.475
June 14, 2016	-0.659	0.639	-0.970	0.697

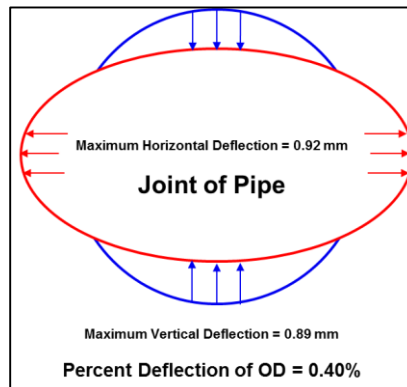
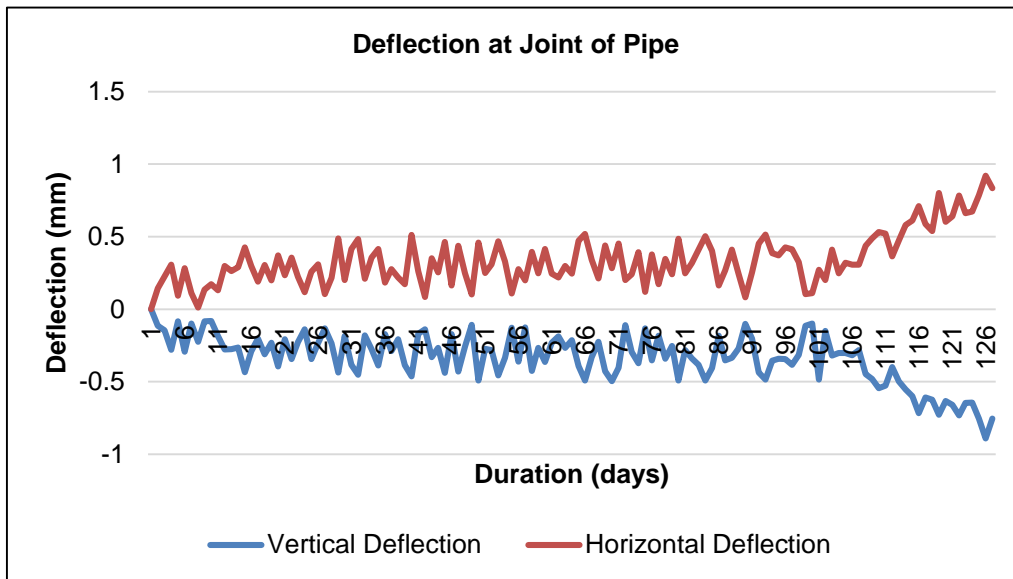


Figure 4-14 Deflection at Joint of Pipe

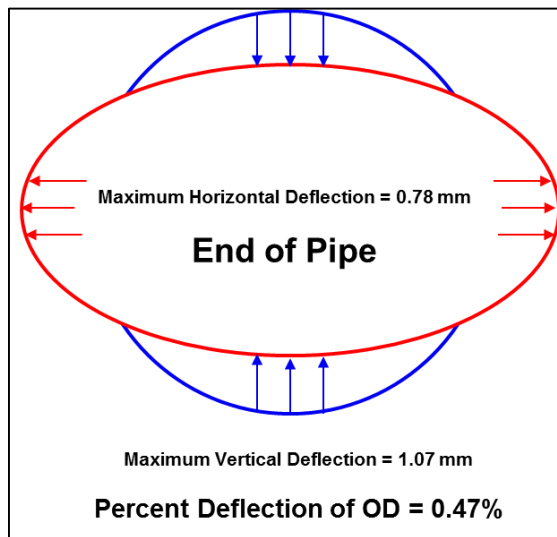
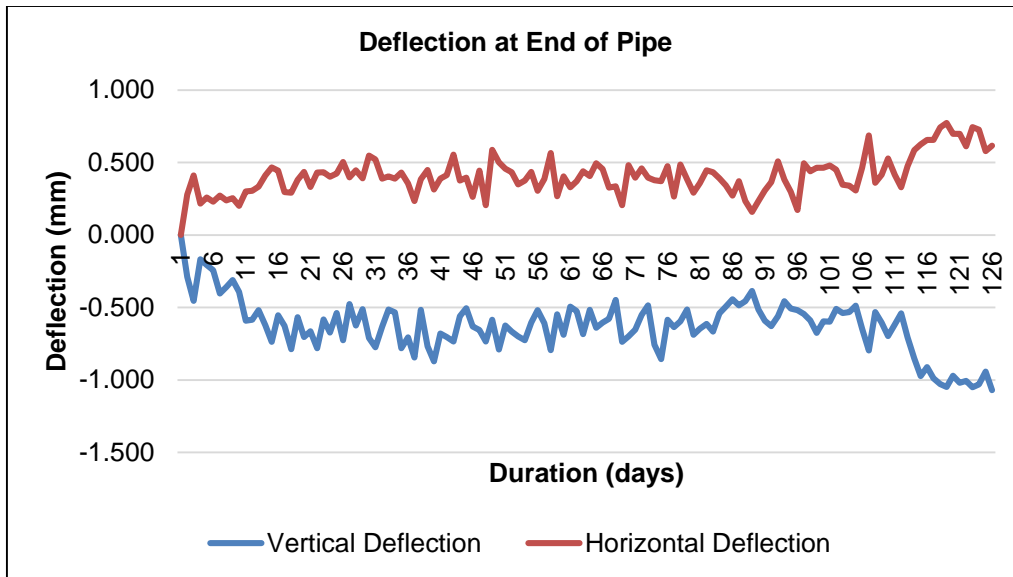


Figure 4-15 Deflection at End of Pipe

Strain gauges were installed at the joint and end of the pipe at 23 locations to measure the strain circumferentially and longitudinally and strains were measured successfully at 20 locations. Table C-1 in Appendix C presents the summary of the strain data at pipe joint and at the end of the pipe. Figure 4-16 and Figure 4-17 illustrate graphical presentation of strain data.

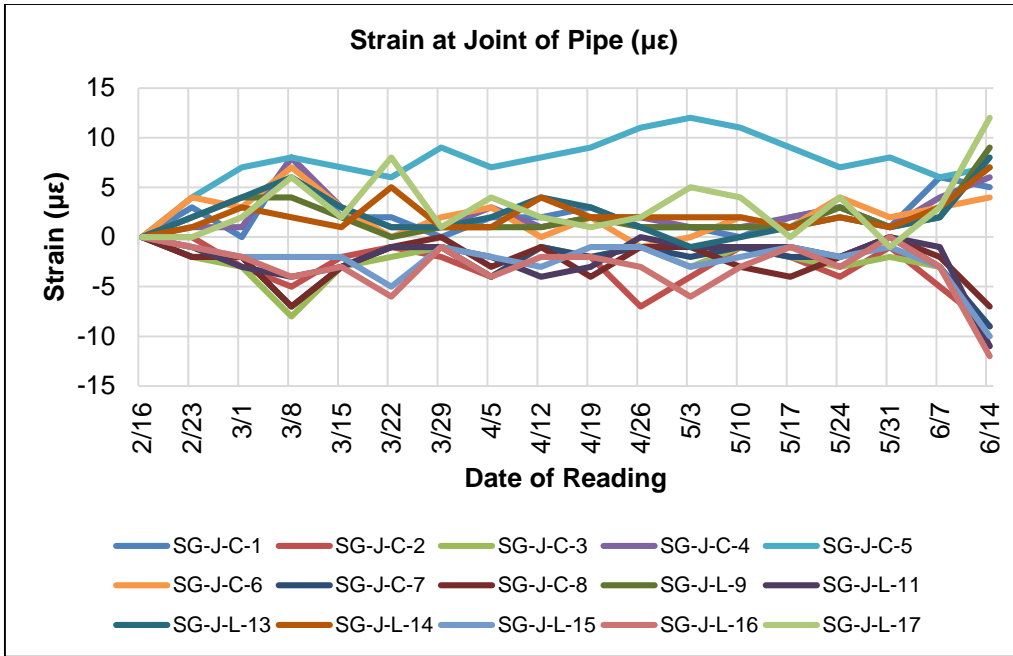


Figure 4-16 Strain Measurements at Joint of Pipe

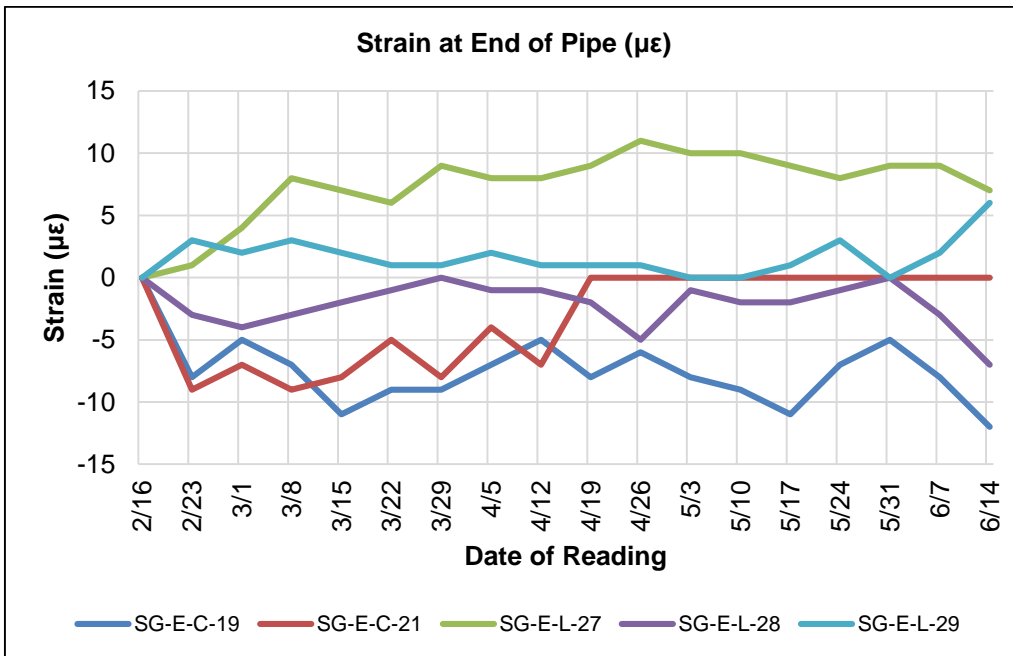


Figure 4-17 Strain Measurements at End of Pipe

Earth pressures were measured at 4 locations at the joint and end of the pipe. The sensors were located around the pipe at crown, south springline, north springline and invert. Table 4-9 presents the recorded pressures at these locations. Figure 4-18 illustrates the graphical presentation of the earth pressure cell data.

Table 4-9 Earth Pressures at Joint and End of Pipe

Date	Joint of Pipe				End of Pipe			
	Invert	North Springline	Crown	South Springline	Invert	North Springline	Crown	South Springline
	EPC-J-VL-1	EPC-J-SL-2	EPC-J-VL-3	EPC-J-SL-4	EPC-E-VL-6	EPC-E-SL-7	EPC-E-VL-8	EPC-E-SL-9
2/16	0.516	0.21	2.259	1.41	1.231	1.658	1.465	1.052
2/23	0.176	0.235	2.564	1.195	1.593	1.011	2.728	1.127
3/1	1.076	0.548	3.059	2.596	2.529	0.529	4.304	1.529
3/8	0.968	0.021	2.692	0.624	2.452	0.32	4.194	1.32
3/15	0.947	0.089	2.533	0.409	2.349	0.181	4.042	1.181
3/22	1.118	0.066	2.59	0.934	2.463	0.178	4.152	1.178
3/29	1.146	0.057	2.592	0.884	2.472	0.213	3.973	1.213
4/5	1.325	0.126	3.175	1.094	2.707	0.866	4.306	1.866
4/12	1.407	0.119	3.104	1.05	2.719	0.773	4.327	1.773
4/19	1.426	0.113	3.094	1.113	2.56	0.761	4.266	1.761
4/26	1.291	0.056	2.924	0.676	2.451	0.612	4.119	1.612
5/3	1.523	0.149	3.037	1.302	2.693	0.796	4.325	1.796
5/10	1.408	0.012	2.849	0.895	2.522	0.598	4.133	1.598
5/17	1.53	0.12	2.917	1.185	2.618	0.687	4.245	1.687
5/24	1.493	0.076	2.869	1.116	2.541	0.624	4.172	1.624
5/31	1.515	0.072	2.88	1.172	2.554	0.676	4.183	1.676
6/7	1.568	0.102	2.88	1.239	2.572	0.693	4.208	1.693
6/14	1.593	0.075	2.904	1.345	2.598	0.766	4.227	1.766

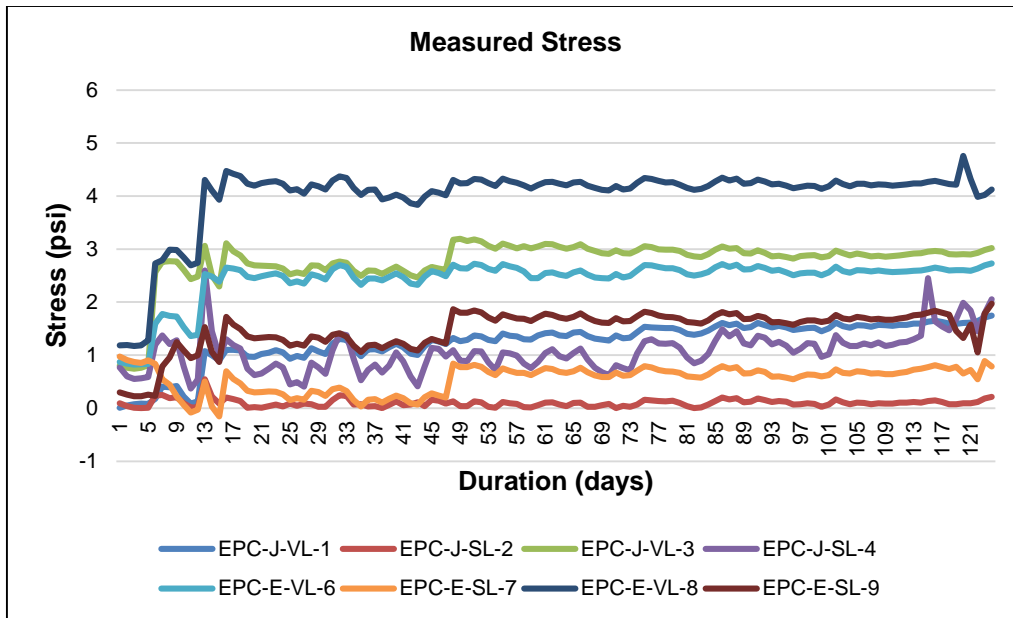


Figure 4-18 Earth Pressures for Bedding Test 2

4.6.2 Effect of Earth plus Truck Load on iPVC pipe

As a part of this project, a live load simulation was created on top of the trench where iPVC pipe was installed. Two scenarios were considered for the testing. A 20-ton truck was run on top of the trench along the length of the pipe for two hours and then halted on top of the pipe for two hours. The truck was filled with heavy gravel to have more weight on top of the trench. The approximate load of the truck including the loaded gravel was about 50,000 lbs. The test helped in checking the effect of the added load on the strain and deflection readings.

The truck load was applied on June 30, 2016. Figure 4-19 shows the actual photographs of the testing. Table 4-10, Table C-2 and Table 4-11 illustrates the deflection, strain and earth pressure readings for 1 hour before, 4 hours during, 1 hour after, 1 week after, and 2 weeks after applying truck load. Figures 4-20 – 4-24 graphically illustrate the vertical deflection, horizontal deflection, strain at joint, strain at end of pipe and earth pressure readings, respectively.



Figure 4-19 20-Ton Truck used to Create Live Load Simulation

Table 4-10 Pipe Deflection at Joint and End of Pipe due to Earth plus Truck Load

Date and Time	Joint of Pipe		End of Pipe	
	Deflection (mm)		Deflection (mm)	
	Vertical	Horizontal	Vertical	Horizontal
6/30 @ 7 AM	-0.673	0.645	-0.982	0.797
6/30 @ 8 AM	-0.914	0.865	-1.104	0.912
6/30 @ 9 AM	-1.323	0.899	-1.554	1.093
6/30 @ 10 AM	-1.617	1.021	-1.913	1.413
6/30 @ 11 AM	-1.591	1.142	-1.902	1.489
6/30 @ 12 noon	-1.571	1.224	-1.895	1.508
6/30 @ 1 PM	-1.488	1.004	-1.501	1.441
7/7 @ 1 PM	-1.035	1.004	-1.230	1.109
7/14 @ 1 PM	-1.016	0.931	-1.198	1.113

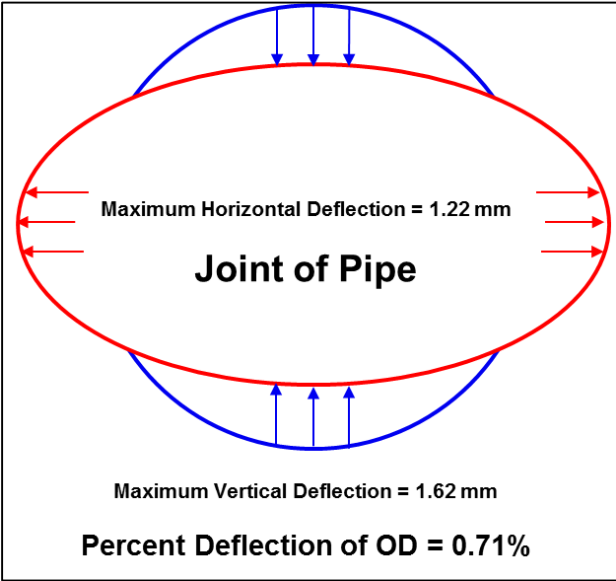
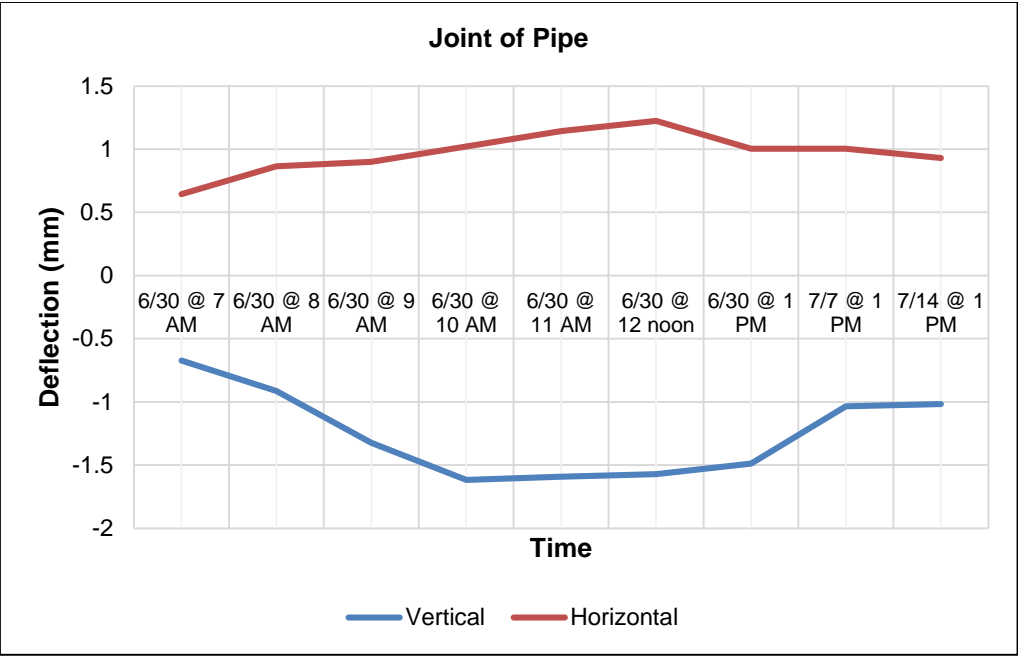


Figure 4-20 Deflection at Joint of Pipe due to Earth plus Truck Load

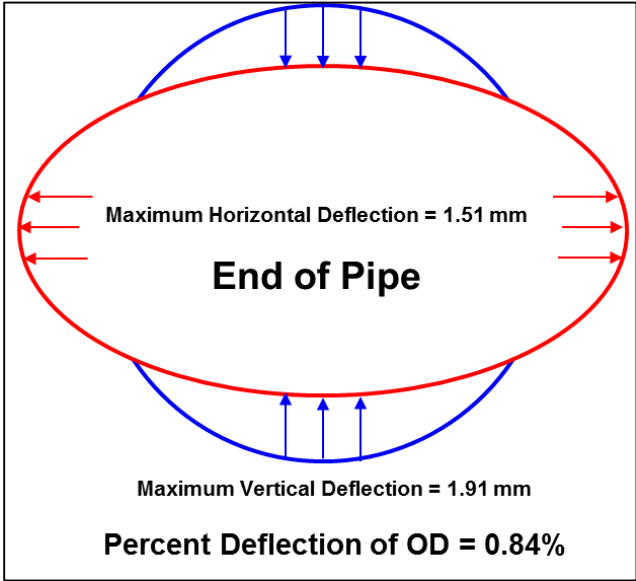
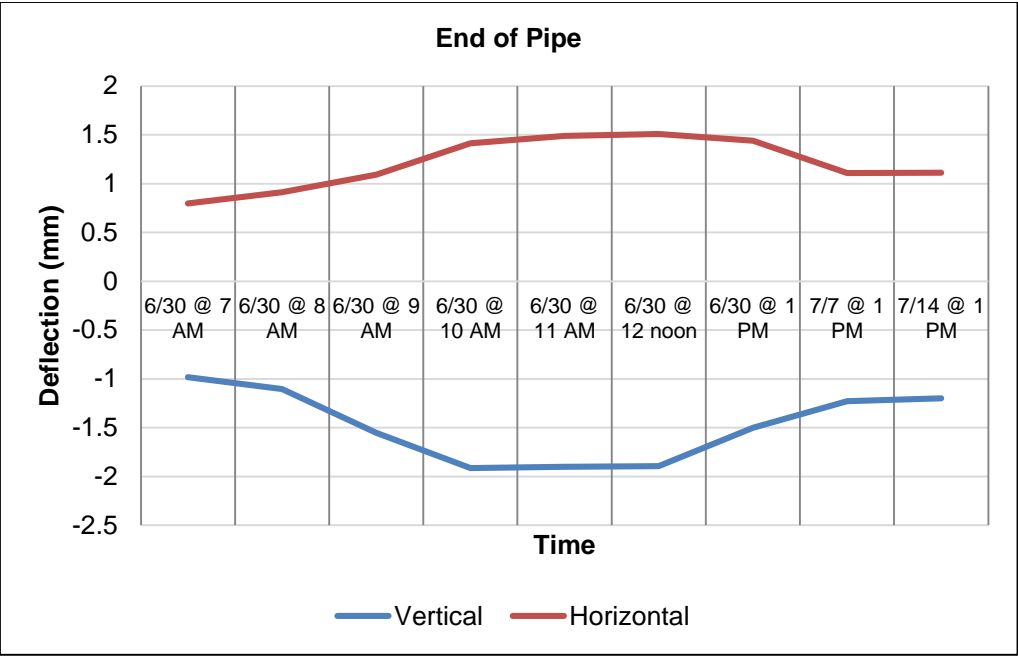


Figure 4-21 Deflection at End of Pipe due to Earth plus Truck Load

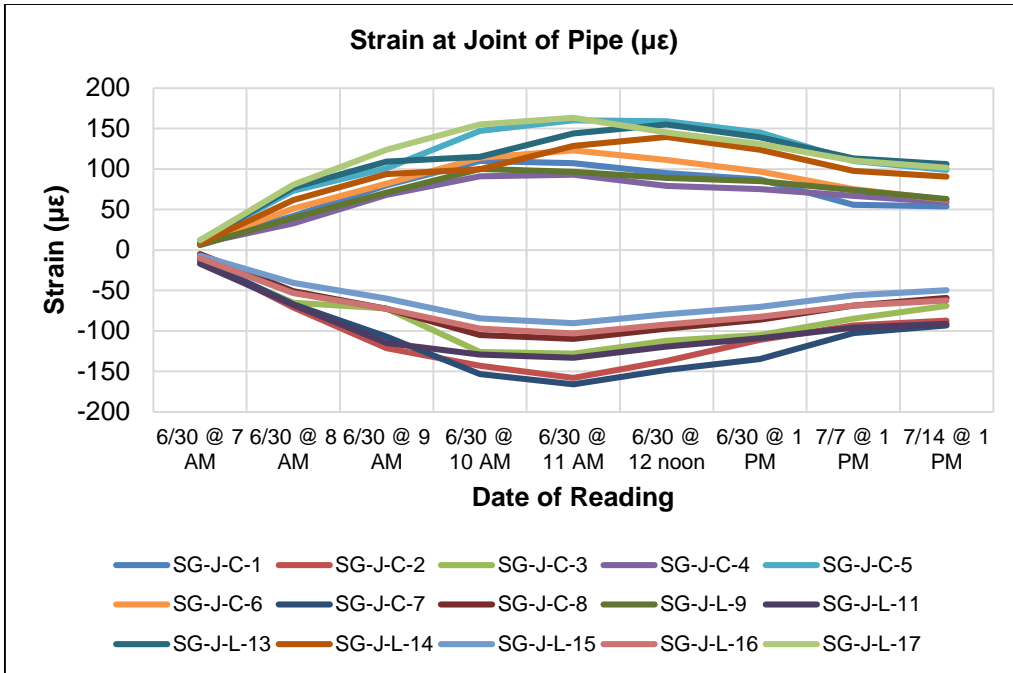


Figure 4-22 Strain Measurements at Joint of Pipe due to Earth plus Truck Load

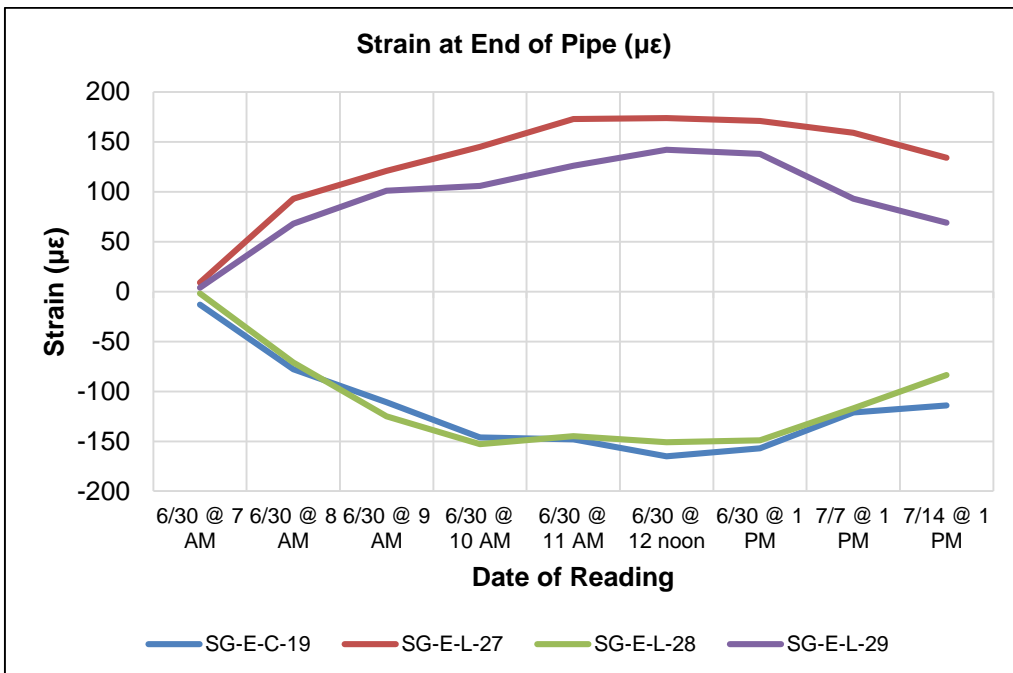


Figure 4-23 Strain Measurements at End of Pipe due to Earth plus Truck Load

Table 4-11 Earth Pressure at Joint and End of Pipe due to Earth plus Truck Load

Date	Joint of Pipe				End of Pipe			
	Invert	North Springline	Crown	South Springline	Invert	North Springline	Crown	South Springline
	EPC-J-VL-1	EPC-J-SL-2	EPC-J-VL-3	EPC-J-SL-4	EPC-E-VL-6	EPC-E-SL-7	EPC-E-VL-8	EPC-E-SL-9
6/30 @ 7 AM	1.732	0.175	2.925	1.456	2.685	1.104	4.285	2.869
6/30 @ 8 AM	1.825	0.244	3.587	1.537	3.582	1.239	5.052	3.615
6/30 @ 9 AM	2.152	1.856	5.189	2.121	4.371	1.337	5.280	3.135
6/30 @ 10 AM	2.325	1.957	6.974	2.564	4.289	1.284	6.497	3.812
6/30 @ 11 AM	2.334	1.948	6.444	2.547	4.237	1.257	6.951	3.760
6/30 @ 12 noon	2.182	1.759	5.314	2.325	4.319	1.302	6.489	3.976
6/30 @ 1 PM	2.630	1.722	4.176	1.856	4.292	1.212	5.291	3.216
7/7 @ 1 PM	1.699	1.203	3.686	1.752	3.569	1.365	4.984	3.154
7/14 @ 1 PM	1.471	1.456	3.184	1.966	2.987	1.157	4.560	2.869

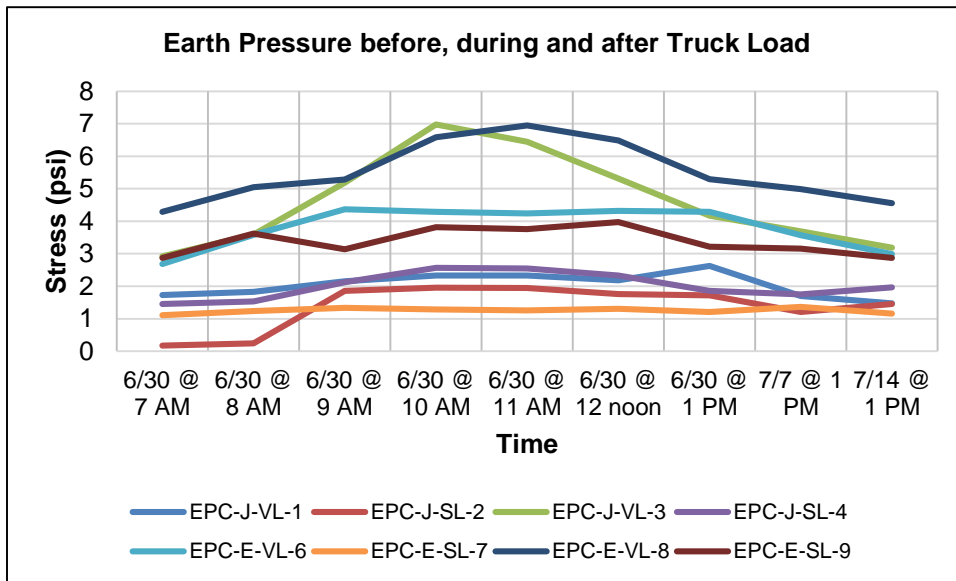


Figure 4-24 Earth Pressures for Bedding Test 2 due to Earth plus Truck Load

4.7 Field Installation of iPVC Pipe

Missouri American Water (MOAW) accepted the task of installing 1,500 ft of 9 in. OD DR 18 iPVC pipe in February 2016 at a St Louis County location with aggressive high clay content soils. The pipe material was provided by PPI from South Korea; shipped on October 24 and received at the MOAW yard on November 16. St. Louis County identified a project in the southern portion of their service territory where an 8 in. inside diameter cast iron pipe needed to be retired due to frequent pipe failure. The MOAW team proceeded with designing the pipe and securing the permits to execute the job. The project site was along the Meramec Bottom Road (southern extreme of St. Louis County not far from the Meramec River). The area has highly corrosive soils and higher operating pressures. The area has experienced flooding in January 2016 (WRF Report No. 4650, 2016).

Armed with much of the test data, MOAW moved forward with a typical PVC pipe installation per AWWA C605. The installation processes included handling, cutting, live tapping (Figure 4-25) and connecting to existing cast iron main. The installation of iPVC pipe can help in evaluating the performance of iPVC pipe in actual field conditions and may be evaluated after a few years in service. Thrust blocks were used at the joint of iPVC pipe. Figure 4-26 presents the actual site photographs of the St. Louis County pipe installation (WRF Report No. 4650, 2016).



Figure 4-25 Tapping of iPVC pipe
(Source: AW)



Figure 4-26 iPVC pipe Pilot Installation by MOAW at Meramec River Bottom Road, St Louis County, MO.
(Source: AW)

4.8 Chapter Summary

This chapter presented the test results for iPVC pipe considering the hydrostatic short term burst pressure test, impact test, tensile test, stiffness test, fatigue test and bedding test. Also, the field installation of iPVC pipe in St. Louis County was discussed in this chapter.

Chapter 5

Discussion of Results

5.1 Introduction

Chapter 4 reported the testing results of iPVC pipe conducted as a part of the WRF Project Report No. 4650 entitled “An Evaluation of the Value of Structurally Enhanced PVC Pipe.” This chapter presents the discussion of the results of the laboratory tests performed. Key parameters required for future designing of iPVC pipe installation such as hoop stress, stiffness factor, fatigue life, bedding conditions, and deflection of iPVC pipe are discussed in depth. The calculations of these parameters are shown.

5.2 Hydrostatic Short-term Burst Pressure Test

The short-term burst pressure test results predict the behavior of iPVC pipe under controlled temperature, time, and applied pressure. This test is conducted to evaluate the maximum pipe loading capacity and ultimate hoop stress developed in the iPVC pipe. The test helps to study the failure pattern of the pipe. Hoop stress is defined as the stress in the circumferential (tangential) direction in cylindrical and non-cylindrical vessels, when loaded by the hydrostatic head of a liquid in a fully- or partially-filled container or by internal or external pressure in a closed vessel. The hoop stress is exerted perpendicular both to the axis and to the radius of the pipe (Figure 5-1). The hoop stress could be calculated as follows:

$$S = \frac{P(D-t)}{2t} \text{ for outside diameter controlled pipe ... Eq. 5.1}$$

or

$$S = \frac{P(d+t)}{2t} \text{ for inside diameter controlled pipe ... Eq. 5.2}$$

where:

S = hoop stress (psi),

P = internal pressure (psi),

D = average outside diameter (in.),

d = average inside diameter (in.), and

t = minimum wall thickness (in.)

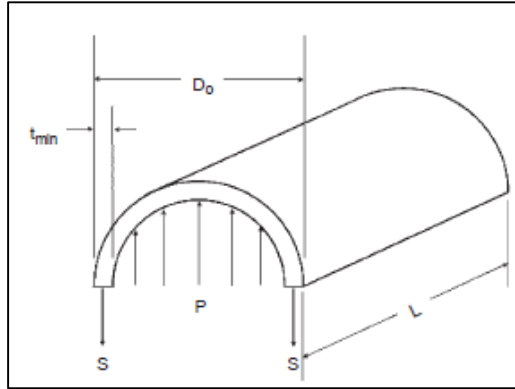


Figure 5-1 Hoop Stress due to Internal Pressure
(Uni-Bell, 2012)

Table 5-1 presents the hoop stress for iPVC pipe based on Equation 5.1 for outside diameter controlled pipe.

Table 5-1 Hoop Stress for iPVC pipe

Sample No.	Failure Pressure (psi)	Hoop Stress (psi)
1	1,070	9,095
2	1,050	8,925
3	1,020	8,670
4	1,050	8,925
5	1,010	8,585
6	1,030	8,755
7	1,030	8,755
8	1,010	8,585
9	1,035	8,798
10	1,020	8,670
11	1,065	9,053
12	1,060	9,010
13	1,060	9,010
14	1,075	9,138
Average	1,042	8,855
Std. Dev.	21	177

Sample Calculation:

For Sample No. 1,

D = 9 in., t = 0.5 in., and P = 1,035 psi.

Using Eq. 5.1, for hoop stress,

$$S = \frac{1,070(9 - 0.5)}{2(0.5)}$$

$$S = 9,095 \text{ psi}$$

The hoop stress for a hydrostatic short-term burst pressure test must meet or exceed the 6,400 psi for a pipe to pass the quick-burst test. This test provides assurance of PVC extrusion quality and demonstrates the surge capacity of PVC pipe. This information is obtained from the Handbook of PVC Pipe Design and Construction (2012).

The short-term rating (STR) for iPVC pipe could be developed using the hoop stress. This STR is determined by dividing short-term strength (STS) by a safety factor. STS is the quick-burst failure pressure obtained during the testing. The STS for C900 DR 18 pipe is 755, considering safety factor of 2. STR for AWWA C900 DR 18 pipe is 376 psi ($755/2 = 376$ psi). The STR rating for a DR 18 iPVC pipe is presented in Table 5-2 considering a safety factor of 2.0.

Table 5-2 STR Rating for iPVC pipe

Sample No.	STS (psi)	STR (psi)
1	1,070	535
2	1,050	525
3	1,020	510
4	1,050	525
5	1,010	505
6	1,030	515
7	1,030	515
8	1,010	505
9	1,035	518
10	1,020	510
11	1,065	533
12	1,060	530
13	1,060	530
14	1,075	538
Average	1,042	521
Std. Dev.	21	10

Figure 5-2 presents the hydrostatic life when PVC pipe operates at the STR value. Based on the graph, the predicted life of PVC would still be in the hundreds of years even when the pipe operates at STR. The average iPVC pipe STR is 521 psi which exceeds the minimum requirement by 28%.

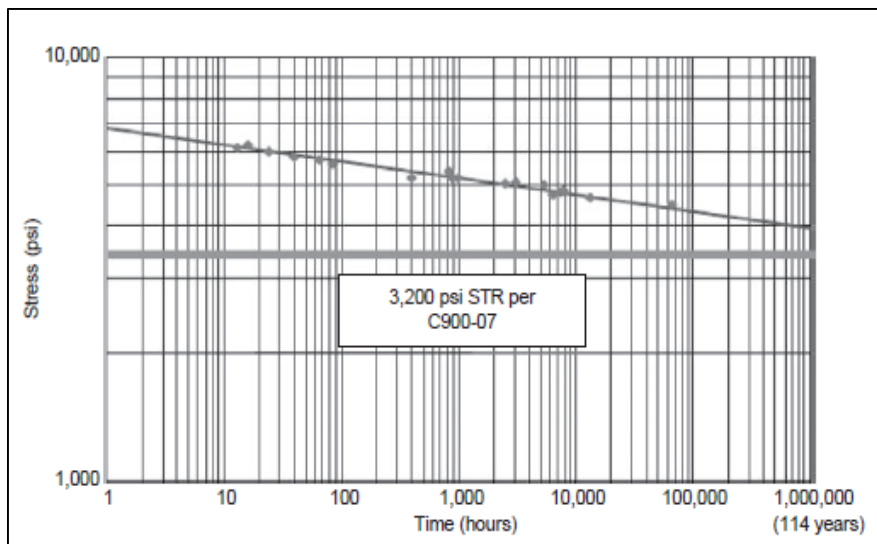


Figure 5-2 Hydrostatic Life of PVC Operation at STR (Uni-Bell, 2012)

5.3 Stiffness Test

The pipe stiffness (PS) calculated in Table 4-5 could be further used to compute the stiffness factor (SF) which is the product of PS and the quantity $0.149r^3$. The PS could be used to calculate the approximate deflections under earth load. For this dissertation, only two points of pipe deformation (95% of OD and 20% of OD) are selected and studied. The minimum AWWA requirements for PS is 364 psi at 95% deformation (AWWA M23 Manual, Table 4-2, Pg. 26). The PS and SF for iPVC pipe samples is presented in Table 5-3.

Sample Calculation for SF:

For Sample R, at 95% OD,

$$SF = PS \times 0.149r^3 = 479 \times 0.149 \times 4.25^3 = 5,554 \text{ in.-lbs}$$

Table 5-3 Stiffness Factor for selected iPVC pipe Samples

Specimen	@ 95% OD		@ 20% OD	
	Pipe Stiffness	Stiffness Factor	Pipe Stiffness	Stiffness Factor
	psi	in.-lbs	psi	in.-lbs
R	479	5,479	153	1,750
Y	462	5,284	148	1,693
W	484	5,536	150	1,716
U	477	5,456	150	1,716
V	482	5,513	151	1,727
AS	481	5,502	149	1,704
AP	489	5,593	153	1,750
AQ	466	5,330	146	1,670
AU	491	5,616	152	1,739
Average	479	5,479	150	1,718
Std. Dev.	10	104	2	25

The flexural modulus could be determined from the SF values calculated using the following equation:

$$EI = SF = 0.149r^3(PS) \dots \text{Eq. 5.2}$$

where:

E = Flexural Modulus, psi

$I = \text{Moment of Inertia} = (\text{thickness of pipe})^3/12$

SF = Stiffness Factor

Although, EI of the pipe is a function of material's flexural modulus (E) and the wall thickness (t), PS and SF are computed values determined from the test resistance at a particular deflection. Hence, PS and SF values are highly dependent on the degree of deflection of pipe wall. The greater the deflection of pipe wall at which PS or SF are determined, the greater magnitude of the deviation from the true EI value. A correction factor $C = [1 + (\Delta Y/2d)]^3$ can be applied, and the PS and SF values can be related to the true EI of the pipe as long as the pipe remains elliptical. Hence, for corrected PS,

$$PS = \frac{F}{\Delta Y} C = \frac{F}{\Delta Y} \left(1 + \frac{\Delta Y}{2d}\right)^3 \dots \text{Eq. 5.3}$$

where: d = initial inside diameter, in.

Table 5-4 presents the corrected values of PS along with the SF and E for iPVC pipe. The calculated values of flexural modulus (E) could be used to study the behavior of the deflected pipe. Figure 5-3 through Figure 5-5 graphically presents the PS, SF and E for 95% and 20% deflection of OD respectively.

Table 5-4 Corrected PS, SF and E for iPVC pipe

Specimen	@ 95% OD			@ 20% OD		
	Corrected Pipe Stiffness	Stiffness Factor	Flexural Modulus (E)	Corrected Pipe Stiffness	Stiffness Factor	Flexural Modulus (E)
	psi	in.-lbs	psi	psi	in.-lbs	psi
R	516	5,900	566,411	165	1,885	180,920
Y	498	5,691	546,308	159	1,823	175,008
W	521	5,962	572,323	162	1,848	177,373
U	514	5,875	564,046	162	1,848	177,373
V	519	5,937	569,958	163	1,860	178,555
AS	518	5,925	568,776	160	1,835	176,190
AP	527	6,023	578,235	165	1,885	180,920
AQ	502	5,740	551,038	157	1,798	172,643
AU	529	6,048	580,600	164	1,872	179,738
Average	516	5,900	566,411	162	1,850	177,636
Std. Dev.	10	112	10,751	2	27	2,601

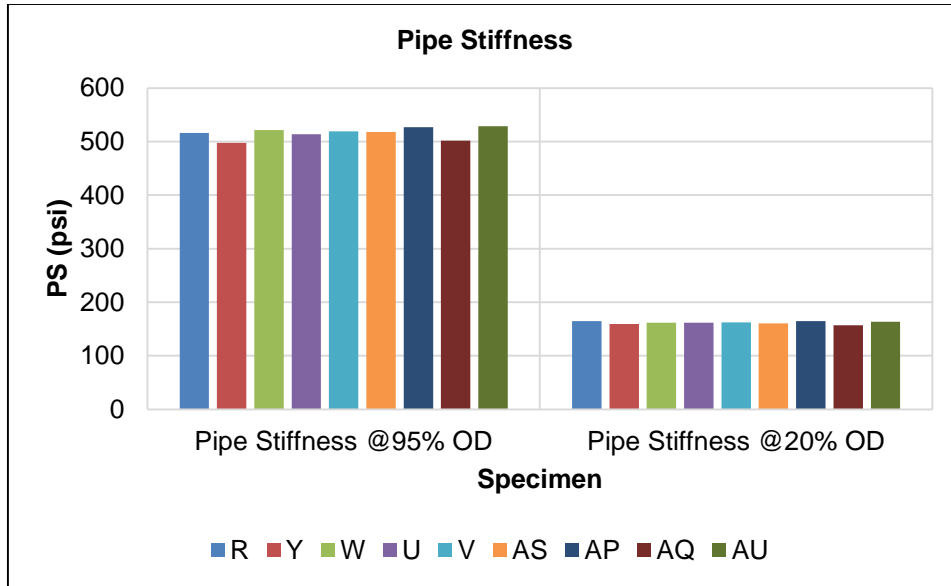


Figure 5-3 Graphical presentation of PS for iPVC pipe

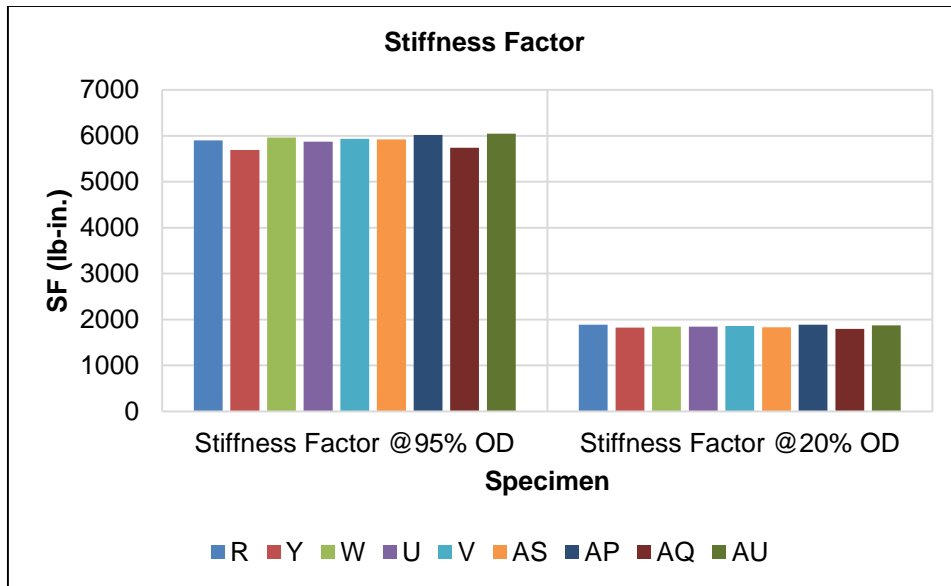


Figure 5-4 Graphical Illustration of SF for iPVC pipe

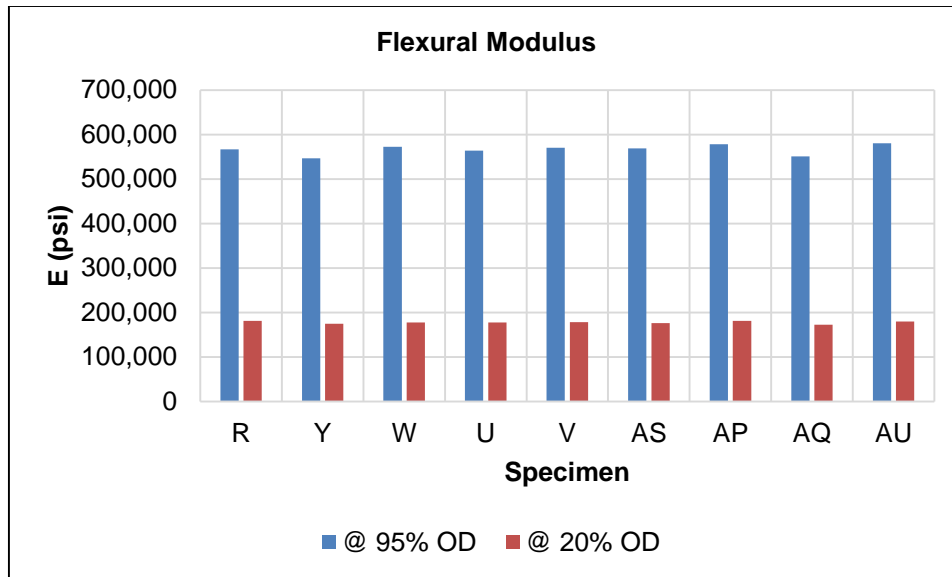


Figure 5-5 Graphical Illustration of Flexural Modulus (E) for iPVC pipe

5.4 Fatigue Test

The fatigue life of 9 in. OD DR 18 iPVC pipe could be estimated based on the equations suggested by Petroff (2013) in Section 2.6 (Eq. 2.2 and Eq. 2.3). The equations are as follows:

$$Number\ of\ Cycles = 10^{\frac{1.708 - \log\left(\frac{Peak\ Stress}{145}\right)}{0.101}}$$

$$Peak\ Stress = (P_{pumping} + P_{surge}) \times \frac{(DR - 1)}{2}$$

The above equations could be used to predict the anticipated number of cycles for failure of the pipe due to fatigue for experimental conditions only. The hydraulic transients during operation of the pipe result in the total pressure (pumping plus surge) to exceed the steady-flow working pressure. AWWA C900 recommends a surge allowance of 1.0 x Pressure Class (PC) of the pipe for occasional surges and a surge allowance of 0.5 x PC for frequent recurring surges.

ASTM D2837-13e1 Standard Test Method for Obtaining Hydrostatic Design Basis for Thermoplastic Pipe Materials or Pressure Design Basis for Thermoplastic Pipe Products helps obtain the hydrostatic design basis (HDB) and long-term hydrostatic strength (LTHS), which could be used in the above equations to predict the fatigue life of the pipe. LTHS is defined in ASTM D2837-13e1 as “the estimated tensile stress in the wall of the pipe in the circumferential orientation that when applied continuously will cause failure of the pipe at 100,000 hrs. This is the intercept of the stress regression line with the 100,000 hrs. coordinate.” HDB is the categorized value of the material's LTHS (ASTM D2837-13e1, 2013).

Hydrostatic design stress (HDS) is defined as the estimated maximum tensile stress the material is capable of continuously withstanding with a high degree of certainty that failure of the pipe will not occur as per ASTM D2837-13e1. These values could be used in the above equations by Petroff (2013) to predict the number of cycles to failure of pipe due to fatigue stress generated by transient surges.

The 50-year LTHS value for iPVC pipe is 3,955 psi (27.27 MPa) determined by PPI, South Korea. Based on the LTHS value, from Figure 5-6, the HDB value for iPVC pipe is 4,000 psi (27.58 MPa). This HDB stress is circumferential when internal hydrostatic water pressure is applied.

Range of Calculated LTHS Values		Hydrostatic Design Basis	
psi	(MPa)	psi	(MPa)
190 to < 240	(1.31 to < 1.65)	200	(1.38)
240 to < 300	(1.65 to < 2.07)	250	(1.72)
300 to < 380	(2.07 to < 2.62)	315	(2.17)
380 to < 480	(2.62 to < 3.31)	400	(2.76)
480 to < 600	(3.31 to < 4.14)	500	(3.45)
600 to < 760	(4.14 to < 5.24)	630	(4.34)
760 to < 960	(5.24 to < 6.62)	800	(5.52)
960 to <1200	(6.62 to < 8.27)	1000	(6.89)
1200 to <1530	(8.27 to <10.55)	1250	(8.62)
1530 to <1730	(10.55 to <11.93)	1600	(11.03)
1730 to <1920	(11.93 to <13.24)	1800	(12.41)
1920 to <2160	(13.24 to <14.89)	2000	(13.79)
2160 to <2400	(14.89 to <16.55)	2250	(15.51)
2400 to <2690	(16.55 to <18.55)	2500	(17.24)
2690 to <3020	(18.55 to <20.82)	2800	(19.30)
3020 to <3410	(20.82 to <23.51)	3150	(21.72)
3410 to <3830	(23.51 to <26.41)	3550	(24.47)
3830 to <4320	(26.41 to <29.78)	4000	(27.58)
4320 to <4800	(29.78 to <33.09)	4500	(31.02)
4800 to <5380	(33.09 to <37.09)	5000	(34.47)
5380 to <6040	(37.09 to <41.62)	5600	(38.61)
6040 to <6810	(41.62 to <46.92)	6300	(43.41)
6810 to <7920	(46.92 to <54.62)	7100	(48.92)

Figure 5-6 Hydrostatic Design Basis Values Corresponding to LTHS Values (ASTM D2837-13e1, 2013)

AS per M23 PVC Pipe Design and Installation Manual,

$$HDS = HDB/SF$$

where,

SF = safety factor = 2.5

Thus,

$$HDS = 4000/2.5 = 1,600 \text{ psi}$$

Considering HDS as our peak stress and using Equation 2.6,

Number of Cycles to failure

$$= 10^{\{[(1.708 - \text{Log}_{10}(1600/145))/0.101]\}}$$

$$= 3,860,000$$

Based on a conservative assumption of 50 surges/day, the experimental fatigue life of 9 in. OD DR 18 iPVC pipe could be predicted to be more than 210 years. However,

210 years design life excludes parameters such as soil conditions, operating pressures, number of connections, pump operation, etc. which could result in a lower life of the pipe.

The HDB testing is less rigorous on the pipe wall as compared to the fatigue test performed in this dissertation. The 190-year life is a prediction based on the HDB testing of iPVC pipe. If we consider the fatigue testing at CUIRE, a total of 2,300,000 cycles were completed. The test proves that the pipe could withstand more than 2,000,000 surges without any failure for a surge pressure range of 150 psi to 225 psi. If we consider the same number of surges per day as earlier, i.e., 50 surges/day, the pipe would have a fatigue life of:

Total surges experienced by pipe without failure = 2,300,000

Daily surge occurrence = 50 surges

Fatigue Life of iPVC pipe = 2,300,000 surge cycles / 50 surges per day
 = 46,000 days = 125 years

The above design life is for the iPVC pipe sample considered in this dissertation. The iPVC pipe sample used for the testing was the 9 in. OD DR 18 with a length of 10 ft. For another diameter and DR of iPVC pipe, the fatigue testing might have different results.

Further, the maximum surge pressure for a change in flow velocity of 2 ft/s could be calculated using the following equations:

$$a = \frac{4,660}{\sqrt{1 + \frac{k}{E}(DR-2)}} \dots\dots\dots \text{Eq. 5.4}$$

where:

a = pressure wave velocity, ft/s

k = fluid bulk modulus, psi (300,000 psi for water)

E = modulus of elasticity of the pipe, psi (461,000 psi for iPVC pipe)

DR = dimension ratio for iPVC pipe (DR = 18 for iPVC pipe)

$$P_s = \frac{a(\Delta V_{max})}{2.31g} \dots\dots\dots \text{Eq. 5.5}$$

where:

P_s = pressure surge, psi

ΔV_{max} = maximum velocity change, ft/s, For conventional PVC, $V_{max} = 2$ ft/s

g = acceleration due to gravity, 32.2 ft/s²

Substituting the values in Eq. 5.4,

$$a = \frac{4,660}{\sqrt{1 + \frac{300,000}{461,000}(18 - 2)}} = 1,380 \text{ ft/s}$$

Further, using Eq. 5.5,

$$P_s \text{ for iPVC} = \frac{1,380(2)}{2.31(32.2)} \sim 37 \text{ psi}$$

5.5 Bedding Test

Bedding test was performed on iPVC pipe to evaluate the performance of iPVC pipe in native soil conditions (lean clay backfill) outside AWWA requirements. The test collected the experimental values of the deflection experienced by the pipe wall under earth load as well as under earth load plus the truck load. Further, the experimental values could be compared to the theoretical values, which could be calculated using the Modified Iowa equation which is based on the dimension ratio of the pipe and modulus of elasticity and Spangler's equation, which is based on the pipe stiffness value of the pipe. A finite element was prepared using PLAXIS 2D and ABAQUS 6.14-3 software which is explained in the next section.

5.5.1 Deflection of iPVC Pipe due to Earth Load

The pipe stiffness determined in this dissertation could be used to calculate approximate deflection of the pipe under earth load and earth load plus live load. From Eq. 3.1,

$$\% \text{ Deflection} = \frac{D_e K (W' + P) 100}{0.149 PS + 0.061 E'}$$

For iPVC pipe,

a deflection lag factor of 1.0 is considered, which is typical for a flexible pipe;

a bedding constant of 0.1 is considered, which is typical for a flexible pipe;

$W' = 0$ for only dead load calculations;

$P = 4.17$ psi from Figure 5-7 as the unit weight of soil used for backfilling in the bedding test is 120 lbs/ft³ and the height of cover for the testing is 5 ft;

$PS = 516$ psi from Table 5-4, and

$E' = 400$ psi is considered from following Figure 5-8 after classifying the soil based on the soil testing carried out in the laboratory.

PRISM LOAD SOIL PRESSURE (LBS/IN2)					
HEIGHT OF COVER (FT)	SOIL UNIT WEIGHT (LBS/FT3)				
	100	110	120	125	130
1	0.69	0.76	0.83	0.87	0.90
2	1.39	1.53	1.67	1.74	1.81
3	2.08	2.29	2.50	2.60	2.71
4	2.78	3.06	3.33	3.47	3.61
5	3.47	3.82	4.17	4.34	4.51
6	4.17	4.58	5.00	5.21	5.42
7	4.86	5.35	5.83	6.08	6.32
8	5.56	6.11	6.67	6.94	7.22
9	6.25	6.88	7.50	7.81	8.13
10	6.94	7.64	8.33	8.68	9.03

Figure 5-7 Standard Prism Load Soil Pressure
(Source: JM Eagle, 2016)

Soil type-pipe bedding material (Unified Classification System) ¹	E' for degree of compaction of bedding (lb/in ²)			
	Dumped	Slight <85% Proctor <40% relative density	Moderate 85-95% Proctor 40-70% relative density	High >95% Proctor >70% relative density
Fine grained soils (LL>50) ² Soils with medium to high plasticity CH, MH, CH-MH	No data available; consult a competent soils engineer; otherwise use E' = 0			
Fine-grained soils (LL<50) Soils with medium to no plasticity CL, ML, ML-CL, with less than 25 percent coarse-grained particles	50	200	400	1000
Fine-grained soils (LL<50) Soils with medium to no plasticity CL, ML, ML-CL, with more than 25 Percent coarse-grained particles	100	400	1000	2000
Coarse-grained soils with fines GM, GC, SM, SC ³ contains more than 12 percent fines				
Coarse-grained soils with little or no fines GW, GP, SW, SP ³ contains less than 12 percent fines	200	1000	2000	3000
Crushed rock	1000	3000		
Accuracy in terms of percent deflection ⁴	±2%	±2%	±1%	±0.5%

¹ ASTM Designation D 2487, USBR Designation E-3.
² LL = liquid limit.
³ Or any borderline soil beginning with one of these symbols (i.e., GM-GC-SC).
⁴ For ± 1 percent accuracy and predicted deflection of 3 percent, actual deflection would be between 2 % and 4 %.

Note:
A. Values applicable only for fills less than 50 ft.
B. Table does not include any safety factor.
C. For use in predicting initial deflections only, appropriate deflection lag factor must be applied for long-term deflections.
D. If bedding falls on the borderline between two compaction categories, select lower E' value or average the two values.
E. Percent Proctor based on laboratory maximum dry density from test standards using about 12 500 ft-lb/ft³ (ASTM D-698, AASHTO T-99, USBR Designation E-11).

Figure 5-8 Bureau of Reclamation Values of E' (for Initial Flexible Pipe Deflection) (Howard, 1977)

Calculation:

$$D_e = 1.0$$

$$K = 0.1$$

$$P = 4.17 \text{ psi}$$

$$PS = 516 \text{ psi}$$

$$E' = 400 \text{ psi}$$

Substituting in Eq. 3.1,

$$\% \text{ Deflection} = \frac{(1.0)(0.1)(0 + 4.17)(100)}{0.149(516) + 0.061(400)} = \frac{41.7}{101.28} = 0.41 \% = 0.94 \text{ mm}$$

Now, using Eq. 3.2, the predicted percent deflection based on the DR and the E of iPVC pipe could be calculated as:

DR = 18 for iPVC pipe,

E = 461,000 psi for iPVC pipe from Table 4-6

$$\% \text{ Deflection} = \frac{(1.0 \times 0.1 \times 4.17 + 0)100}{\{2(461,000)/[3(18 - 1)^3]\} + 0.061(400)} = \frac{41.7}{87.01} = 0.48 \% = 1.09 \text{ mm}$$

The maximum stress experienced was 4.759 psi on crown part at the end of the iPVC pipe test pipe which exceeds the expected soil load of 4.17 psi from Figure 5-7.

5.5.2 Deflection of iPVC Pipe due to Earth plus Truck Load

As explained earlier, a live load simulation was created on top of the trench with a 20 ton truck. The truck was run on top of the trench along the length of the pipe for 2 hours and then halted on top of the pipe for 2 hours. Using Figure 5-9, the expected live load transmitted to the pipe from the traffic could be considered in predicting the percent deflections using Eq. 3.1 and Eq. 3.2.

LIVE LOADS ON PVC PIPE			
HEIGHT OF COVER (FT)	LIVE LOAD TRANSFERRED TO PIPE, (LBS/IN ²)		
	HIGHWAY H20 ¹	RAILWAY E80 ²	AIRPORT ³
1	12.50		
2	5.56	26.39	13.14
3	4.17	23.61	12.28
4	2.78	18.40	11.27
5	1.74	16.67	10.09
6	1.39	15.63	8.79
7	1.22	12.15	7.85
8	0.69	11.11	6.93
10	*	7.64	6.09

Figure 5-9 Transmitted Live Loads to Pipe
(Source: JM Eagle, 2016)

Using Eq. 3.1, and considering all the values used in Section 5.5.1,

$W' = 1.74$ psi from Figure 5-9,

$$\% \text{ Deflection} = \frac{(1.0)(0.1)(1.74 + 4.17)(100)}{0.149(516) + 0.061(400)} = \frac{59.1}{101.28} = 0.58 \% = 1.33 \text{ mm}$$

Using Eq. 3.2,

$$\% \text{ Deflection} = \frac{(1.0 \times 0.1 \times 4.17 + 0.1 \times 1.74)100}{\{2(461,000)/[3(18 - 1)^3]\} + 0.061(400)} = \frac{59.1}{87.01} = 0.68 \% = 1.55 \text{ mm}$$

5.6 Pipe-Soil Interaction with Finite Element analyses

5.6.1 Introduction

This section presents the pipe-soil interaction using finite element models. The models were developed in order to study the deformation and stress experienced by iPVC pipe under different loading conditions. The finite element models are analyzed by using PLAXIS 2D and ABAQUS 6.14-3 software. The results of the analysis are compared to the actual test results in order to validate the models. The validation facilitates the use of the finite element method to do further analyses without having to perform the actual installation for testing. The properties and parameters of the finite element analyses (FEA) model elements and soil and pipe models are described and the results are presented.

5.6.2 Assumptions and Parameters for FEM Model

The analysis was performed in PLAXIS 2D initially and, hence, the results were obtained under plane strain conditions. The strains normal to x-y plane ϵ_z and shear strains γ_{xz} and γ_{yz} were assumed to be zero. The Mohr-Coulomb model was used to model the behavior of soil in the FEM analysis on PLAXIS 2D and ABAQUS 6.14-3. The Mohr-Coulomb model involves four input parameters, i.e., Young's modulus E and Poisson's ratio (ν) for soil elasticity; friction angle ($\phi - \text{phi}$) and the dilatancy angle ($\psi - \text{psi}$) for soil plasticity. Table 5-5 presents the properties of soil used in this dissertation to perform the FEM analysis.

Table 5-5 Soil Properties for FEM Analysis
(Source: Sharma, 2013)

Parameter	Value
Modulus of Soil Reaction (E')	400 psi (57,600 psf)
Poisson's ratio (ν)	0.30
Friction angle (ϕ)	35 °
Dilatancy angle (ψ)	5 °

5.6.3 FEM Analysis in PLAXIS 2D

iPVC pipe was modeled by using plate elements (line elements) feature of PLAXIS 2D. The iPVC pipe was modeled as a linear elastic material with a modulus of elasticity of 461,000 psi (from Table 4-6) and a Poisson's ratio of 0.3. Figure 5-10 and Figure 5-11 illustrates the screenshot of the soil and iPVC pipe properties defined in the model.

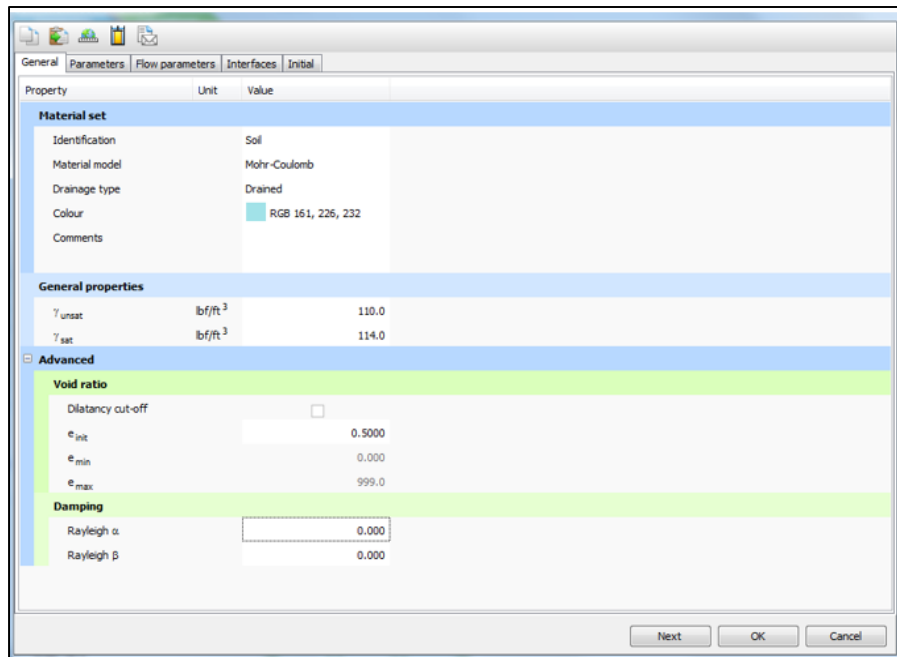


Figure 5-10 Screenshot of Soil Properties used for FEM analysis

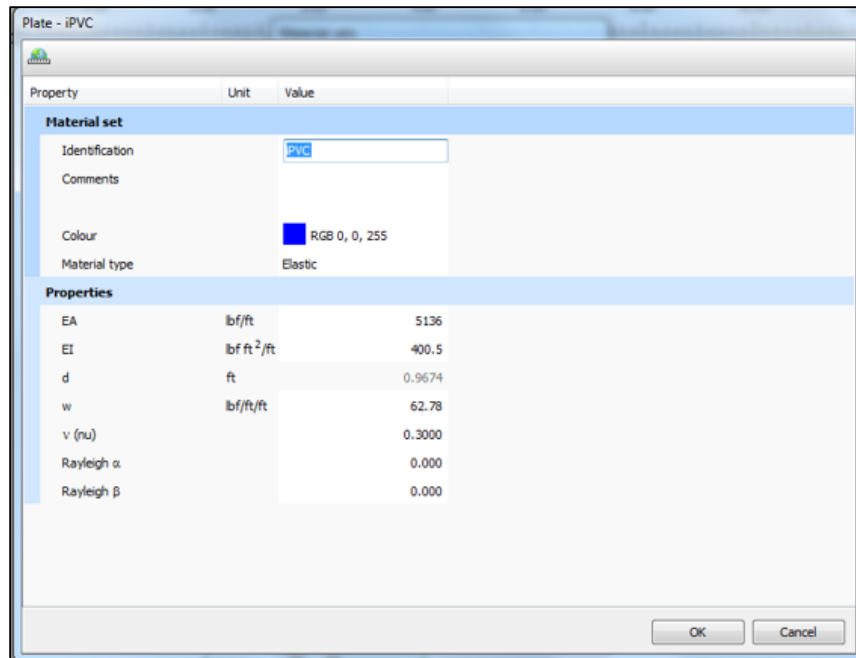


Figure 5-11 Screenshot of iPVC pipe Properties used for FEM Analysis

The model was developed for unfavorable conditions of pipe installation in the trench. The unfavorable conditions refer to improper bedding or no bedding support beneath the pipe. Hence, the model does not include a separate bedding for the pipe and only has soil all around the pipe. Bedding (trench bottom) acts as a support to the pipe; hence, the pipe is under less stress if proper bedding is provided. But, in absence of bedding, pipe experiences more stress and maximum deflection can be expected in the pipe walls. Hence, the model was developed for the maximum deflection conditions due to unfavorable conditions of installation. The analysis was performed on the end of the pipe rather than at the joint of the pipe as the maximum deflection is expected to be at the end of pipe as compared to the joint of the pipe.

A 4 ft wide × 5 ft deep soil box was considered as it nearly represents the actual trench conditions of the experimental bedding test. A uniformly distributed load of 50,000 lbs was considered on top of the soil box to simulate the live load application by the 20-ton

truck in the experimental testing as explained in Chapter 3 Section 3.3.7. Figure 5-12 presents the model developed in PLAXIS 2D before the FEM calculations.

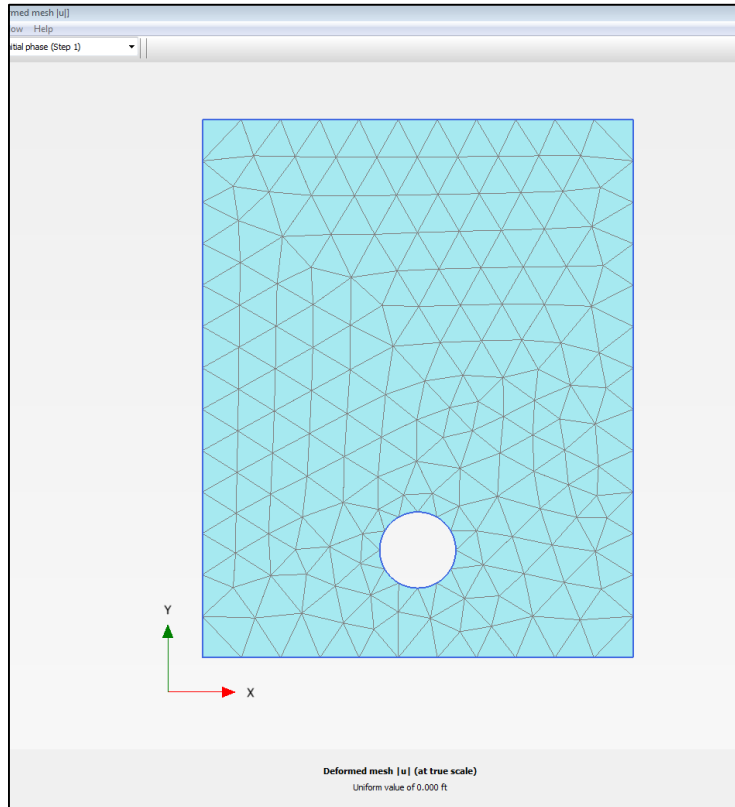


Figure 5-12 Distribution of Mesh for Soil Box in Initial Phase using Plaxis 2D

The calculations were run for the soil box and iPVC pipe and a load of 50,000 pounds was applied uniformly on top of the trench to demonstrate the deflection of the pipe under the soil and truck load application. Figures 5-13 to 5-17 illustrate the initial phase without any FEM analysis, vertical deflection due to earth load and earth load plus truck load, and horizontal deflection due to earth load and earth load plus truck load. The deflection results from the FEM analysis are summarized in Table 5-8.

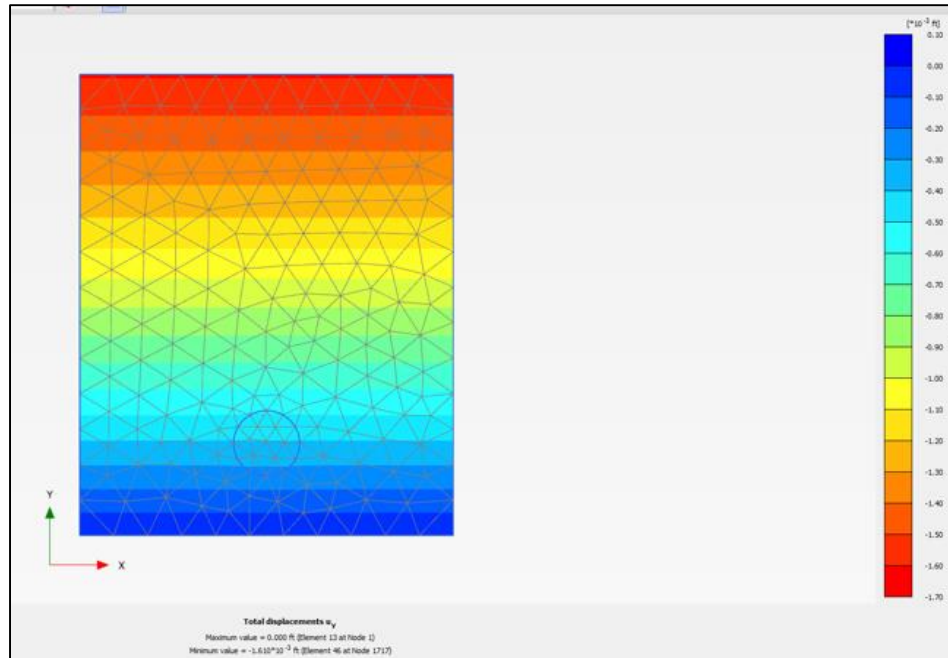


Figure 5-13 Initial Phase before FEM Analysis

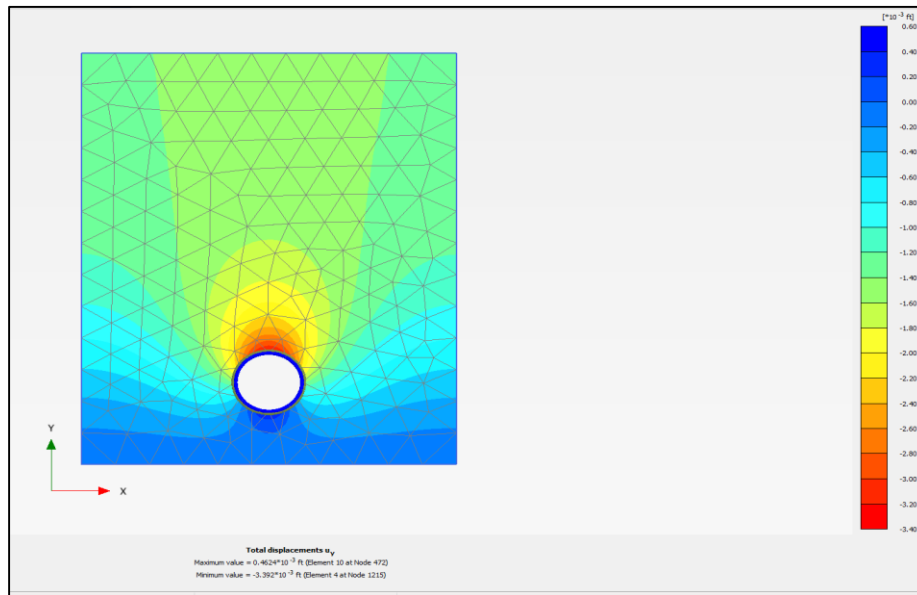


Figure 5-14 Vertical Displacement due to Earth Load

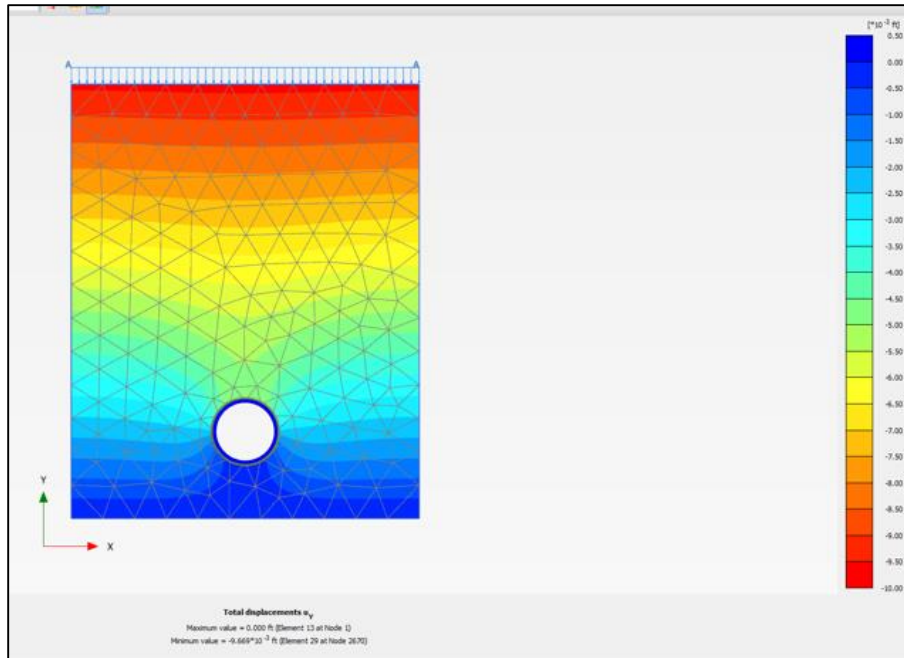


Figure 5-15 Vertical Displacement due to Earth plus Truck Load

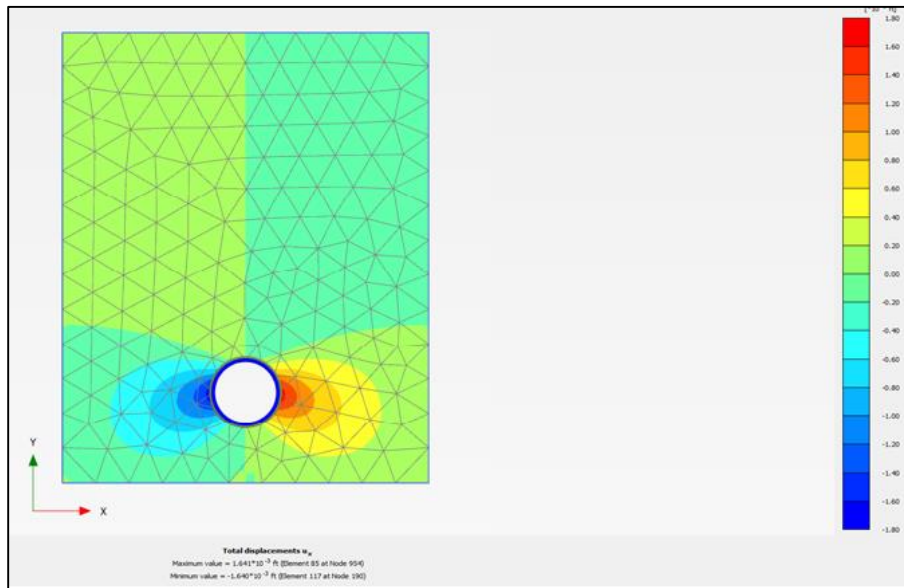


Figure 5-16 Horizontal Displacement due to Earth Load

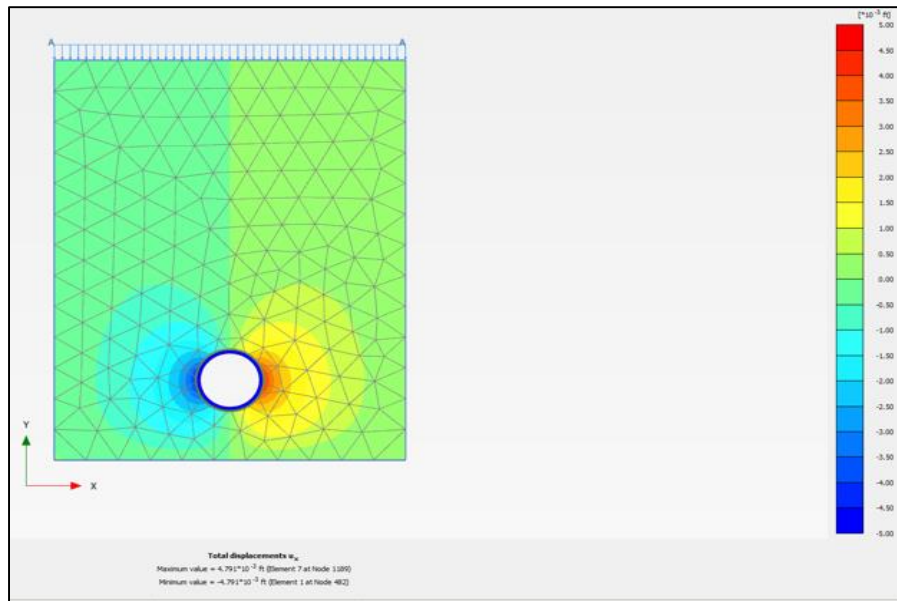


Figure 5-17 Horizontal Displacement due to Earth plus Truck Load

5.6.4 FEM Analysis in ABAQUS 6.14-3

A 3D FE analysis with ABAQUS was performed for the bedding test 2, considering a soil box (3 ft wide, 1 ft long and 4.5 ft high). The soil box size was slightly modified to see the change in deflection due to less cover on top of the pipe and less width of the trench. Both soil box and iPVC pipe were modeled as 3D solid sections and the soil material was defined by Mohr-Coulomb plasticity model. The soil box was modeled in different layers to illustrate layers of bedding, compacted clay and lean clay and was partitioned to enable different meshing techniques. These factors were not considered in PLAXIS 2D software. Also, a surface to surface contact between soil and pipe was defined.

For the soil box, C3D8R element is used. Element type for the soil is structured hexagonal shape, but a swept wedge shape element was considered for the curved region of the soil around the pipe. C3D6 element is used for the pipe. The mesh sizes for the soil box, the curved region of soil around the pipe and the pipe, are 0.7, 0.5 and 0.7, respectively. Earth load is defined as the gravity load through all layers of the soil and live

load is defined as a distributed load to prevent stress concentration under the axles of the truck.

Figure 5-18 through 5-21 illustrate geometry of the model, contact surface between soil and pipe, meshing, and vertical deflection contours respectively. Table 5-6 summarizes the vertical and horizontal deflection values of FE analysis by ABAQUS 6.14-3 considering earth load only. Figure 5-22 through 5-24 illustrate vertical deflection contours due to the earth plus truck load and the direction of resultant deflection in pipe and soil. Table 5-7 summarizes the vertical and horizontal deflection values as per the FE analysis for earth plus truck loads.

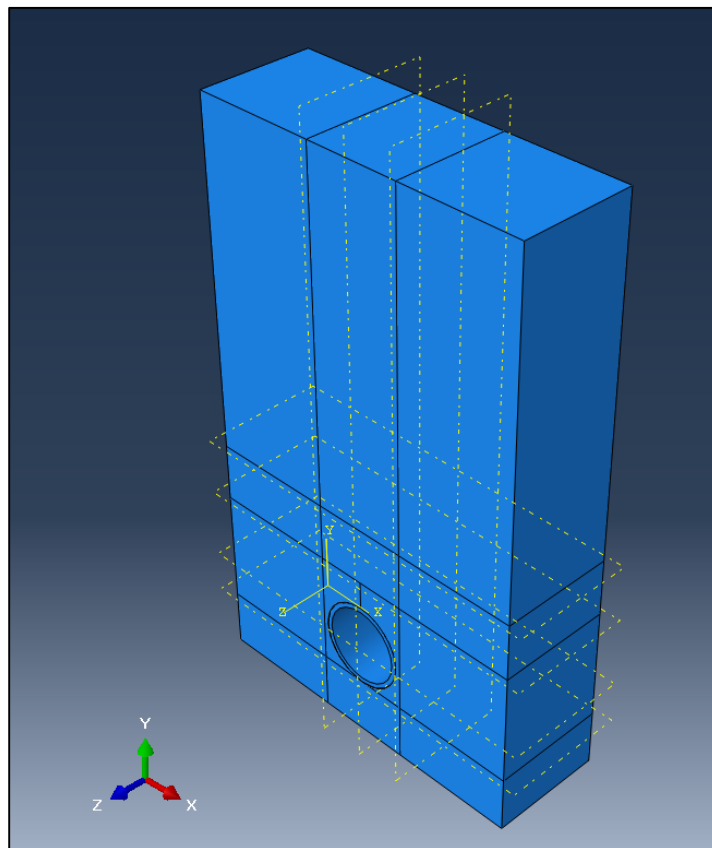


Figure 5-18 Geometry of Pipe-Soil Model in ABAQUS

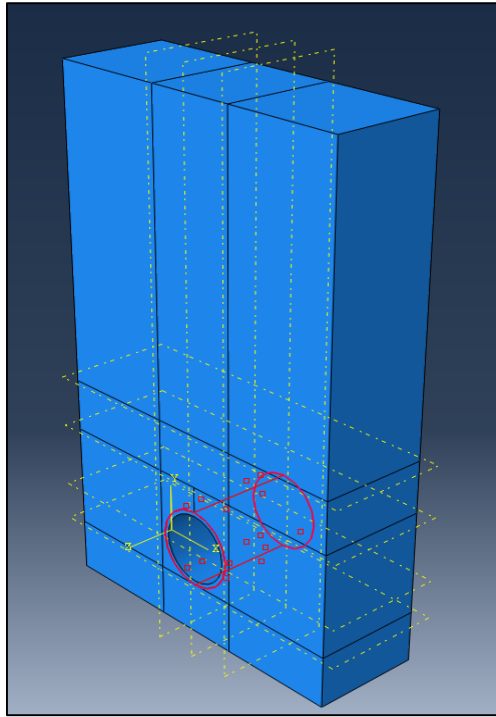


Figure 5-19 Contact Surface between Soil and Pipe

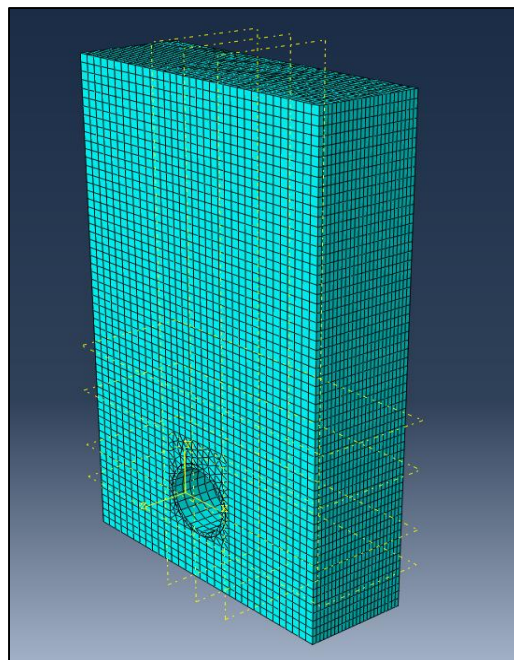
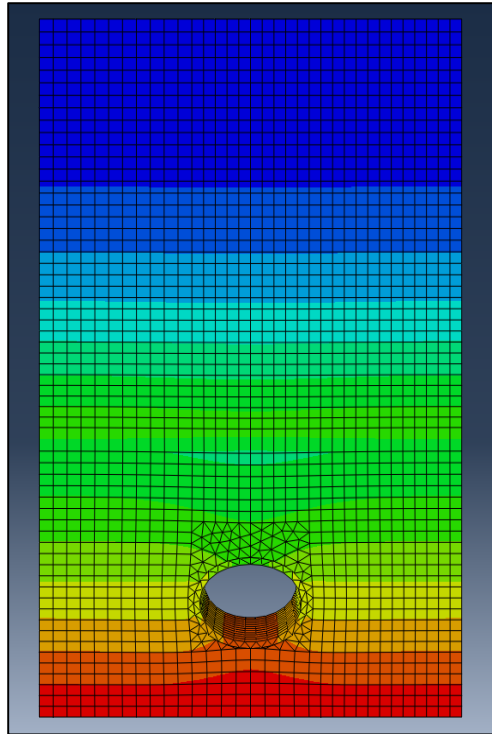
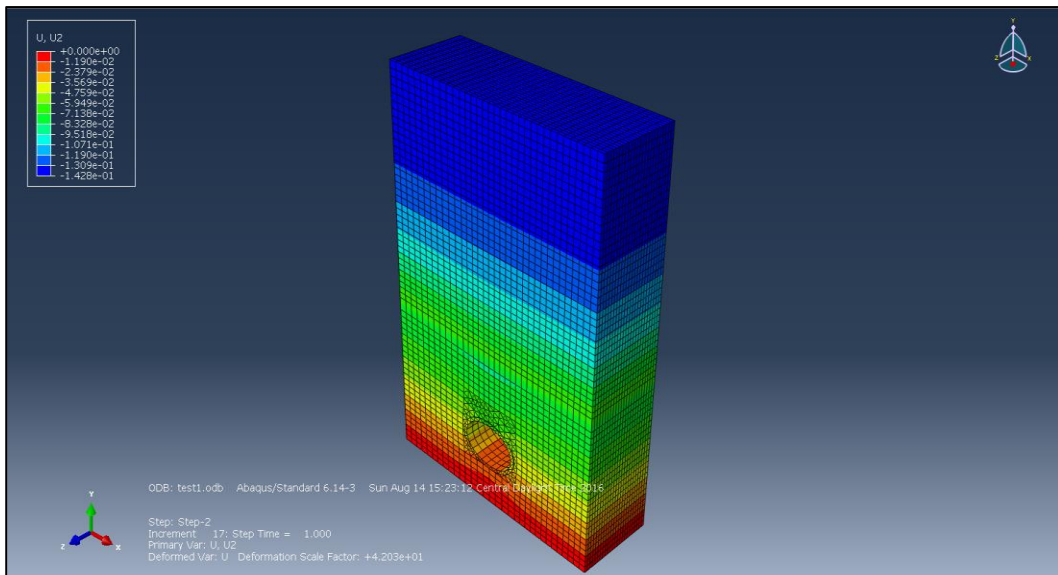


Figure 5-20 Meshing of Model in ABAQUS



(a)



(b)

Figure 5-21 Vertical Deflection Contours (a) Front View (b) 3D View

Table 5-6 Summary of Vertical and Horizontal Deflections for Earth Load only

Step time	Vertical Deflection (in.)	Horizontal Deflection (in.)
0	0	0
0.001	-2.24E-05	1.41859E-05
0.002	-4.48E-05	2.84319E-05
0.0035	-7.85E-05	4.98048E-05
0.00575	-0.000129001	8.18662E-05
0.009125	-0.000204733	0.000129963
0.014188	-0.000318297	0.000202119
0.021781	-0.000488564	0.000310378
0.033172	-0.000743792	0.000472816
0.050258	-0.00112625	0.000716582
0.075887	-0.0016991	0.00108246
0.11433	-0.00255654	0.00163171
0.171995	-0.00383883	0.00245638
0.258493	-0.00575424	0.00369463
0.388239	-0.00861119	0.00555388
0.582859	-0.0128652	0.00834441
0.874788	-0.0191899	0.0125292
1	-0.0218855	0.014323
1.001	-0.0219267	0.0143484
1.0035	-0.0220295	0.0144118
1.00575	-0.0221221	0.0144689
1.00912	-0.0222609	0.0145545
1.01419	-0.022469	0.014683
1.02178	-0.022781	0.0148755
1.03317	-0.0232488	0.0151642
1.05026	-0.0239498	0.0155969
1.07589	-0.0249999	0.0162453
1.11433	-0.026572	0.0172163
1.172	-0.0289235	0.0186697
1.25849	-0.0324825	0.0208827
1.38824	-0.0379046	0.0242817
1.58286	-0.0460733	0.0294269
1.87479	-0.0583248	0.0371918
2	-0.0635855	0.0405167

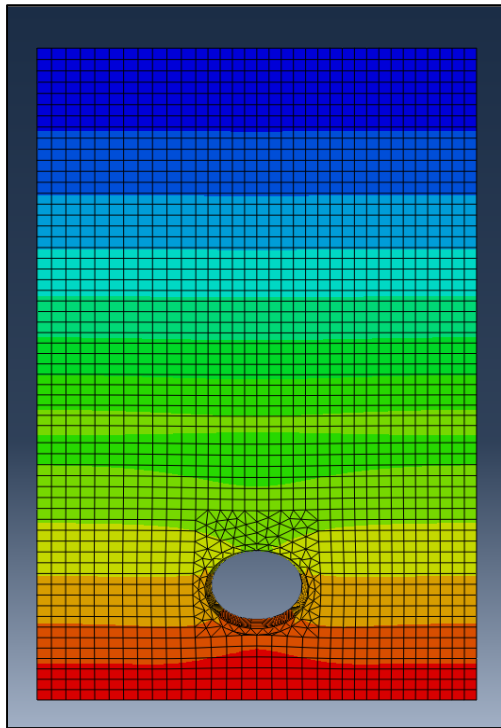


Figure 5-22 Vertical Deflection Contours - Front View

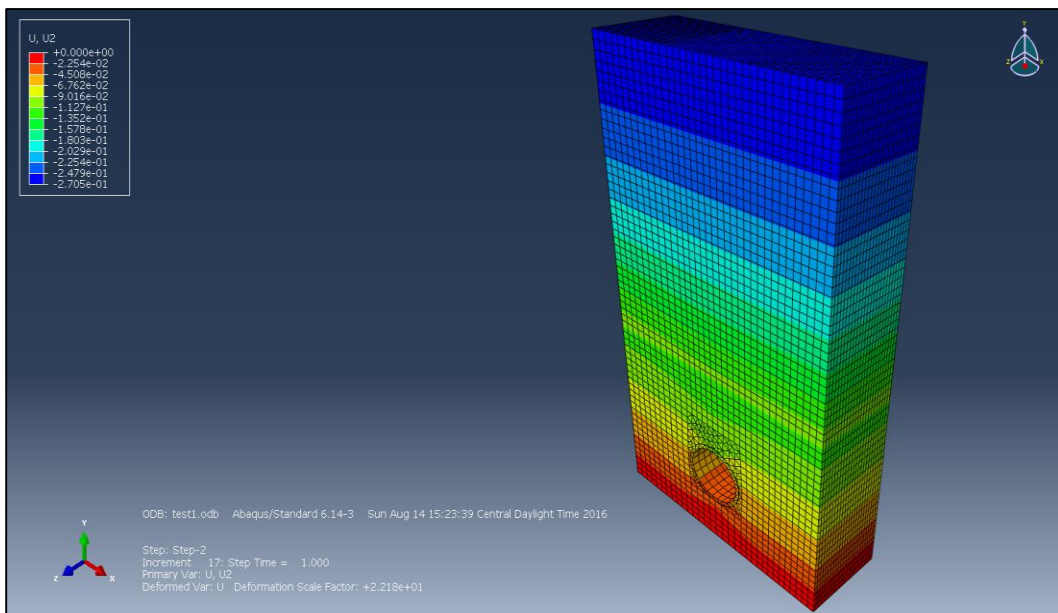


Figure 5-23 Vertical Deflection Contours - 3D View

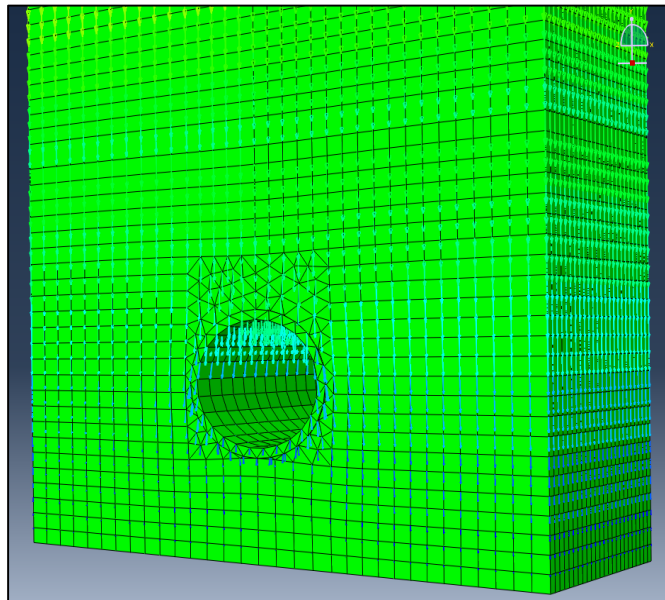
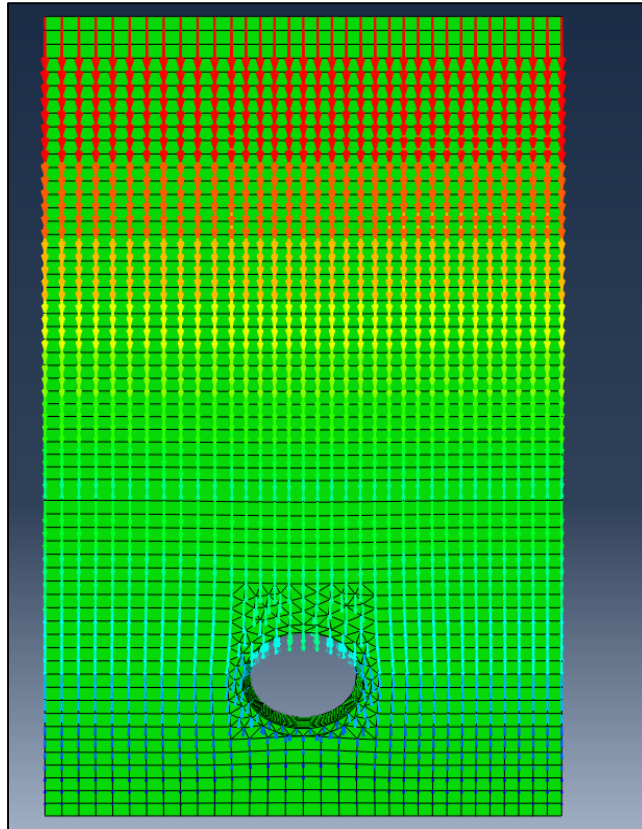


Figure 5-24 Arrows showing the Direction of Resultant Deflection in Pipe

Table 5-7 Summary of Vertical and Horizontal Deflections for Earth plus Truck Loads

Step time	Vertical Deflection (in.)	Horizontal Deflection (in.)
0	0	0
0.001	-2.41E-05	0.000015476
0.002	-4.82E-05	3.10268E-05
0.0035	-8.44E-05	5.43583E-05
0.00575	-0.000138662	8.93584E-05
0.009125	-0.000220064	0.000141865
0.014188	-0.000342133	0.00022064
0.021781	-0.000525158	0.000338834
0.033172	-0.000799523	0.000516195
0.050258	-0.00121069	0.000782385
0.075887	-0.00182659	0.00118198
0.11433	-0.00274862	0.00178199
0.171995	-0.00412778	0.00268315
0.258493	-0.0061885	0.00403685
0.388239	-0.00926337	0.00607054
0.582859	-0.0138442	0.00912486
0.874788	-0.0206594	0.0137087
1	-0.0235651	0.0156745
1.002	-0.0237027	0.0157613
1.0035	-0.0238059	0.0158265
1.00575	-0.0239606	0.0159242
1.00912	-0.0241927	0.0160706
1.01419	-0.0245406	0.0162903
1.02178	-0.0250622	0.0166195
1.03317	-0.0258438	0.017113
1.05026	-0.0270146	0.0178524
1.07589	-0.0287676	0.0189597
1.11433	-0.0313898	0.0206169
1.172	-0.0353693	0.0231439
1.25849	-0.0414452	0.0270244
1.38824	-0.0506077	0.0329094
1.58286	-0.0643709	0.0418006
1.87479	-0.0851396	0.0551743
2	-0.094074	0.0609078

Soil is a heterogeneous material. Different environmental conditions, level of compaction and etc., play an important role in the behavior of the soil, so, defining the exact material properties of soil was difficult. When FE model has some complexities such as contacts and when the exact data are not available, i.e. exact soil properties, the errors greater than 20% could be expected and be acceptable. Based on the complexity of the FE modeling in this study, the results of the FE analysis match acceptably with the experimental results.

Table 5-8 Deflection Values obtained from FEM Analysis

Scenario	PLAXIS 2D		ABAQUS 6.14-3	
	Horizontal Deflection (mm)	Vertical Deflection (mm)	Horizontal Deflection (mm)	Vertical Deflection (mm)
Initial	0	0	0	0
Earth Load	0.99	1.15	1.03	1.61
Earth + Truck Load	2.91	2.95	1.54	2.38

Figure 5-25 and Figure 5-26 compares the deflection values obtained by the theoretical methods, experimental testing and FEM analysis of iPVC pipe for earth load and earth plus truck load application respectively. The deflection calculated by the theoretical methods (Spangler's equation and Modified Iowa equation) is considered equal in vertical and horizontal direction. The values are the absolute values of deflection in mm. Vertical deflection was negative whereas horizontal deflection was positive throughout the testing.

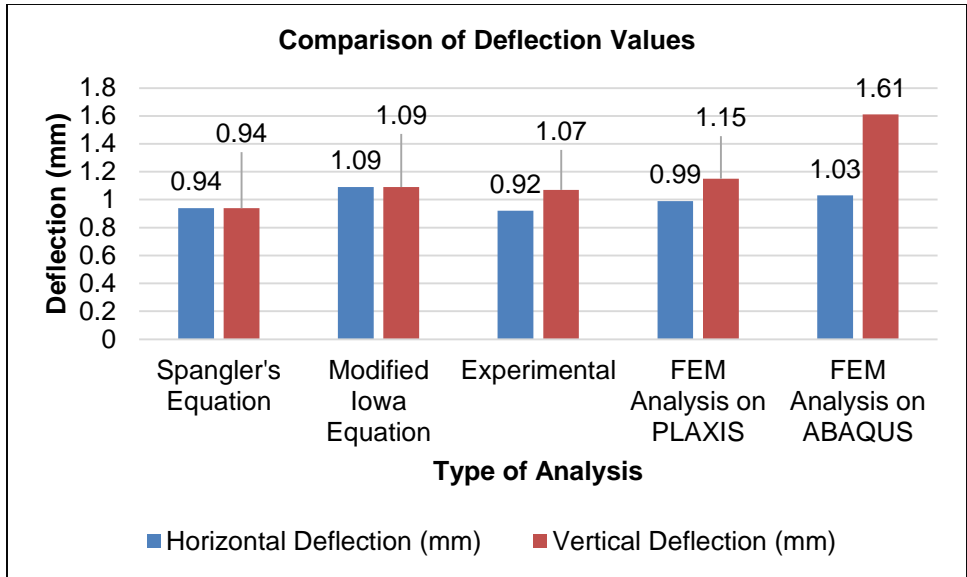


Figure 5-25 Deflection Values for Earth Load Application

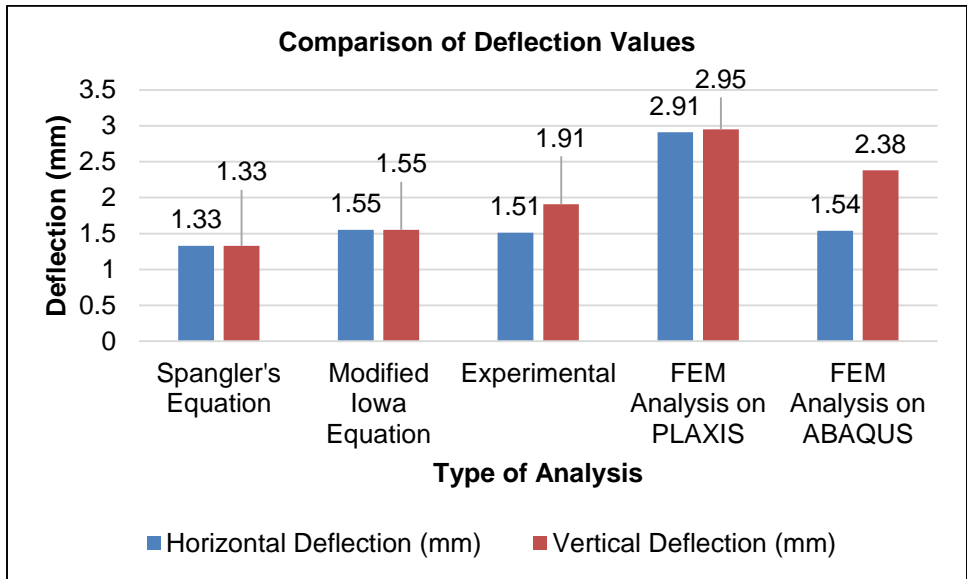


Figure 5-26 Deflection Values for Earth plus Truck Load Application

FEM analysis considering earth load only calculated the maximum absolute value of horizontal deflection as 1.03 mm and maximum absolute vertical deflection value of

1.61 mm in ABAQUS 6.14-3. The maximum experimental absolute value obtained due to the earth load is 0.92 mm for horizontal deflection and 1.07 mm for vertical deflection.

FEM analysis calculated the maximum horizontal and vertical deflection value of 2.92 and 2.95 mm, respectively, under earth plus truck load. The maximum absolute experimental values of horizontal and vertical deflection are 1.51 mm and 1.91 mm, respectively, at the end of the pipe.

The reason for the vertical deflection experimental value exceeding both the theoretical values in the earth plus truck loading condition could be due to the decrease in depth of soil cover provided during the live load simulation. The loaded truck completed 76 cycles running on top of the trench in 2 hours (from 8:00 am to 10:00 am). This scenario was followed by the loaded truck stationed on top of the trench for 2 hours (from 10:00 am to 12:00 noon). A noticeable settlement of soil was witnessed on top of the trench after the two continuous hours of truck operation. The depth of cover was reduced from 5 ft to 4.5 ft. This might have caused the pipe to deflect more than the deflection calculated using the formulae.

The deflection values obtained by all four methods are negligible as compared to the allowable limits of deflection set at 7.5% by ASTM (for a 9-in. OD PVC where allowed deflection = 17.15 mm) and 5% by AWWA (for a 9-in. OD PVC where allowed deflection = 11.43 mm) for flexible pipes.

Considering the values obtained by the theoretical formulae based on the pipe stiffness and modulus of elasticity of the iPVC pipe, and also the results of FE analysis by ABAQUS, it could be concluded that the deflection values for iPVC pipe by the experimental bedding test are in agreement with other values, thus, validating the experiment conducted.

5.7 Contribution to the Body of Knowledge

5.7.1 *Overall Approach to Evaluate a New Pipe*

There is a lot of information readily available for pipe materials such as ductile iron, PVC, and HDPE. Introducing a new pipe material into the market dominated by these three pipe materials would need a comprehensive research on the new pipe material. The iPVC pipe is a new pipe material which is not known to the U.S. market. The first part of this dissertation was to develop a holistic approach to perform the tests on iPVC pipe, which would provide information about the pipe material and will help introduce the pipe material to the U.S. market. The six tests performed in this WRF funded project provide enough information about iPVC pipe to be considered by water utilities while selecting the pipe materials for water application. The overall testing approach developed in this WRF funded project can be used for introducing new pipe materials in the future.

5.7.2 *Uniqueness of Fatigue and Bedding Test*

The first four tests in this WRF funded project, hydrostatic short-term burst pressure test, impact test, stiffness test, and tensile test, have standard ASTM manuals explaining the testing procedure, expected results and analysis of results. But, the other two tests, fatigue test and bedding test, do not have any specific standards.

The fatigue test is an important test for pipe material evaluation considering the effect of surges on pipelines. Pipelines could fail due to high surges and, hence, designers need to consider surge pressure while designing the installation. Since, there was no standard available for considering the effects of surges and to estimate the fatigue life cycle, development of fatigue testing for iPVC pipe was a challenge. It was important to understand the effects of surges on iPVC pipe. Water utilities experience a lot of failures due to surges and, hence, the testing results for iPVC pipe can provide a lot of information

to the utilities, which can be used during the design or implementation of surge control techniques to minimize the effect of surges.

Bedding tests provided valuable information on deflection of the pipe wall. It is imperative that the pipe walls buckle under loads, but it is important to have as little deflection as less than the AWWA allowable deflection. Similar to fatigue testing, there is no set standard to perform the bedding test on pipe materials. A testing procedure was developed solely as a part of this research project aligning with the experimental procedure conducted at the Kansas University (Khatri, 2014) and from guidance provided by the AW engineers to collect the results for the stress, strain, and deflection experienced by the pipe wall. The deflection results from the testing were satisfactory and negligible compared to the set standard values of deflection. The live load simulation with a 20-ton truck was a significant addition to the testing procedure as it helped to understand the behavior of iPVC pipe and deflection under earth plus live load. The testing results could be used by water utility designers to compare the material performance with other pipe materials and consider what loading conditions the pipe could withstand during and after installation.

5.7.3 Comparison of Evaluation of New Pipe with Other Pipe Materials

The parameters obtained in this dissertation along with the parameters available from previous testing on iPVC pipe are compared to other pipe materials such as ductile iron (DI), regular PVC, and HDPE. Table 5-9 compares the properties of iPVC pipe with other pipe materials.

Table 5-9 Comparison of DI, PVC, HDPE and iPVC pipe
(Source: DIPRA, Uni-Bell, Plastics Pipe Institute)

Parameter	DI Pipe	PVC Pipe	HDPE Pipe	iPVC pipe
Trade organization	DIPRA	Uni-Bell	PPI	Not available
AWWA designation	C151	C900 and C905	C906	C900
Diameter range	3 in. – 64 in.	4 in. – 12 in. (C900) 14 in. - 48 in. (C905)	4 in. – 65 in.	4 in. – 12 in. (Anticipated up to 24 in.)
Hydrostatic Burst Pressure	4,150 psi	755 psi	814 psi	1,042 psi
Impact strength (ASTM F2444)	Not available	Not available	Not available	1,200 ft-lbs
Pipe stiffness	4,843 psi	364 psi	218 psi	479 psi
Tensile strength	60,000 psi	7,000 psi	3,500 psi	7,930 psi
Modulus of elasticity	24,000,000 psi	400,000 psi	130,000 psi	461,000 psi
Ductile or brittle	Ductile	Brittle	Ductile	Ductile
Corrosion resistance (int. + ext.)	Poor	Excellent	Excellent	Excellent
Cement lining and PE encasement	Required	Not applicable	Not applicable	Not applicable
UV resistance	Excellent	Gradual strength decline	Excellent	Not available
Cyclic resistance	Excellent	Poor	Excellent	Excellent
Standard pipe lengths (8 in.)	18 ft or 20 ft	20 ft	40 ft - 50 ft	20 ft

Table 5-9 — *Continued*

Parameter	DI Pipe	PVC Pipe	HDPE Pipe	iPVC pipe
Type of joints	Push-on or mechanical	Push-on, mechanical	Fusion (ASTM F2620-13 and F1055-15) or mechanical	Push-on, mechanical
Compatible w/ DI fittings	Yes	Yes	Yes	Yes
Need for joint restraint	Yes	Yes	No	Yes
Ability to locate underground	Excellent	Needs tracer wire	Needs tracer wire	Needs tracer wire

5.7.4 Marketing of iPVC Pipe in U.S.

The Pyungwha Pipe Industry, Inc. (PPI), South Korea, is the manufacturer of iPVC pipe and intends to introduce iPVC pipe as a pipe material to the U.S. Currently, iPVC pipe is manufactured in South Korea, but a manufacturing plant could be set up by the manufacturer in the U.S. in the future. This WRF funded research project serves as a basis to validate iPVC pipe engineering properties and provide confidence for using the pipe for water applications.

The initial testing results of this project has been presented and published in conference proceedings (ASCE, 2016; ACE, 2016; NASTT, 2016). The publication of conference papers, and technical reports by WRF will act as a marketing tool and will create awareness among the water utilities about the new iPVC pipe. The pilot installation by Missouri American Water in St. Louis County, MO and their evaluation of the iPVC pipe in service will provide confidence in the performance of iPVC pipe. The overall project results will develop confidence among water utilities and will generate interest to explore the new iPVC pipe in water applications in the future.

5.8 Chapter Summary

This chapter presented the discussion of results of the laboratory tests performed as part of this dissertation. Key parameters such as hoop stress, short-term rating of iPVC pipe, pipe stiffness and stiffness factor, flexural modulus, design fatigue life, strain and stress values in iPVC pipe during the bedding test along with the experimental values of deflections, theoretical values of deflection based on pipe stiffness and based on modulus of elasticity and DR of iPVC pipe were discussed in detail. The finite element analyses of iPVC pipe in a soil box was simulated and discussed in this chapter. The chapter concludes with comparison of key iPVC pipe parameters with other pipe materials such as ductile iron, regular PVC and HDPE.

Chapter 6

Conclusions and Recommendations for Future Research

Chapter 5 discussed the research results analysis and its significance as well as its contribution to the body of knowledge to the research community through proceedings publications and this dissertation. This chapter concludes the research results and makes recommendations for future research of pipe materials.

6.1 Conclusions

The results of this dissertation and WRF Project Report No. 4650 introduced iPVC pipe as an alternative pipe material for water applications. The testing carried out by CUIRE and Microbac under the leadership of AW provided information about iPVC pipe material characteristics.

1. The test results exceeded the standard requirements set by AWWA for PVC pipes as follow:
 - Average hydrostatic short-term burst pressure was recorded as 1,042 psi (40% higher than AWWA standard requirements). Ductile and brittle failure was observed in the pipe samples.
 - Average hoop stress was calculated as 8,855 psi (38% higher than AWWA standards requirement).
 - Average impact strength was recorded as 1,200 foot-pounds at 73 °F (12 times higher than AWWA requirements) and 1,080 foot-pounds at 32 °F (10 times higher than AWWA requirements).
 - Average pipe stiffness was recorded as 479 psi (32% higher than AWWA standard requirements).
 - Average tensile strength was recorded as 7,930 psi (13% higher than AWWA standard requirements).

- Average modulus of elasticity was recorded as 461,000 psi (15% higher than AWWA standard requirements).
- Fatigue design life for 9 in. OD DR 18 iPVC pipe is 125 years considering only the surge pressure experienced by the pipe. Other parameters may influence the life of the pipe.
- Maximum Deflection of iPVC pipe under earth load:
 - Theoretical based on Pipe Stiffness = 0.94 mm
 - Theoretical based on Modulus of Elasticity = 1.09 mm
 - Experimental = 0.92 mm (Horizontal)
 - Experimental = 1.07 mm (Vertical)
 - Finite Element analyses on PLAXIS 2D = 0.99 mm (Horizontal)
 - Finite Element analyses on PLAXIS 2D = 1.15 mm (Vertical)
 - Finite Element analyses on ABAQUS = 1.03 mm (Horizontal)
 - Finite Element analyses on ABAQUS = 1.61 mm (Vertical)
- Maximum Deflection of iPVC pipe under earth plus live (truck) loads (50,000 lbs):
 - Theoretical based on Pipe Stiffness = 1.33 mm
 - Theoretical based on Modulus of Elasticity = 1.55 mm
 - Experimental = 1.51 mm (Horizontal)
 - Experimental = 1.91 mm (Vertical)
 - Finite Element analyses on PLAXIS 2D = 2.91 mm (Horizontal)
 - Finite Element analyses on PLAXIS 2D = 2.95 mm (Vertical)
 - Finite Element analyses on ABAQUS = 1.54 mm (Horizontal)
 - Finite Element analyses on ABAQUS = 2.38 mm (Vertical)

- AWWA maximum allowable deflection for 8 in. DR 18 PVC pipe is 5% (11.43 mm). The experimental values observed are much lesser than the AWWA requirements.
2. Burst test results illustrates the pipe material's resistance to hydrostatic pressure. iPVC pipe exceeded the AWWA standard requirements displaying higher resistance to circumferential stress (hoop stress).
 3. Impact strength of pipe materials is an important characteristic considered during the handling, shipping and installation of PVC. The higher impact strength of iPVC pipe will provide a better resistance to sudden impacts that could be experienced by iPVC pipe during handling, shipping and installation.
 4. A lower pipe stiffness would result in increased deflection of pipe, increased reliance on soil to carry the load to minimize deflection, distortion of pipe shape reducing hydraulic capacity and increased strain in wall, which might lead to failure or crack in the pipe. The higher pipe stiffness of iPVC pipe compared to the AWWA PVC standards would help in less deflection of pipe walls reducing the reliance on soil for support in carrying loads, less distortion of pipe shape and less strain in pipe walls.
 5. The bedding test for iPVC pipe confirmed that the native trench conditions in accordance with AWWA C605 are adequate for the iPVC pipe installation and no special considerations are required for bedding or trench for iPVC pipe. The deflections observed in the iPVC pipe were within the recommended limits.
 6. Test results showed that iPVC pipe material has exceeded the AWWA requirements and it displays properties of ductile, stiffness and robustness and can be used in any trench conditions.

6.2 Recommendations for Future Research

Recommendations for future research can be summarized as follows:

1. The joint of iPVC pipe considered for this dissertation was an unrestrained gasketed bell and spigot joint. A new joint could be developed similar to the BRS joint mentioned in this dissertation which would be suitable for iPVC pipe.
2. The fatigue test can be continued until pipe failure with using strain gauges to collect information about the pipe strain due to pressure surges. The fatigue test in this dissertation was performed on a 9 in. OD DR 18 iPVC pipe. A different diameter size with a different wall thickness might have different test results as compared to the results in this dissertation.
3. The bedding test can be performed in different types of soils and bedding materials in a laboratory for a controlled environment testing. The ground water pressure was not taken into consideration and was not measured during the testing. Future tests could make arrangements in the test setup to measure the water pressure. Use of more earth pressure cells in bedding test to understand the distribution of lateral pressure on pipe and trench walls.
4. The bedding test setup did not have sensors to measure the temperature change in the soil. It would have been interesting to measure the impact of temperature on the deformation of iPVC pipe.
5. iPVC pipe was deformed due to the loading on the pipe in the bedding test. The deformation might affect the overall flow capacity of the pipe. The change on the flow capacity was not measured or considered during the testing.
6. Pyungwha Pipe Industry (PPI), manufacturer of iPVC pipe, has assessed the aseismic property of iPVC pipe and concluded that the product is safe at potential seismic zones (up to 7 magnitude on Richter scale) and soft ground conditions. A

full scale testing program to assess the seismic performance of iPVC pipe should be conducted to verify the results obtained by PPI.

7. Saddle tapping is performed on iPVC pipe for lateral service connections. Other tapping methods need to be evaluated to determine the most suitable method of tapping. The minimum distance between two taps or connections need to be determined to avoid longitudinal cracking of iPVC pipe.
8. Applicability of iPVC pipe in trenchless installations should be studied.

Appendix A
Abbreviations

AC – Asbestos-Cement Pipe

ACE – Annual Conference and Exposition by AWWA

ANSI – American National Standards Institute

ASCE – American Society of Civil Engineers

ASME – American Society of Mechanical Engineers

ASTM – American Society for Testing and Materials

AW – American Water

AWWA – American Water Works Association

AwwaRF – American Water Works Association Research Foundation

B.C. – Before Christ

BRS – Bulldog Restrained Joint System

BWP – Bar-wrapped Steel-cylinder Concrete Pipe

CDS – Cable-extension Displacement Sensor

CIP – Cast Iron Pipe

CISPI – Cast Iron Soil Pipe and Fittings Handbook

CLSM – Controlled Low Strength Material

CPVC – Chlorinated Polyvinyl Chloride Pipe

CUIRE – Center for Underground Infrastructure Research and Education

DIP – Ductile Iron Pipe

DIPRA – Ductile Iron Pipe Research Association

DR – Dimension Ratio

DS – Displacement Sensor

EPC – Earth Pressure Cell

FEA – Finite Element analyses

FEM – Finite Element Model

FHWA – Federal Highway Administration

GRP – Glass Reinforced Pipe

HDB – Hydrostatic Design Basis

HDD – Horizontal Directional Drilling

HDPE – High Density Polyethylene Pipe

HDS – Hydrostatic Design Stress

HS – High Strength Wire

ID – Inside Diameter

iPVC pipe – Structurally enhanced/ Improved PVC Pipe

JSWA – Japanese Sewage Works Association

LPT – Linear-Position Transducer

LTHS – Long-Term Hydrostatic Strength

LVDT – Linear Variable Differential Transformer

MDPE – Medium Density Polyethylene Pipe

MOAW – Missouri American Water

NASTT – North American Society for Trenchless Technology

NRCC – National Research Council of Canada

OD – Outside Diameter

PA1 – Polyamide 1

PA2 – Polyamide 2

PC – Pressure Class

PCCP – Prestressed Concrete Cylinder Pipe

PE – Polyethylene Pipe

PPI – Plastics Pipe Institute

PPI – Pyungwha Pipe Industry Inc., South Korea (Manufacturer of iPVC pipe)

PS – Pipe Stiffness

PVC/ PVC-U – Un-plasticized (regular) Polyvinyl Chloride Pipe

PVC-M – Modified Polyvinyl Chloride Pipe

PVC-O – Oriented Polyvinyl Chloride Pipe

RCP – Rapid Crack Propagation

RCP – Reinforced Concrete Pipe

RTP – Reinforced Thermoplastic Pipe

SEM – Scanning Electron Microscope

SF – Stiffness Factor

SG – Strain Gauge

SL – Side Load

SP – Steel Pipe

SRHDPE – Steel Reinforced High Density Polyethylene

Std. Dev. – Standard Deviation

STR – Short Term Rating

U.S. – United States

UTA – University of Texas at Arlington

UV – Ultraviolet

VCM – Vinyl Chloride Monomer

VCP – Vitrified Clay Pipe

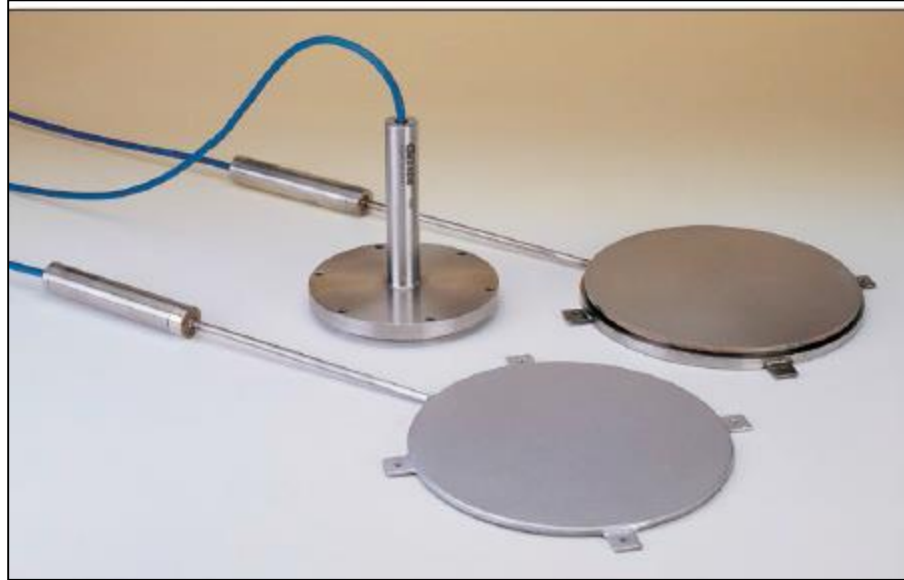
VL – Vertical load

WRF – Water Research Foundation

Y/T – Yield to Tensile Ratio

Appendix B
Bedding Test Instrumentation

Earth Pressure Cell (Geokon)



Technical Specifications

	4800	4810	4815	4820	4830	4855	3500
Transducer Type	Vibrating Wire	Vibrating Wire	Vibrating Wire	Vibrating Wire	Vibrating Wire	Vibrating Wire	Semiconductor
Output	2000-3000 Hz	2000-3000 Hz	2000-3000 Hz	2000-3000 Hz	2000-3000 Hz	2000-3000 Hz	2 mV/V, 0-5 VDC or 4-20 mA
Standard Ranges ¹	70, 170, 350, 700 kPa; 1, 2, 3, 5, 7.5, 20 MPa	350, 700 kPa; 1, 2, 3, 5 MPa	350, 700 kPa; 1, 2, 3, 5 MPa	350, 700 kPa; 1, 2, 3, 5 MPa	70, 170, 350, 700 kPa; 1, 2, 3, 5 MPa	2, 3, 5, 7.5, 10, 20 MPa	100, 250, 400, 600 kPa; 1, 2.5, 6 MPa
Over Range	150% F.S. (max)	150% F.S. (max)	150% F.S. (max)	150% F.S. (max)	150% F.S. (max)	150% F.S. (max)	150% F.S. (max)
Resolution	±0.025% F.S.	±0.025% F.S.	±0.025% F.S.	±0.025% F.S.	±0.025% F.S.	±0.025% F.S.	Infinite
Accuracy ²	±0.1% F.S.	±0.1% F.S.	±0.1% F.S.	±0.1% F.S.	±0.1% F.S.	±0.1% F.S.	±0.5% F.S.
Linearity	< 0.5% F.S.	< 0.5% F.S.	< 0.5% F.S.	< 0.5% F.S.	< 0.5% F.S.	< 0.5% F.S.	< 0.5% F.S.
Thermal Effect on Zero	< 0.05% F.S.	< 0.05% F.S.	< 0.05% F.S.	< 0.05% F.S.	< 0.05% F.S.	< 0.05% F.S.	< 0.05% F.S.
Typical Long-Term Drift	< 0.02% F.S./yr	< 0.02% F.S./yr	< 0.02% F.S./yr	< 0.02% F.S./yr	< 0.02% F.S./yr	< 0.02% F.S./yr	< ±0.02% F.S./yr
Cell Dimensions ³ (H × D)	6 × 230 mm	12 × 230 mm	26 × 230 mm	12 × 150 mm	12 × 150 mm	50 × 600 mm	6 × 230 mm
Transducer Dimensions (L × D)	150 × 25 mm	150 × 25 mm	150 × 25 mm	150 × 25 mm	150 × 25 mm	(included in above)	150 × 32 mm
Excitation Voltage	2.5-12 V swept square wave	2.5-12 V swept square wave	2.5-12 V swept square wave	2.5-12 V swept square wave	2.5-12 V swept square wave	2.5-12 V swept square wave	10 V maximum
Excitation Frequency	1400-3500 Hz	1400-3500 Hz	1400-3500 Hz	1400-3500 Hz	1400-3500 Hz	1400-3500 Hz	n/a
Material	316 Stainless Steel	316 Stainless Steel	316 Stainless Steel	316 Stainless Steel	316 Stainless Steel	316 Stainless Steel	316 Stainless Steel
Temperature Range ¹	-20°C to +80°C	-20°C to +80°C	-20°C to +80°C	-20°C to +80°C	-20°C to +80°C	-20°C to +80°C	-20°C to +80°C

Note: PSI = kPa × 0.14503, or MPa × 145.03

¹Other ranges available on request.

²Stated accuracy is for the pressure transducer alone. The total system accuracy (pressure transducer + pressure cell) is subject to site-specific variables.

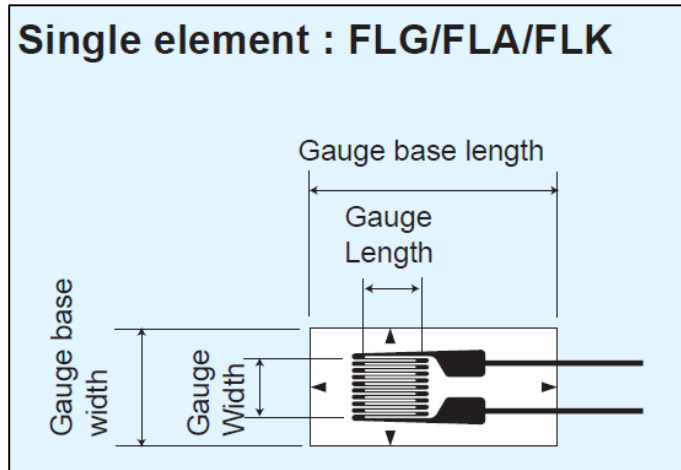
³Other sizes available on request.

Displacement Sensors (Deflectometers) (Vishay/Micromeritics)



SPECIFICATIONS							
MODEL		CDS-05	CDS-10	CDS-20	CDS-30	CDS-40	CDS-50
Measurement Range	in [mm]	5 [127 mm]	10 [254 mm]	20 [508 mm]	30 [762 mm]	40 [1016 mm]	50 [1270 mm]
Accuracy	% FS	0.25	0.15	0.10	0.10	0.10	0.10
Resolution		Analog (Effectively infinite, limited only by instrumentation)					
Repeatability		Greater of ± 0.001 in [± 0.025 mm] or 0.02% FS					
Cable Retraction Force (min)	oz. [N]	3.5 [1.0]	8.4 [2.3]	8.4 [2.3]	6.3 [1.8]	4.2 [1.1]	3.5 [1.0]
Cable Extension Force (max)	oz. [N]	6.5 [1.8]	15.6 [4.3]	15.6 [4.3]	11.7 [3.3]	7.8 [2.2]	6.5 [1.8]
Cable Acceleration	g	3	11	11	5	4	3
Vibration	g, Hz	Up to 10, 0 - 2000					
Shock	g, mS	100, 0.1					
Sensor		Plastic-hybrid precision potentiometer					
Resistance	ohms	500					
Maximum Supply Voltage - Potentiometer	V	30					
Maximum Supply Voltage - Bridge	V	30					
Output - Bridge	mV/V FS	3.0 typical					
Case		Powder-painted aluminum alloy					
Cable		Nylon-coated stainless steel, 0.019 in [0.48 mm] diameter					
Electrical Connector		RJ-45 receptacle					
Weight	lb [kg]	2 [1] typ.					
Operating Temperature	$^{\circ}$ F [$^{\circ}$ C]	- 40 to + 200 [- 40 to 93]					
TC of Sensor	ppm/ $^{\circ}$ F [ppm/ $^{\circ}$ C]	88 [157]					
Humidity	% RH	100 at 90 $^{\circ}$ F [32 $^{\circ}$ C]					

Strain Gauges (Tokyo Sokki Kenkyujo Co., Ltd.)



Type	Gauge length (mm)	Gauge width (mm)	Backing length (mm)	Backing width (mm)	Resistance (Ω)	Lead wire pre-attached	Type name of lead wire preattached
FLA-1-11 FLA-1-17 FLA-1-23	1	1.3	5	2.5	120	Paralleled 1m Paralleled 3m Paralleled 5m 3-wire 3m 3-wire 5m	-1L -3L -5L -3LT -5LT
FLA-2-11 FLA-2-17 FLA-2-23	2	1.5	6.5	3	120	Paralleled 1m Paralleled 3m Paralleled 5m 3-wire 3m 3-wire 5m	-1L -3L -5L -3LT -5LT
FLA-3-11 FLA-3-17 FLA-3-23	3	1.7	8.8	3.5	120	Paralleled 1m Paralleled 3m Paralleled 5m 3-wire 3m 3-wire 5m	-1L -3L -5L -3LT -5LT
FLA-5-11 FLA-5-17 FLA-5-23	5	1.5	10	3	120	Paralleled 1m Paralleled 3m Paralleled 5m 3-wire 3m 3-wire 5m	-1L -3L -5L -3LT -5LT
FLA-6-11 FLA-6-17 FLA-6-23	6	2.2	12.5	4.3	120	Paralleled 1m Paralleled 3m Paralleled 5m 3-wire 3m 3-wire 5m	-1L -3L -5L -3LT -5LT


Data Loggers

1. Geokon™ 8002-16

Technical Specifications			
	Single-Channel	4-Channel	16-Channel
	LC-2, LC-2A	LC-2x4	LC-2x16
Measurement Accuracy	±0.05% F.S. (450-4000 Hz)	±0.05% F.S. (450-4000 Hz)	±0.05% F.S. (450-4000 Hz)
Measurement Resolution	1 part in 20,000	1 part in 20,000	1 part in 20,000
Program Memory	24K FLASH	24K FLASH	24K FLASH
Data Memory	320K EEPROM	320K EEPROM	320K EEPROM
Data Connection	RS-232, USB or RS-485	RS-232, USB or RS-485	RS-232, USB or RS-485
Storage Capacity (Arrays)	16,000 ¹	10,666	3,555
Temperature Range	-30°C to +50°C	-30°C to +50°C	-30°C to +50°C
Temperature Measurement	(accuracy) 2.0% F.S. (resolution) 0.1°C	(accuracy) 2.0% F.S. (resolution) 0.1°C	(accuracy) 2.0% F.S. (resolution) 0.1°C
Communication Speed	9600 bps	9600 bps	9600 bps
Communication Parameters	8 data bits, no parity, 1 stop bit	8 data bits, no parity, 1 stop bit	8 data bits, no parity, 1 stop bit
Power Supply	3 VDC (2 Alkaline 'D' cells)	3 VDC (2 Alkaline 'D' cells)	3 VDC (4 Alkaline 'D' cells)
Communication Current	< 100 mA	< 100 mA	< 100 mA
Measurement Current	< 200 mA	< 200 mA	< 200 mA
Quiescent Current	< 500 µA	< 500 µA	< 500 µA
Scan Interval	3 - 86,400 seconds (24 hours)	10 - 86,400 seconds (24 hours)	30 - 86,400 seconds (24 hours)
Operating Time (20°C)	3 days - 3 years, depending on scan interval	8 days - 2 years, depending on scan interval	8 days - 2 years, depending on scan interval
Sensor Connection	(LC-2) Hard wired (LC-2A) 10-pin Connector	Hard wired	Hard wired
L × W × H	122 × 120 × 91 mm	260 × 160 × 91 mm	318 × 277 × 159 mm ²

¹8,000 arrays when used with LogWare software.
²Does not include mounting feet.

2. Vishay™ System 7000 32 channel

<p>LCD DISPLAY 64 x 128 white LED-backlit display</p> <p>LED PANEL 32 individual red/green LEDs; one per channel</p> <p>KEYPAD Membrane. 20-key; 12-key numeric keypad, 5 key navigation keypad, and three soft-keys</p> <p>INPUT POWER 11–32 VDC, 30A max</p> <p>POWER INDICATION Green LED (illuminated when power is on)</p> <p>ETHERNET INTERFACE IEEE 802.3, 802.3u 10Base-T, 100Base-TX, half- and full-duplex, auto-detect</p> <p>COMPACT FLASH® CAPACITY 1 GB supplied (removable)</p> <p>PROCESSOR 250 MHz floating point digital signal processor</p> <p>MEMORY 64 MB SDRAM</p> <p>INTERNAL COMMUNICATION Asynchronous command bus, synchronous data bus</p> <p>SYSTEM SYNCHRONIZATION Connections: Sync In, Sync Out Topology: Daisy-chain Cable Connection: TIA/EIA RJ-45, Category 5 Max. Distance: 100m</p> <p>SYSTEM CALIBRATION REFERENCE Firmware-controlled Drift: 1.9 ppm/°C ± 0.6 µV/°C typical, 9.4 ppm/°C ± 2.1 µV/°C maximum Resolution: 150 µV nominal Voltage Range: ±5V</p> <p>DIMENSIONS 7.5 H x 7.1 W x 13.5 D in (190 x 180 x 343 mm)</p> <p>WEIGHT 10.1 lb (4.6 kg)</p>	<p>STRAIN GAGE INPUT CARDS</p>  <p>A choice of two Strain Gage Input Cards (7003-8-SG or 7003-8-SG-A) are used in conjunction with the Model 7003-8-A-I Analog Input Card to perform bridge excitation, bridge completion, shunt calibration, and signal conditioning for eight quarter, half, and full bridges. Note that the 7003-8-SG-A Strain Gage Input Card with Analog Output has an analog output which provides an amplified representation of the input source.</p> <p>CHANNELS Eight per card</p> <p>INPUTS Software selectable for S+/S-, VCAL+/VCAL-, or excitation Strain Gage: 120Ω, 350Ω, 1000Ω quarter-bridges; 60Ω to 5000Ω half- and full-bridges Input Impedance: 220 MΩ nominal each input Source Current: ±5 nA per volt excitation</p> <p>ANALOG OUTPUT (MODEL 7003-8-SG-A ONLY) Fixed Gain: 50.3 V/V ±1% Output Range: ±10V min Output Load: 2000Ω min Bandwidth: DC to 4.2 kHz (-3 dB ±0.25 dB)</p> <p>MEASUREMENT RANGE AND RESOLUTION Total range depends on excitation setting (see table). Resolution: 0.5 µε (GF=2)</p> <table border="1" data-bbox="878 1329 1334 1663"> <thead> <tr> <th rowspan="2">EXCITATION VOLTS</th> <th colspan="2">MEASURING RANGE</th> </tr> <tr> <th colspan="2">Includes Full Scale Imbalance</th> </tr> <tr> <th></th> <th>µε @ GF=2</th> <th>mV/V</th> </tr> </thead> <tbody> <tr><td>0</td><td>48,000</td><td>24*</td></tr> <tr><td>0.25</td><td>100,000</td><td>50</td></tr> <tr><td>0.5</td><td>96,000</td><td>48</td></tr> <tr><td>0.75</td><td>70,000</td><td>35</td></tr> <tr><td>1</td><td>48,000</td><td>24</td></tr> <tr><td>2</td><td>24,000</td><td>12</td></tr> <tr><td>3</td><td>16,000</td><td>8</td></tr> <tr><td>4</td><td>50,000</td><td>25</td></tr> <tr><td>5</td><td>40,000</td><td>20</td></tr> <tr><td>6</td><td>35,000</td><td>17.5</td></tr> <tr><td>7</td><td>30,000</td><td>15</td></tr> <tr><td>8</td><td>25,000</td><td>12.5</td></tr> <tr><td>9</td><td>20,000</td><td>10</td></tr> <tr><td>10</td><td>20,000</td><td>10</td></tr> </tbody> </table>	EXCITATION VOLTS	MEASURING RANGE		Includes Full Scale Imbalance			µε @ GF=2	mV/V	0	48,000	24*	0.25	100,000	50	0.5	96,000	48	0.75	70,000	35	1	48,000	24	2	24,000	12	3	16,000	8	4	50,000	25	5	40,000	20	6	35,000	17.5	7	30,000	15	8	25,000	12.5	9	20,000	10	10	20,000	10
EXCITATION VOLTS	MEASURING RANGE																																																		
	Includes Full Scale Imbalance																																																		
	µε @ GF=2	mV/V																																																	
0	48,000	24*																																																	
0.25	100,000	50																																																	
0.5	96,000	48																																																	
0.75	70,000	35																																																	
1	48,000	24																																																	
2	24,000	12																																																	
3	16,000	8																																																	
4	50,000	25																																																	
5	40,000	20																																																	
6	35,000	17.5																																																	
7	30,000	15																																																	
8	25,000	12.5																																																	
9	20,000	10																																																	
10	20,000	10																																																	

Appendix C
Strain Gauge Readings

Table C-1 Strain in iPVC pipe at joint and end of pipe

Date	Joint of Pipe (µε)															End of Pipe (µε)				
	S G- J- C- 1	S G- J- C- 2	S G- J- C- 3	S G- J- C- 4	S G- J- C- 5	S G- J- C- 6	S G- J- C- 7	S G- J- C- 8	S G- J- L- 9	SG -J- L- 11	SG -J- L- 13	SG -J- L- 14	SG -J- L- 15	SG -J- L- 16	SG -J- L- 17	SG -E- C- 19	SG -E- C- 21	SG -E- L- 27	SG -E- L- 28	SG -E- L- 29
2 / 1 6	0	0	0	0	0	0	0	0	0	0	0	0	0	0	0	0	0	0	0	0
2 / 2 3	3	0	-2	1	4	4	-2	-2	2	-1	2	1	-1	-1	0	-8	-9	1	-3	3
3 / 1 1	0	-3	-3	1	7	3	-2	-2	4	-3	4	3	-2	-2	2	-5	-7	4	-4	2
3 / 8	8	-5	-8	8	8	7	-7	-7	4	-4	6	2	-2	-4	6	-7	-9	8	-3	3
3 / 1 5	2	-2	-3	3	7	3	-3	-3	2	-3	3	1	-2	-3	2	-11	-8	7	-2	2
3 / 2 2	2	-1	-2	1	6	0	-1	-1	0	-1	1	5	-5	-6	8	-9	-5	6	-1	1
3 / 2 9	0	-2	-1	1	9	2	-1	0	1	-1	1	1	-1	-1	1	-9	-8	9	0	1
4 / 5	2	-4	-4	3	7	3	-4	-3	1	-2	2	1	-2	-4	4	-7	-4	8	-1	2
4 / 1 2	2	-1	-1	1	8	0	-1	-1	1	-4	4	4	-3	-2	2	-5	-7	8	-1	1
4 / 1 9	3	-2	-2	2	9	2	-2	-4	2	-3	3	2	-1	-2	1	-8	-	9	-2	1
4 / 2 6	1	-7	-1	2	11	-1	-1	-1	1	0	1	2	-1	-3	2	-6	-	11	-5	1
5 / 3	1	-4	-3	1	12	0	-2	-1	1	-1	-1	2	-3	-6	5	-8	-	10	-1	0
5 / 1 0	0	-1	-1	1	11	2	-1	-3	1	-1	0	2	-2	-3	4	-9	-	10	-2	0
5 / 1 7	2	-2	-2	2	9	1	-2	-4	1	-1	1	1	-1	-1	0	-11	-	9	-2	1
5 / 2 4	3	-4	-3	3	7	4	-2	-2	3	-2	2	2	-2	-3	4	-7	-	8	-1	3
5 / 3 1	1	-1	-2	1	8	2	0	0	1	0	1	1	-1	0	-1	-5	-	9	0	0
6 / 7	6	-5	-3	4	6	3	-3	-2	2	-1	2	3	-3	-3	3	-8	-	9	-3	2
6 / 1 4	5	-9	-11	6	7	4	-9	-7	9	-11	8	7	-10	-12	12	-12	-	7	-7	6

Table C-2 Strain in iPVC pipe at joint and end of pipe due to earth plus truck load

Time	Joint of Pipe ($\mu\epsilon$)															End of Pipe ($\mu\epsilon$)			
	SG-J-C-1	SG-J-C-2	SG-J-C-3	SG-J-C-4	SG-J-C-5	SG-J-C-6	SG-J-C-7	SG-J-C-8	SG-J-L-9	SG-J-L-11	SG-J-L-13	SG-J-L-14	SG-J-L-15	SG-J-L-16	SG-J-L-17	SG-E-C-19	SG-E-L-27	SG-E-L-28	SG-E-L-29
6/30 @ 7 A M	9	-12	-16	8	12	9	-12	-5	6	-17	11	8	-7	-10	12	-13	9	-2	4
6/30 @ 8 A M	42	-71	-65	33	73	51	-67	-51	40	-68	77	62	-41	-53	81	-78	93	-71	68
6/30 @ 9 A M	80	-121	-72	68	101	82	-107	-73	71	-115	109	94	-60	-73	124	-111	121	-125	101
6/30 @ 10 A M	110	-143	-126	91	147	114	-153	-105	100	-129	115	100	-84	-97	155	-146	145	-153	106
6/30 @ 11 A M	107	-158	-128	93	160	123	-166	-110	97	-133	144	129	-90	-103	163	-148	173	-145	126
6/30 @ 12 noon	95	-137	-112	79	159	111	-148	-97	89	-119	155	140	-79	-92	145	-165	174	-151	142
6/30 @ 1 P M	87	-111	-105	75	145	97	-135	-86	85	-109	139	124	-70	-83	131	-157	171	-149	138
7/7 @ 1 P M	56	-93	-85	67	110	75	-103	-69	74	-96	113	98	-56	-69	110	-121	159	-117	93
7/14 @ 1 P M	54	-87	-69	59	99	62	-93	-59	63	-91	106	91	-50	-62	102	-114	134	-84	69

References

ABAQUS 6.14-3. Software available at:

www.3ds.com/products-services/simulia/products/abaqus

Alam, S., and Allouche, E.N. (2010). Experimental Investigation of Pipe Soil Friction Coefficients for Direct Buried PVC Pipes. American Society of Civil Engineers. Pipelines Conference 2010.

Al-Barqawi, H., and Zayed, T. (2006). "Condition Rating Model for Underground Infrastructure Sustainable Water Mains." *Journal of Performance of Constructed Facilities*, American Society of Civil Engineers (ASCE), Vol. 20:2, Reston, VA.

American Chemistry Council (2008). The Economic benefits of Polyvinyl Chloride in the United States and Canada. Whitfield and Associates, Naperville, IL.

American Water Works Association (2002). "M23 PVC Pipe - Design and Installation, Second Edition." American Water Works Association, Denver, CO.

American Water Works Association (2007). "C900 - Polyvinyl Chloride (PVC) Pressure Pipe and Fabricated Fittings, 4 in. through 12 in. (100 mm through 300 mm), for Water Transmission and Distribution." American Water Works Association, Denver, CO.

American Water Works Association (2009). "C909-09 Molecularly Oriented Polyvinyl Chloride (PVCO) Pressure Pipe, 4 in. through 24 in. (100 mm through 600 mm) for Water, Wastewater, and Reclaimed Water Service." American Water Works Association, Denver, CO.

American Water Works Association (2010). "C905 - Polyvinyl Chloride (PVC) Pressure Pipe and Fabricated Fittings, 14 in. through 48 in. (350 mm through 1,200 mm) for Water Transmission and Distribution." American Water Works Association, Denver, CO.

- American Water Works Association (2012). "C907 - Injection-Molded Polyvinyl Chloride (PVC) Pressure Fittings, 4 in. through 12 in. (100 mm through 300 mm), for Water, Wastewater, and Reclaimed Water Service." American Water Works Association, Denver, CO.
- American Water Works Association (2014). "C605-13 Underground Installation of Polyvinyl Chloride (PVC) and Molecularly Oriented Polyvinyl Chloride (PVCO) Pressure Pipe and Fittings." American Water Works Association, Denver, CO.
- Antaki, G. A. (2003). *Piping and Pipeline Engineering: Design, Construction, Maintenance, Integrity, and Repair*. Marcel Dekker, New York.
- Arnaout, S. (2000). "Design and Installation of Concrete Bar-Wrapped Cylinder Pipe:(AWWA C303 - Type Pipe)." *Environmental and Pipeline Engineering*, American Society of Civil Engineers (ASCE), Reston, VA.
- ASTM D1599-14 (2010). "Standard Test Method for Resistance to Short-Time Hydraulic Pressure of Plastic Pipe, Tubing, and Fittings." American Society for Testing and Materials, West Conshohocken, Pa.
- ASTM D1784-11. "Standard Specification for Rigid Poly(Vinyl Chloride) (PVC) Compounds and Chlorinated Poly(Vinyl Chloride) (CPVC) Compounds." American Society for Testing and Materials, West Conshohocken, Pa.
- ASTM D2321-14e1 (2005). *Standard Practice for Underground Installation of Thermoplastic Pipe for Sewers and Other Gravity-Flow Applications*. American Society for Testing and Materials, West Conshohocken, PA.
- ASTM D2444-99 (2011). "Standard Test Method for Determination of the Impact Resistance of Thermoplastic Pipe and Fittings by Means of a Tup (Falling Weight)." American Society for Testing and Materials, West Conshohocken, PA.

- ASTM D5947-11 (2010). "Standard Test Methods for Physical Dimensions of Solid Plastics Specimens." American Society for Testing and Materials, West Conshohocken, PA.
- ASTM D638-14 (2010). "Standard Test Method for Tensile Properties of Plastics." American Society for Testing and Materials, West Conshohocken, Pa.
- Bai, Q., and Bai, Y. (2014). Burst Strength of Reinforced Thermoplastic Pipe (RTP). *Subsea Pipeline Design, Analysis, and Installation*. Elsevier Inc., Ottawa, Canada.
- Balkaya, M., Moore, I., and Saglamer, A. (2012). "Study of Non-uniform Bedding Due to Voids under Jointed PVC Water Distribution Pipes." *Geotextiles and Geomembranes*, Elsevier Science Ltd., Vol. 34, Ottawa, Canada.
- Balkaya, M., Moore, I.D., and Saglamer, A. (2013). Study of Non-uniform Bedding Support under Continuous PVC Water Distribution Pipes. *Tunneling and Underground Space Technology*, Vol. 35, pp. 99-108. Elsevier Ltd., Amsterdam, Netherlands.
- Bar-wrapped Pipe (2016). www.puretechltd.com/types-of-pipe/bar-wrapped-pipe-c303 (Accessed on: April 20, 2016).
- Bazoune, A. (2012). Artificial Dry Heat Temperature Effects on Tensile Properties of Chlorinated Poly (Vinyl Chloride). *Advanced Materials Research*, Vol. 445, pp. 853-858. Trans Tech Publications Inc., Switzerland.
- Beamer, R.E., Kendall, D.R., and Romer, A.E. (2009). Several Failures of a 16-inch PVC Transmission Main within 12 years. American Society of Civil Engineers. Pipelines Conference 2009.
- Bowman, J.A. (1990). *The fatigue response of polyvinyl chloride and polyethylene pipe systems. Buried Plastic Pipe Technology*. ASTM STP 1093, ed. George S. Buczala and Michael J. Cassady. Philadelphia, PA: American Society for Testing and Materials.

- Burn, S., Davis, P., Schiller, T., Tiganis, B., Tjandraatmadja, G., Cardy, M., Gould, S., Sadler, P., and Whittle, A. (2005). "Long-term Performance Prediction for PVC Pipes." AWWA Research Foundation, Denver, CO.
- C. Brad. *Transient and Surge Related Pipe Bursts, Water Loss and Damage Prevention*. Singer Valve Inc.: Surrey, B.C., Canada. p. 19.
- Chan, J.H., Yee Foo, D.C., Kumaresan, S., Aziz, R.A., and Abu-Hassan, M.A. (2007). An Integrated Approach for Water Minimization in a PVC Manufacturing Process. *Clean Technology Environmental Policy*, Springer-Verlag, Berlin, Germany.
- Chapman, P.G., and Agren, L. (1998). A New Technology for In-line Manufacturing of Biaxially Oriented PVC Pipes. *Proceedings of Plastic Pipes X*, Gothenberg, Sweden.
- CISPI (2006). "Cast Iron Soil Pipe and Fittings Handbook." Rep. No. 86071884, Cast Iron Soil Pipe Institute (CISPI), Chattanooga, TN.
- Deeble, V. C. (1994). "Effectiveness of PVC Coatings as Thermal Insulation for Domestic Hot-water Piping." *Applied Energy*, Vol. 48:1, Elsevier Science Ltd., Ottawa, Canada.
- Divyashree, D., Najafi, M., Sever, F., and Entezarmahdi, A. (2015). "Development of a Testing Protocol for Fatigue Testing of Large Diameter HDPE Pipes." Proceedings of ASCE Pipelines Conference 2015, Baltimore, Maryland.
- Ductile Iron Pipe Research Association (2016). www.dipra.org (Accessed on July 20, 2016).
- Fragher, E., Fleming, P.R., and Rogers, C.D.F. (2000). Analysis of Repeated-Load Field Testing of Embedded Plastic Pipes. Transportation Research Record 1514, Transportation Research Board, Washington, DC, pp. 271–277.

- Federal Highway Administration (FHWA) (2002). *Corrosion Cost and Preventive Strategies in the United States*, FHWA-RD-01-156, McLean, VA.
- Folkman, S. (2014). PVC Pipe Longevity Report – A Comprehensive Study on PVC Pipe Excavations, Testing, and Life Cycle Analysis.
- Gabet, C., Chicheportiche, S., Vivet, R., Taravel-Condât, C. (2011). Small and Full Scale Testing of Flexible Pipes in Cold Environment for Arctic Use. Arctic Technology Conference 2011, Houston, TX.
- Geokon™ (2016). <www.geokon.com/8002-16> (April 22, 2016).
- Gere, J.M., and Timoshenko, S.P. (1997). *Mechanics of materials, 4th ed.* PWS Publishing Company, Boston.
- Howard, A. (2015). *Pipeline Installation 2.0*. Relativity Publishing, Lakewood, CO.
- Hucks, R. T. (1972). *Design of PVC water-distribution pipe*. Civil Engineering ASCE 42, no. 6:70-73.
- Hughes, D., Venkatesh, C., Lee, A.G., Paradkar, A. and Najafi, M. (2016). Development, Evaluation, and Installation of a New Improved PVC (iPVC pipe) Pipe for Water Applications. *Proc., Pipelines Conference 2016*, American Society of Civil Engineers, Reston, VA. pp. 1046-1060.
- Hughes, D., Venkatesh, C., Paradkar, A. and Najafi, M. (2016). The Innovative Plastic Pipe: Ductile iPVC pipe. *Proc. AWWA Annual Conference and Exposition 2016*, American Water Works Association, Denver, CO.
- Japanese Sewage Works Association [JSWA] (1999). *The design guidelines for fiberglass reinforced plastic mortar pipe*. JSWA, Tokyo.
- Jeffrey, J.D. (2012). Long-term cyclic testing of 6-inch PVC pipe. Thesis for the Degree of Master of Science from Utah State University, Logan, UT.

- Jeffrey, J.D., Moser, A.P., and Folkman, S.L. (2004). Long-term cyclic testing of PVC pipe. Buried Structures Laboratory, Utah State University, Logan, UT.
- JM Eagle (2016). Depth of Burial for PVC Pipe. www.jmeagle.com/pdfs/Technical%20Bulletins/TB06DepthofBurialforPVC.pdf (Accessed on July 18, 2016).
- JM Eagle (2016). Frequently Asked Questions on PVC. www.jmeagle.com/plastic-pipe/faq.html#flexible-conduit (Accessed on July 18, 2016).
- Kawabata, T., Ling, H.I., Mohri, Y., and Shoda, D. (2006). Behavior of Buried Flexible Pipe under High Fills and Design Implications. *Journal of Geotechnical and Geoenvironmental Engineering*. American Society of Civil Engineers, Reston, VA.
- Khatri, D.K. (2014). "Laboratory and Field Performance of Buried Steel-Reinforced High Density Polyethylene (SRHDPE) Pipes in a Ditch Condition under a Shallow Cover." PhD dissertation, University of Kansas, KS.
- Kim, S. H., Seong-Yong, A., and Seung-Yeop, K. (2008). "Suppression of Dioxin Emission in Incineration of Poly Vinyl Chloride (PVC) as Hybridized with Titanium Dioxide (TiO₂) Nanoparticles." *Applied Catalysis B: Environmental*, Vol. 79:3, Elsevier Science Ltd., Ottawa, Canada.
- Lackey, K. A. (2010). "When Pump Design Goes Wrong." *NCAWWA Spring Conference*, New Bern, NC.
- Law, M., and Bowie, G. (2007). Prediction of Failure Strain and Burst Pressure in High Yield-to-Tensile Strength Ratio Linepipe. *International Journal of Pressure Vessels and Piping*. Elsevier Science Ltd., Vol. 84, pp. 487-492. Ottawa, Canada.
- Makar, J. M., Desnoyers, R., and McDonald, S. E. (2001). "Failure Modes and Mechanisms in Gray Cast Iron Pipes." *Underground Infrastructure Research 2001 - Waterloo, Ontario*. National Research Council, Canada.

- Marshall, G.P., Brogden, S. and Shepherd, M.A. (1998). *Evaluation of the surge and fatigue resistance of PVC and P E pipeline materials for use in the U.K. water industry*. Information and Guidance Note. London, UK: Water Industry's Trade Association.
- Mays, L. W. (2000). *Water Distribution Systems Handbook*. McGraw-Hill, New York.
- Meikle, J. (1995). "American Plastic: A Cultural History." Rutgers University Press, New Brunswick, NJ.
- Moser, A.P. (2001). *Cyclic life of PVC pipe*. Utah State University, College of Engineering, Logan, UT.
- Moser, A.P. and Folkman, S. (2008). *Buried Pipe Design*. McGraw-Hill, New York.
- Mulder, K., and Knot, M. (2001). "PVC Plastic: A History of Systems Development and Entrenchment." *Technology in Society*, Elsevier Science Ltd., Vol.23:2, Ottawa, Canada.
- Najafi, M. (2010). *Trenchless Technology Piping: Installation and Inspection*. McGraw-Hill, New York.
- Najafi, M., and Gokhale, S. (2005). *Trenchless Technology: Pipeline and Utility Design, Construction and Renewal*. McGraw-Hill, New York.
- Najafi, M., Fisher, C., Kanchawala, M., and Kulkarni, T. (2011-a). "Cost Comparison of PVC Water Pipe for Horizontal Directional Drilling (HDD) and Open-cut Installations." North American Society for Trenchless Technology, No-Dig Show 2010, Washington, D.C.
- Najafi, M., Fisher, C., Sharma, J.R., and Jain, A. (2011-b). "Testing of Segmental PVC Pipe for HDD Applications." North American Society for Trenchless Technology, No-Dig Show 2010, Washington, D.C.

- Najafi, M., Habibian, A., and Sever, F.V. (2015). "Durability and Reliability of Large Diameter (16-inch and Larger) HDPE Pipe for Water Main Applications." Water Research Foundation, Denver, CO.
- Najafi, M., Sharma, J.R., Marshall, D., and Jain, A. (2013). "Thin-walled Large Diameter Steel Pipe Response to Various Embedment Conditions." American Society of Civil Engineers. Pipelines Conference 2013.
- Najafi, M., Sharma, J.R., Marshall, D., Jain, A., and Rahjoo, S. (2011). "Testing and Evaluation of Statically-loaded Large Diameter Steel Pipe with Native Backfill Soils." American Society of Civil Engineers. Pipelines Conference 2011.
- Netto, T.A., Ferraz, U.S., and Estefen, S.F. (2005). The Effect of Corrosion Defects on the Burst Pressure of Pipelines. *Journal of Constructional Steel Research*. Elsevier Science Ltd., Vol. 61, pp. 1185-1204, Ottawa, Canada.
- Oliphant, K., Conrad, M., and Bryce, W. (2012). Fatigue of Plastic Water Pipe: A Technical Review with Recommendations for PE4710 Pipe Design Fatigue. Jana Laboratories, Aurora, Ontario.
- Ong, S. K., Gaunt, J. A., Mao, F., Cheng, C., Hurburgh, C., and Esteve-Agelet, L. (2008). "Impact of Hydrocarbons on PE/PVC pipes and pipe gaskets." AWWA Research Foundation, Denver, CO.
- Parisher, R. A., and Rhea, R. A. (2012). "Chapter 2- Steel Pipe - *Pipe Drafting and Design*." Gulf Publishing Company, Elsevier Science Ltd., Houston, TX.
- Petroff, L.J. (2013). Occasional and Recurring Surge Design Considerations for HDPE pipe. *Proceedings of ASCE Pipelines Conference 2013*, Fort Worth, TX.
- Plastics Additives and Compounding (2004). Impact Modifiers: How to make your Compound Tougher. Elsevier Science Ltd., Ottawa, Canada.
- Plastics Pipe Institute (2016). www.plasticpipe.org (Accessed on July 20, 2016).

- Plaxis 2D Version 2010.01. www.plaxis.nl
- Potyondy, J.G. (1961). Skin Friction between Various Soil and Construction Materials. *Geotechnique*, Vol. XI, No. 4, pp. 339-353.
- Pyungwha Pipe Industry, Inc. (2015). www.iPVC pipepipe.com
- Rahman, S. and Farrell, H. (2015). "Municipal Pipeline Thrust Restraint: Next Generation of Products for Thermoplastic Pipes." Texas ASCE Sectional Paper. www.bulldogrestraintsystem.com/TexasASCESectionalPaper.pdf (Accessed on November 20, 2015).
- Rahman, S., and Watkins, R. (2005). "Longitudinal Mechanics of Buried Thermoplastic Pipe: Analysis of PVC Pipes of Various Joint Types." *Pipelines Conference 2005*, American Society of Civil Engineers (ASCE), Reston, VA.
- Saeki, Y., and Emura, T. (2002). "Technical progresses for PVC production." *Progress in Polymer Science*, Elsevier Science Ltd., Vol. 27:10, Ottawa, Canada.
- Sargand, S.M., Hazen, G.A., and Masada, T. (1998). Structural Evaluation and Performance of Plastic Pipe. *Report FHWA-OH-98-011*. FHWA, U.S. Department of Transportation, Washington, D.C.
- Schluter, C.J., and Shade, J.W. (1999). Flexibility Factor or Pipe Stiffness, Significant Stiffness Considerations. *Transportation Research Record 1656*, pp. 45-50. Washington, D.C.
- Sewer History (2016). Milestones in PVC Sewer Pipe History. www.sewerhistory.org/articles/compon/pdfs/pvc_water_milestones.pdf (Accessed on: May 15, 2016).
- Sharma, J.R. (2013). Development of a Model for Estimation of Buried Large Diameter Thin-Walled Steel Pipe Deflection due to External Loads. Presented to the Faculty

of the Graduate School of The University of Texas at Arlington in Partial Fulfillment of Requirements for the Degree of Doctor of Philosophy.

Shigley, E.J., and Mischke, C.R. (1989). *Mechanical engineering design, 5th ed.* McGraw-Hill Inc., New York.

Spangler, M. G. (1941). "The structural design of flexible pipe culverts." *Bulletin 153*, Iowa Engineering Experiment Station, Ames, Iowa.

Storm, T. S. and Rasmussen, S. C. (2011). "100+ Years of Plastic." Leo Baekeland and Beyond, American Chemical Society, printed by Oxford University Press, Inc.

Terzi, N.U., Yilmazturk, F., Yildirim, S., and Kilic, H. (2010). Experimental Investigations of Backfill Conditions on the Performance of High-Density Polyethylene Pipes. *Experimental Techniques*, pp. 40-49. Society of Experimental Mechanics.

Think Pipes, Think PVC (2016). Benefits of PVC Pipes.

www.thinkpipethinkpvc.com.au/benefits-of-pvc-pipes (Accessed on August 15, 2016).

Thornton, J. (2002). "Environmental Impacts of Polyvinyl Chloride Building Materials - A Healthy Building Network Report." Healthy Building Network, Washington, D.C.

Tseng, A.A., Borrosky, M.A., O'Connor, S.M., and Knotts, J.J. (1991). Impact Behavior of Modified PVC for Outdoor Applications. *Proc., Advances in Polymer Technology, Vol. 10, No. 3, 205-218*. John Wiley and Sons, Inc., Hoboken, NJ.

Underground Solutions (2016). Fusing Fusible C900 in Pit Fusion.

www.undergroundsolutions.com/pipe-fusion.php (Accessed on August 24, 2016).

Uni-Bell (2012). Handbook of PVC Pipe Design and Construction Fifth Edition. Industrial Press Inc., New York, NY. Uni-Bell PVC Pipe Association. ISBN: 9780831134501.

Uni-Bell (2013). Installation guide for gasketed-joint PVC pressure pipe. Uni-Bell PVC Pipe Association, Dallas, TX.

- Uni-Bell (2015). Technical Brief. Uni-Bell PVC Pipe Association, Dallas, TX.
- Uni-Bell (2016). www.uni-bell.org (Accessed on July 20, 2016).
- Venkatesh, C. (2012). Performance Comparison of High Density Polyethylene Pipe (HDPE) in Municipal Water Applications. Presented to the Faculty of the Graduate School of The University of Texas at Arlington in Partial Fulfillment of Requirements for the Degree of Master of Science in Civil Engineering.
- Venkatesh, C., Paradkar, A., Hughes, D., and Najafi, M. (2016). Preliminary Test Results of a New Structurally Improved PVC (iPVC pipe) Water Pipe Material. *Proc. No-Dig Show (Dallas), 2016*, North American Society for Trenchless Technology, Cleveland, OH.
- Vinson, H.W. (1981). *Response of PVC pipe to large, repetitive pressure surges. Proceedings of the international conference on underground plastic pipe held in New Orleans 30 March - 1 April 1981*, edited by B. Jay Schrock, 485-494., American Society of Civil Engineers, VA.
- Vinyl Institute (2016). How is Vinyl made? www.vinylinfo.com/vinyl/facts (Accessed on May 2, 2016).
- Vinyl Pipes (2016). Benefits of PVC Pipes. www.vinylpipes.com/wp-content/uploads/2014/01/BENEFITS-OF-PVC-PIPE.pdf (Accessed on August 15, 2016).
- Vishay™ (2016). <www.vishaypg.com/docs/11102/p3.pdf> (April 23, 2016).
- Walski, T. M. (2006). "A History of Water Distribution." Vol. 98, No. 3, American Water Works Association, Denver, CO.
- Wang, D., Cullimore, R., Hu, Y., and Chowdhury, R. (2011). "Biodeterioration of Asbestos Cement (AC) Pipe in Drinking Water Distribution Systems." *International*

Biodeterioration & Biodegradation. Elsevier Science Ltd., Vol. 65:6, Ottawa, Canada.

Watkins, R.K., and Anderson, L.R. (2000). *Structural Mechanics of Buried Pipes*. CRC Press LLC, Boca Raton, FL.

West, D.B., and Truss, R.W. (2011). *Stochastic fatigue limits and fatigue life variability in oriented-PVC pipe*. Elsevier, Oxford, U.K.

WRF Report No. 4650 (2016). *An Evaluation of the Value of Structurally Enhanced PVC Pipe*. Water Research Foundation Report No. 4650 prepared by David Hughes, Chandan Venkatesh and Mohammad Najafi as part of iPVC pipe project.

Zhan, C., and Rajani, B. (1997). *Load Transfer Analyses of Buried Pipe in Different Backfills*. *Journal of Transportation Engineering*, Vol. 123, No. 6. American Society of Civil Engineers, Reston, VA.

Biographical Information

Ameya Paradkar graduated with a Master of Science Degree in Civil Engineering with a focus on Construction Engineering and Management from the University of Texas at Arlington (UTA) in December 2012. He was a teaching assistant at UTA and was involved in teaching Construction Estimating, Construction Scheduling, and Construction Productivity courses. He taught construction scheduling (Primavera Ver. 7.0) and construction estimating (Sage Timberline). He was fully funded throughout his Doctoral studies and also received a Doctoral Dissertation Fellowship from the University in his final semester. Paradkar has served as the president of the UTA student chapter of the North American Society of Trenchless Technology (NASTT) and has been an active ASCE student member.